LUT UNIVERSITY
LUT School of Energy Systems
LUT Mechanical Engineering

Eetu Holstein

CONCEPTUALIZATION OF PARAMETER OPTIMIZATION OF NEW MATERIALS IN VAT PHOTOPOLYMERIZATION FOR DENTAL APPLICATIONS.

Helsinki 15.6.2020

Examiner(s): Professor Heidi Piili, D. Sc. (Tech.)
Product Development Director Helka Ojanperä, M. Sc. (Tech.)

TIIVISTELMÄ

LUT-Yliopisto
LUT School of Energy Systems
LUT Kone

Eetu Holstein

Parametrikehityksen konseptointi uusille materiaaleille allasvalokovetuksessa hammaslääketieteellisissä sovelluksissa.

Diplomityö

2020

108 sivua, 60 kuvaa, 17 taulukkoa ja 5 liitettä

Tarkastajat: Professori Heidi Piili, TkT
Tuotekehitysjohtaja Helka Ojanperä, DI

Hakusanat: Allasvalokovetus, 3D-tulostus, lisäävä valmistus, hartsi, hammaslääketiede, parametrien optimointi

Diplomityön tavoitteena oli määrittää vakioitu, dokumentoitu, toistettava sekä jäljitettävä prosessi, uusien hammaslääketieteellisten materiaalien parametrikehitykselle Planmeca Oy:lle. Määritetty prosessi mahdollistaa uusien hammaslääketieteessä käytettävien hartsien tehokkaamman testaamisen. Diplomityö koostui kahdesta osasta, kirjallisuuskatsauksesta sekä kokeellisesta osasta. Kirjallisuuskatsauksessa etsittiin tietoa erilaisista koesuunnittelumenetelmistä, joita on käytetty 3D-tulostamisessa sekä tietoa allasvalokovetuksen merkittävimmistä parametreistä. Kokeellisessa osassa luotiin prosessi parametrikehitykselle sekä testattiin kyseinen prosessi käytännössä.

Kirjallisuuskatsaus osoitti Taguchin metodin olevan laajasti hyödynnetty koesuunnittelumenetelmä optimoitaessa parametrejä 3D-tulostusprosessissa. Käyttämällä Taguchin monimuuttujakoesuunnittelua, kokeiden määrää voidaan vähentää huomattavasti. Kriittisten parametrien tunnistaminen sekä vasteen tarkka määrittäminen ovat tärkeimmät osa-alueet onnistuneen koesuunnittelun saavuttamiseksi. Merkittävimmät parametrit hartsien 3D-tulostamisessa todettiin olevan kerrospaksuus, valotusaika, hartsin koostumus, UV-valon ominaisuudet, tilavuusalkion koko sekä kappaleen asemointi yhdessä tukirakenteiden kanssa.

Kokeellisessa osassa luotiin sekä testattiin kolmivaiheinen, toistettavissa oleva optimointiprosessi. Jokaisessa vaiheessa tulostettiin koesarja, joka arvioitiin visuaalisesti. Optimointiprosessille luotiin työnkulkukaavio. Lisäksi parametrit jaettiin kolmeen ryhmään selkeyttämään parametrien hallintaa sekä kalanruotokaavio luotiin havainnollistamaan tulostuslaatuun vaikuttavia parametrejä Creo C5 3D-tulostimella. Diplomityö osoitti, että hyödyntämällä monimuuttujakoesuunnittelua, kokeiden määrä voidaan vähentää 81:stä yhdeksään kokeeseen testisarjaa kohti. Optimointiprosessilla kyettiin nopeuttamaan tulostusprosessia 13.7%, säilyttäen tulostuslaatu halutulla tasolla.

ABSTRACT

LUT University
LUT School of Energy Systems
LUT Mechanical Engineering

Eetu Holstein

Conceptualization of parameter optimization of new materials in vat photopolymerization for dental applications.

Master's thesis

2020

108 pages, 60 figures, 17 tables and 5 appendices

Examiners: Professor Heidi Piili, D. Sc. (Tech.)
Product Development Director Helka Ojanperä, M. Sc. (Tech.)

Keywords: Vat photopolymerization, 3D printing, additive manufacturing, resin, dentistry, parameter optimization

The goal of this master thesis was to determine a standardized, documented, repeatable, and traceable procedure for parameter optimization process used with new materials of dental applications by Planmeca corporation. Determined process enables more efficient testing of new dental 3D printing resins. This thesis consists of two parts. First literature review was carried out and then experimental part was executed based on the knowledge collected in the literature review. In literature review it was concentrated on finding knowledge of different design of experiment processes used among 3D printing and the most critical parameters in vat photopolymerization. The parameter optimization process was created and tested in experimental part.

The literature review showed that Taguchi method is widely utilized design of experiments process when 3D printing parameters are optimized. The number of experiments can be remarkably reduced by using Taguchi multivariable design of experiments. According the literature review, identification of the critical parameters and determination of the response carefully, are the key issues to have a succeeded design of experiments. The most important parameters for resin 3D printing are layer thickness, exposure time, resin composition, UV light characteristics, voxel size, and build angle with support structure settings.

The optimization process of three steps was created in experimental part. The process was tested and re-executed in practice. Test series of experiments were printed in each step and all the experiments were visually examined. Flow chart was created for the optimization process. Furthermore, fishbone diagram was created, and parameters were divided into three groups to clarify which parameters are affecting to printing quality in Creo C5 3D printer. This thesis showed that the amount of experiments can be reduced from 81 experiments down to only 9 experiments per test series. The created optimization process resulted 13.7% faster printing times while maintaining printing quality at desired level.

ACKNOWLEDGEMENTS

First, I would like to thank Planmeca Oy and especially Helka Ojanperä (Product Development Director) for the opportunity to execute my master thesis at Planmeca about the topic I was interested in. I want to thank Professor Heidi Piili from LUT University of the guidance she has provided during my studies among additive manufacturing as well as during my thesis. I would like to show my gratitude also to my colleagues at Planmeca, who have helped me whenever I needed help.

Special thanks to all my friends who I have met during my studies in Finland and abroad, you have provided me inspiration and support whenever I have needed it. I would especially like to thank Markus Korpela, for his help with this thesis and guidance into academic writing in English. I am also very grateful for every second I got to spent in Lappeenranta as a student, community spirit of LUT University and student organizations was exceptional.

Last and the foremost, I want to thank my parents for all the support and believe in me during my life. Without you, me graduating as a Master of Science in Technology, would not be possible. Mum and Dad, you have given me the strength to believe in myself.

Eetu Holstein

Eetu Holstein
Helsinki 15.6.2020

TABLE OF CONTENTS

LIST OF SYMBOLS AND ABBREVIATIONS

E_D	Exposure dose [mJ/cm^2]
E_I	Irradiance [mW/cm^2]
t_E	Exposure time [sec]
t_{E1}	Exposure time of the sheet to the bottom of the vat [sec]
$t_{E,B}$	Exposure time of the bottom layers [sec]
t_X	Exposure time [sec]
v_{uX}	Speed up [mm/min]
v_{dX}	Speed down [mm/min]
z_X	Lift distance [mm]
$\bar{X}$	Arithmetic mean

AM	Additive Manufacturing
CAD	Computer Aided Design
CAM	Computer Aided Manufacturing
CBCT	Cone Beam Computed Tomography
DOE	Design of Experiments
DMD	Digital Micromirror Device
DLP	Digital Light Processing
IFU	Instructions For Use
IR	Infrared
LCD	Liquid Crystal Display
LED	Light-Emitted Diode
OVAT	One Variable At a Time
PDMS	Polydimethylsiloxane
RMSE	Root Mean Squared Error
SLA	Stereolithography
UV	Ultraviolet
VTT	Technical Research Centre of Finland

1 INTRODUCTION

Additive manufacturing (AM) is rapidly developing manufacturing technique among industry, but especially a large growth of technology among dental industry has been noticed. Specifically, the high customization of the final product in dental industry has led to utilization of additive manufacturing as customization is the one of the main advantages of the technology. Therefore, Planmeca is manufacturing 3D printer for dental use, name of the printer is Creo C5. Like other industries, dentistry is also moving towards digital workflow. This means in practice in dentistry, that teeth are scanned with intraoral scanner (only if treatment that needs scanning is executed) and then for example the required surgical guides are designed with computer aided design (CAD) software. Computer aided manufacturing (CAM) is made with 3D printer based on the CAD model. This way high improvements in surgical accuracy and so on in recovery times are achieved. Digital dentistry and digital workflow (Figure 1) are also enabling "one day dentistry" concept, that all the needed operations could be done in one day. (Anderson 2017, p. 30; Bhargav et al. 2018, pp. 2058–2059; Roland 2020; Shah & Chong 2018, pp. 641–642.)

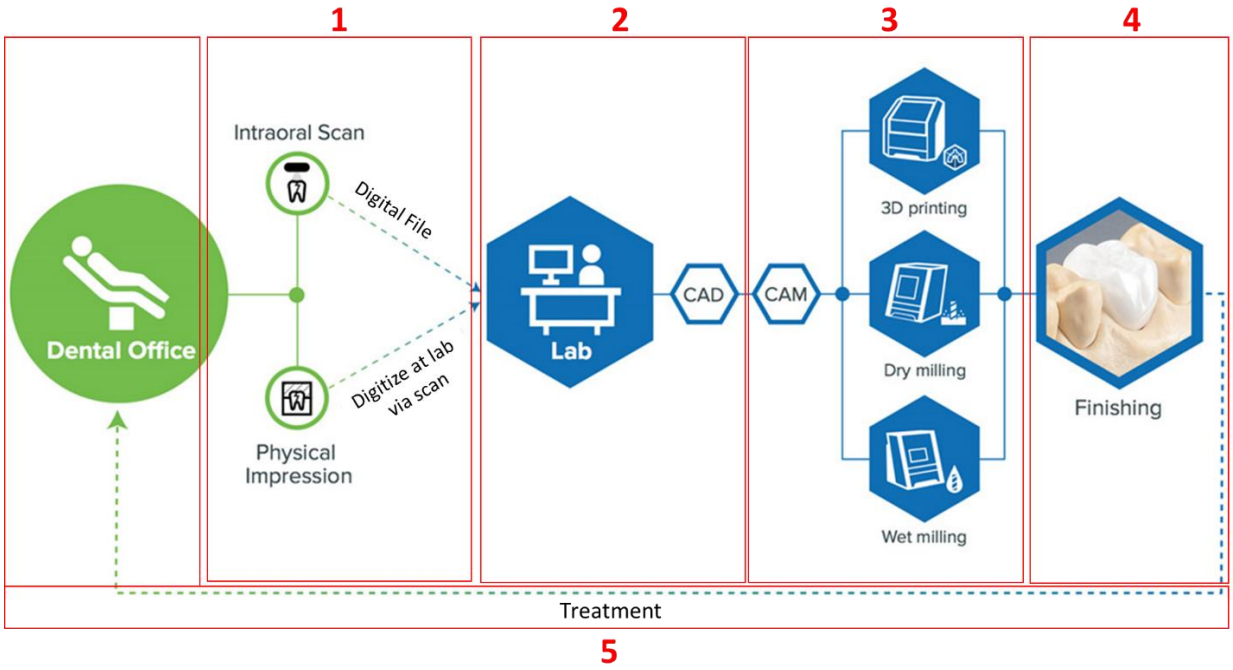

Figure 1. Digital workflow in dentistry (Modified from Roland 2020).

Figure 1 presents how the workflow goes in dentistry. In phase 1, the scanning is done by the dentist at the office. After scanning, the digital file is sent to the dental laboratory where the design and manufacturing is done by the dental technicians. In phase 2 the design is done with the dental design software. In phase 3, the manufacturing is done either by milling or 3D printing. 3D printers used in dental applications are usually resin 3D printers. Resin 3D printer is a printer which cures liquid polymer with the help of light. In phase 4, the part is post processed and finished, for example via polishing. Phase 5 contains treatment of the patient at the dentist office. However, the whole workflow could be done also inside one office, if there are dental technicians. (Roland 2020.)

Planmeca is a well-known brand all over the world among the dentistry. Planmeca Group is a Finnish family owned company operating in the health care technology business. The Group consists of six companies and the Planmeca Oy as a parent company forms the core of the Group's business activities, which is high technology dental equipment. Planmeca was founded in 1971 in Helsinki, Finland, by Heikki Kyöstilä and it was manufacturing dental stools and instrument cabinets. Planmeca Group is nowadays manufacturing dental units, 2D and 3D imaging devices, CAD/CAM products, and software solutions. Planmeca is able to cover every step with all these products, in digital work flow path. One of the most important innovations has been Planmeca Romexis which was the first dental software to combine the whole work flow into same platform. Planmeca Group employs approximately. 2800 people worldwide and approximately 1000 of them work in Finland. The turnover of the group in 2019 was 745.7 million euro and equity ratio were 78.3 percentage. (Planmeca 2019; Taloussanomat 2019.)

This thesis was executed in co-operation with Research Group of Laser Materials Processing and Additive Manufacturing of LUT University (Lappeenranta, Finland) and Planmeca Oy (Helsinki, Finland).

1.1 Goals and methods

The goal of this thesis was to determine a standardized, documented, repeatable and traceable procedure for parameter optimization process so that the same process can be repeated with needed dental 3D printing materials. In this context, repeatable means that the procedure can be repeated with similar way every time and traceable means that the process

has numerical values which helps Planmeca with the predictability of the material releases. Standardized means that there is certain protocol how the tests are executed and how they are documented. This is why the main research question is:

- What are the steps for successful parameter optimization process for Planmeca?

The sub-questions, which are supporting the main research question, are:

1. Which parameters are the most important ones in resin 3D printing?
2. Which parameters are the critical ones in Creo C5 printer?
3. What kind of optimization processes are used among other studies for 3D printing parameter optimization?

These questions are answered in this thesis. The research questions lead to research problem which is also solved in this thesis. The research problem is: “There are only three different materials at the markets for Creo C5, because efficient parameter optimization process does not exist”. In this context, efficient means process that is well explained and has certain clear steps so that everyone who is aware of resin 3D printing can execute the plan. Every step has clear meaning and the plan will be followed, no modifies of test matrix in between. The documentation is a critical part of the process, everything has to be documented. Documentation should include the information about the time used for every step, so that the document can be used as a tool in decision making.

At the moment, the standardization at dental 3D printing field is coming way behind that the technology is developing. Therefore, the end users (in this case the dentists and dental technicians) have a lot of possibilities to execute the manufacturing process. This has led to usage of unstandardized manufacturing processes, which is not good. There is no standardized process established, how dental 3D prints should be manufactured. This means that the end user can print, wash and post cure, for example surgical guide, with any device and material from any material manufacturer. That is why now it is highly important to have wide range of suitable materials for the Creo C5 printer to stay in the business, which drives the need of efficient process for parameter optimization. On the other hand, it is assumed that in the future the standard will determine the whole process flow, so that there has to be a certain printer, certain material, certain washer and certain post curing device, with right parameters in order to get acceptable printed applications that can be used in dental

healthcare especially intraorally. Creo C5 is aiming to that solution with the technical solutions that have designed into the printer.

Literature review is executed to find basic knowledge of vat photopolymerization process in general and especially about 3D printing processes that are curing the whole layer at once. The goal of the literature review is to find a concrete examples of different parameter optimization processes and how the optimization process is validated. It is also important to find out, which parameters are the most critical ones and how are they affecting to the printing quality and what is printing quality.

In experimental part, the goal is to utilize the key findings from the literature review in order to create a clear and efficient parameter optimization process. The experimental part is executed at 3D printing laboratory of Planmeca in Helsinki, Finland and Creo C5 is used as a printer.

1.2 Limitations of the thesis

The literature review is focusing only in references considering vat photopolymerization and especially digital light processing (DLP) technology as a manufacturing technology. References considering about 3D printing in dental applications are examined. Design of experiment (DOE) process in 3D printing is researched.

Only references published after 2009 are accepted but main aim is to concentrate in references which are published after or at the year of 2017. This is done because the 3D printing industry is developing rapidly, and knowledge is expiring rapidly as well. Only few exceptions are allowed, these references are considering about basic physics or methods that are not changed during the years. LUT Finna is used in order to search information from different databases like Science Direct, Scopus and Springer. Also Google Scholar, Google and ResearchGate were used when references were searched. The key words used in literature research were: vat photopolymerization, resin 3D printing, 3D printing in dental applications, digital light processing, parameter optimization for resin 3D printing and parameter optimization in 3D printing. The amount of publications among resin 3D printing has increased enormously during last seven years, as shown in figure 2. (Scopus 2020a.)

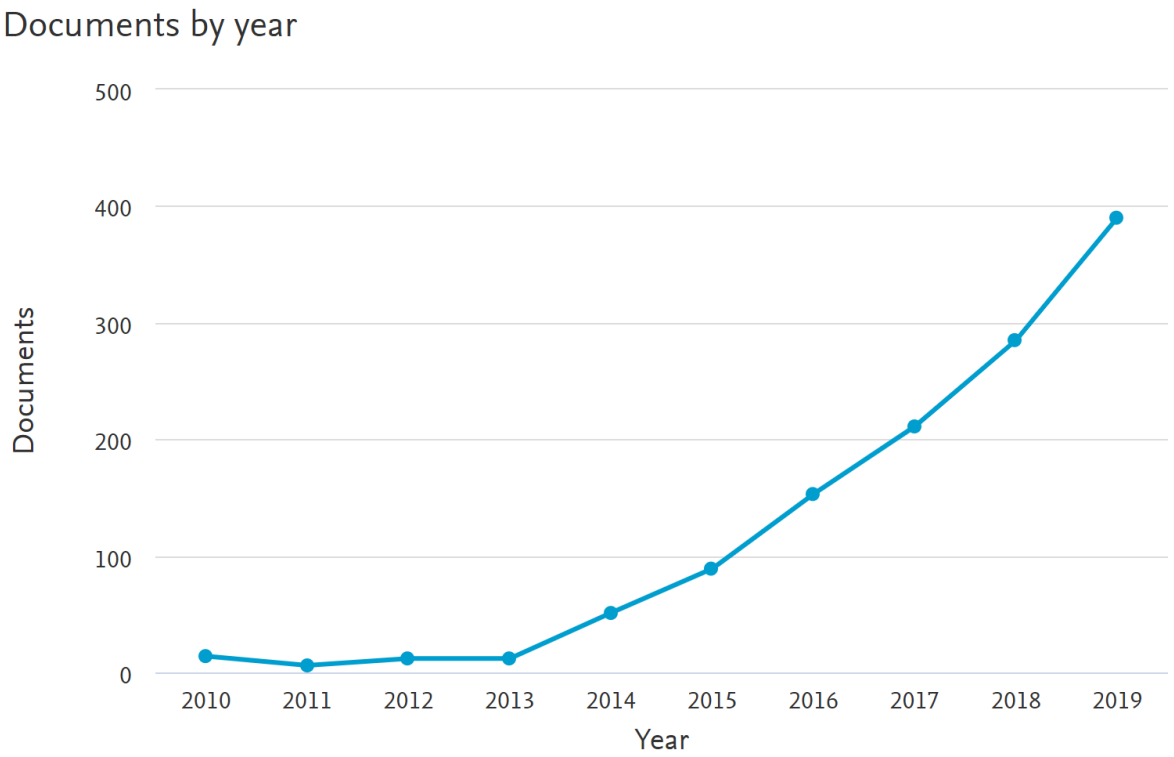

Figure 2. Number of publications per year when resin 3D printing was searched (Scopus 2020a).

Figure 2 shows that there is huge increase in scientific publications published during last seven years. Altogether there are 1317 publications (3.2.2020) considering this topic and 1235 of them have been published after year 2013. It is possible that the same trend will continue during year 2020. (Scopus 2020a.) Figure 3 shows how amount of publications considering 3D printing in dental applications has increased.

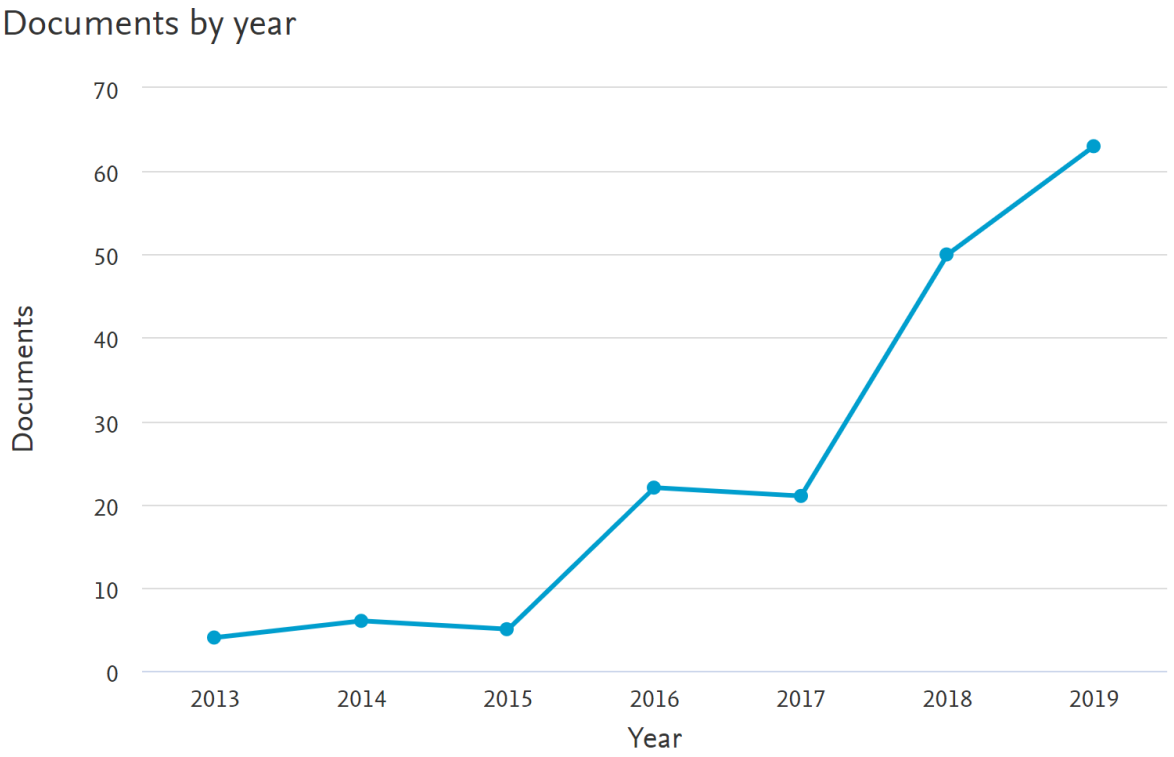

Figure 3. Amount of publications per year when 3D printing in dental applications was used as keyword (Scopus 2020b).

As it can be seen from the figure 3, the amount of scientific publications has increased rapidly after year 2015. Altogether there were 180 documents published so far (3.2.2020) and 167 of them have been published after year 2015. It might be that 3D printing in dental applications will continue to grow as a topic of publications if the trend continues to be the same. (Scopus 2020b.)

Experimental part is limited to consider only one material when the parameter optimization process is tested. Second material is used to test if the created process is possible to repeat with concrete results. Other critical limitation of the thesis is that the material and machine parameters are not variated in order to keep the procedure as simple as possible. But also, that the amount of experiments can be restricted to be reasonable. It is known that these parameters are also affecting to the printing quality, but with these limitations the amount of experiments can be kept controllable. In the experimental part Planmeca test plate and two cubes were used as a test print part.

2 3D PRINTING IN DENTAL APPLICATIONS

This section concentrates only in dental applications made by vat photopolymerization technique, although there are also many dental applications in the field of metal additive manufacturing. When digital manufacturing processes are becoming more common, it means that the whole workflow in dentistry is moving towards totally digital workflow. Digital impression of teeth is used to create a 3D model instead of traditional manual impression with impression trays. The whole planning can be done digitally with the 3D model. Model of the mouth can be printed (if necessary), and the planned operation can be checked before the treatment to get the dental care done by one time. Many of the cases can be executed during one visit. However, if the treatment includes difficult operations, several visits are required. The digital impression is done via intraoral scanners, shown in figure 4. (All3DP 2019; Lättemaa 2020; 3Dnatives 2018.)

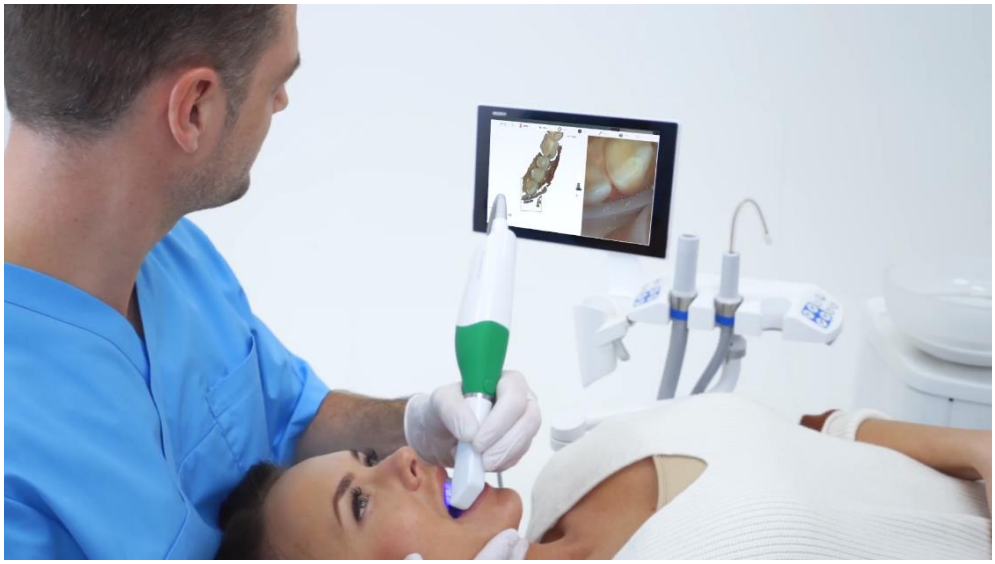

Figure 4. Dentist scanning patient's teeth with intraoral scanner which creates the digital file of the patient's teeth that can be modified later (Planmeca 2020).

As figure 4 shows, the dentist is scanning the teeth of patient with intraoral scanner. After scanning the treatment planning and modelling can be done digitally. There are few major areas of applications in dentistry which are utilizing 3D printing, the most common ones are night guards and aligners. Night guards are shown in figure 5. (All3DP 2019; Lättemaa 2020.)

Figure 5. 3D printed night guard places on top of the teeth (All3DP 2019).

As shown in figure 5, night guards are placed on top of the teeth over night to prevent attrition of the teeth during night. Aligners are used as alternative for orthodontics, instead of conventional braces. Aligners are not yet printed, but the model of the teeth is printed and the aligner itself is then thermoformed on top of the model. This creates the fact that both applications need to be accurate. Accuracy applies also to surgical guides which is one popular application of dental 3D printing. (All3DP 2019; Lättemaa 2020.)

When oral surgeries need to be done, they have to be very precise. The 3D printed guide is designed to fit perfectly on top of the teeth, and it is really important tool for dentist during the surgery. The guide looks similar to aligner, but it has accurate holes exact where the implant is placed, see the figure 6. (All3DP 2019; Lättemaa 2020.)

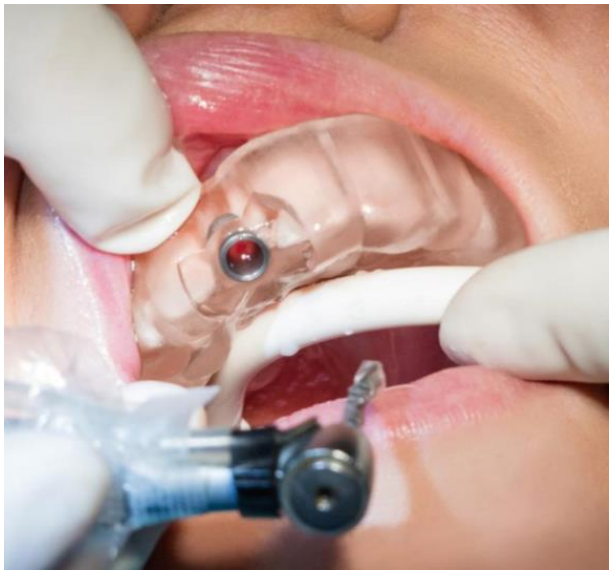

Figure 6. Surgical guide used in surgery (Formlabs 2019b).

The surgical guides are designed based on the anatomical data from the intraoral scanner with high accuracy and data from cone beam computed tomography (CBCT). CBCT imaging is necessary for dentist for example to know the position of the jawbone. After planning the guide and whole surgery, the guide is printed. The placement of guide during the surgery is guaranteed as printed guide fits perfectly to teeth of patient and the risks of surgical complications are decreased and clinical results improved. (All3DP 2019; Lättemaa 2020.)

Model of the teeth and jaw in dentistry are often printed beforehand and the fitting for example of the aligner, night guard, guide or crown can be checked and ensured that they will fit well. Figure 7 illustrates printed teeth model (in beige color) and surgical guide fitted on top of one of these models. The fitting is a critical phase of patient care, since then the appointment times can be reduced to minimum, and it is cheaper for customer and the dentist can have maximum utilization rate for reception. (All3DP 2019; Lättemaa 2020.)

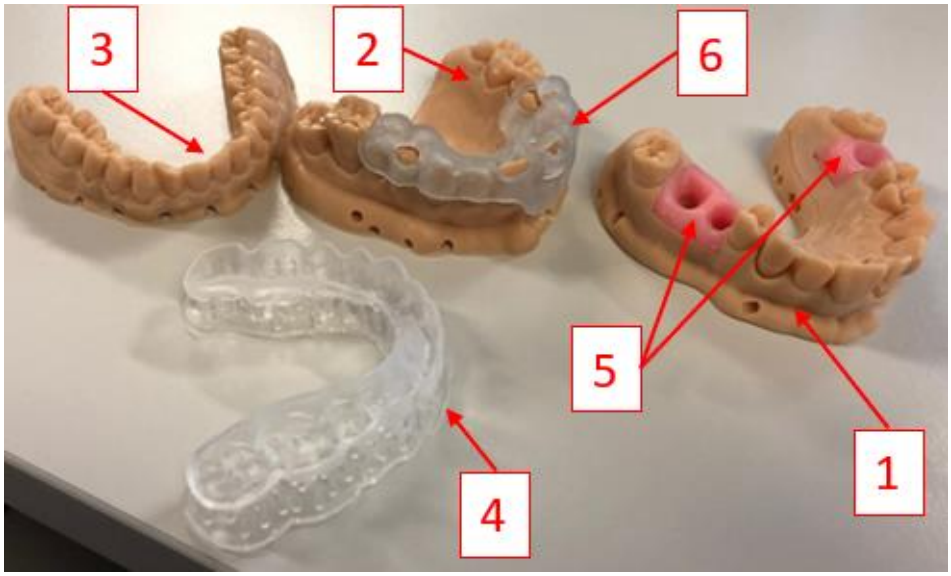

Figure 7. Teeth models (1, 2 &3) printed and surgical guide (6) fitted on top of model, also tissues (5) and aligner (4).

Figure 7 introduces two upper jaw models, (numbers 1 and 2). Two pink tissues (figure 7, number 5) are fitted into model to demonstrate gum. A surgical guide (figure 7, number 6) is placed on top of the upper jaw model (figure 7, number 2) and lower jaw model (figure 7, number 3) is also printed. In front of lower jaw there is printed aligner (figure 7, number 4) which is still attached unremoved supports and base.

3 VAT PHOTOPOLYMERIZATION

The additive manufacturing processes can be divided in seven different categories. The categories can be seen in the figure 8. This thesis concentrates only into vat photopolymerization as it is the most used technology among dental 3D printing and Creo C5 is using this technology. (Davoudinejad et al. 2018, p. 98; EN ISO 17296-2 2016, pp. 7–12; EN ISO/ASTM 52900 2017, p. 19.)

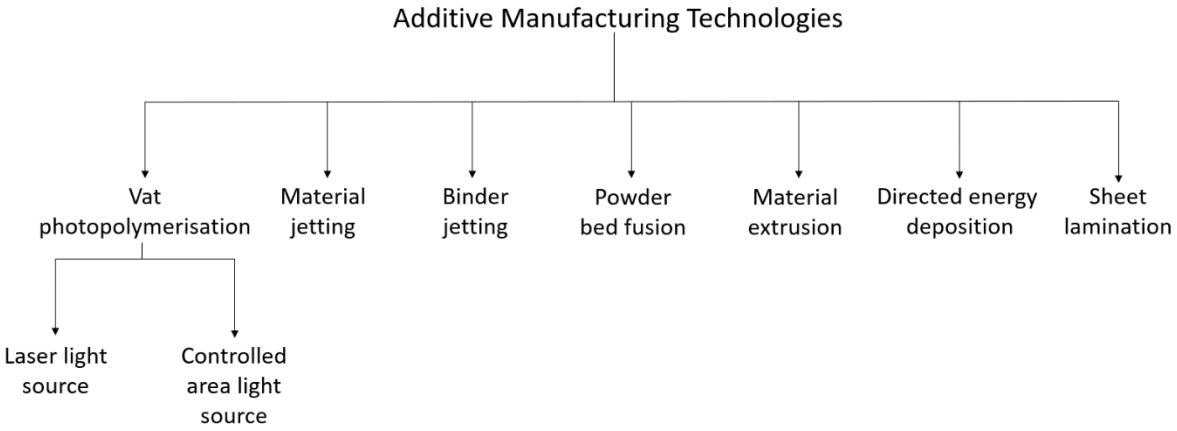

Figure 8. Existing process categories of the AM processes (Modified from EN ISO 17296-2 2016, pp. 7–12; EN ISO/ASTM 52900 2017, p. 19).

As it can be seen from the figure 8, additive manufacturing is divided into seven main process categories. These are vat photopolymerization, material jetting, binder jetting, powder bed fusion, material extrusion, direct energy deposition and sheet lamination. Furthermore, six out of seven process categories can be applied for polymers. These six process categories are vat photopolymerization, material jetting, binder jetting, powder bed fusion, material extrusion and sheet lamination. Vat photopolymerization technology is based on curing the light reactive liquid polymer layer by layer, with the help of light. This light very often is ultraviolet (UV) light. Light actives the polymerization reaction which creates the solid layer and further after layerwise fabrication the solid part. (Davoudinejad et al. 2018, p. 99; EN ISO 17296-2 2016, pp. 7–12; EN ISO/ASTM 52900 2017, p. 19; Taormina et al. 2018, pp. 151–153.)

It can be also observed from figure 8, that vat photopolymerization is dived into two different subprocesses: 1) vat photopolymerization by laser light source, stereolithography (SLA), and 2) vat photolymerization by controlled area light source, for example digital light processing (DLP). These technologies are using UV light to start the polymerization reaction. The difference is that SLA is utilizing focused laser beam which scans the whole layer while DLP is utilizing light (created mainly by projector) which exposes the whole layer at once. This makes DLP faster process, since it selectively cures the whole resin layer at once. Figure 9 shows principle of SLA technique. (Davoudinejad et al. 2018, p. 99; EN ISO 17296-2 2016, pp. 7–12; EN ISO/ASTM 52900 2017, p. 19; Formlabs 2019a; Taormina et al. 2018, pp. 152–153; Wang et al. 2017, p. 156–157.)

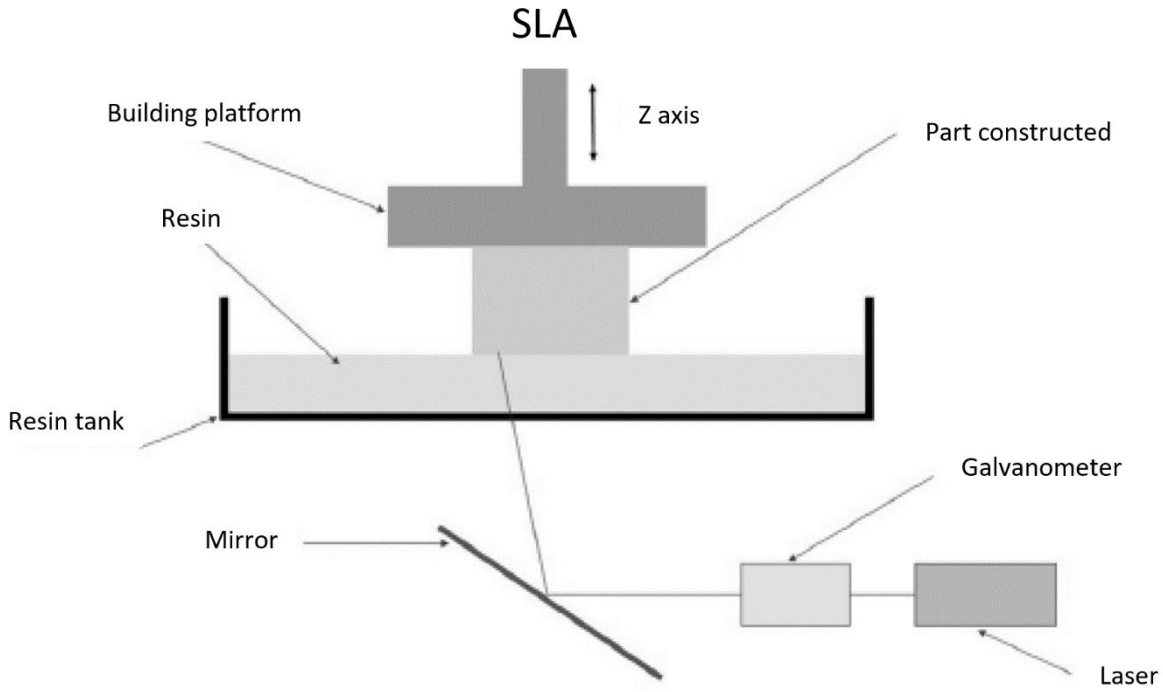

Figure 9. The principle of SLA technique (Taormina et al. 2018, p. 152).

As it can be seen from figure 9, the laser beam scans the whole layer with the help of moving mirror. Since the wavelength of used laser is in wavelength area of UV light, it cures the resin. Resin is in the resin tank and building platform is lifted upwards the height of one layer, after laser has scanned the whole area. Usually the layer height is between 50-200 microns, which determinates the resolution of z-axis. The size of the laser spot size and increments of the laser control determine the resolution in xy-plane. (Stansbury & Idacavage 2016, pp. 54–57; Formlabs 2019a.)

DLP technique uses digital light projector to create the light and digital micromirror device (DMD) to create the picture of the layer and reflect it to the resin, as shown in the figure 10. (Davoudinejad et al. 2018, p. 99; Formlabs 2019a; Taormina et al. 2018, pp. 152-153; Wang et al. 2017, p. 156–157.)

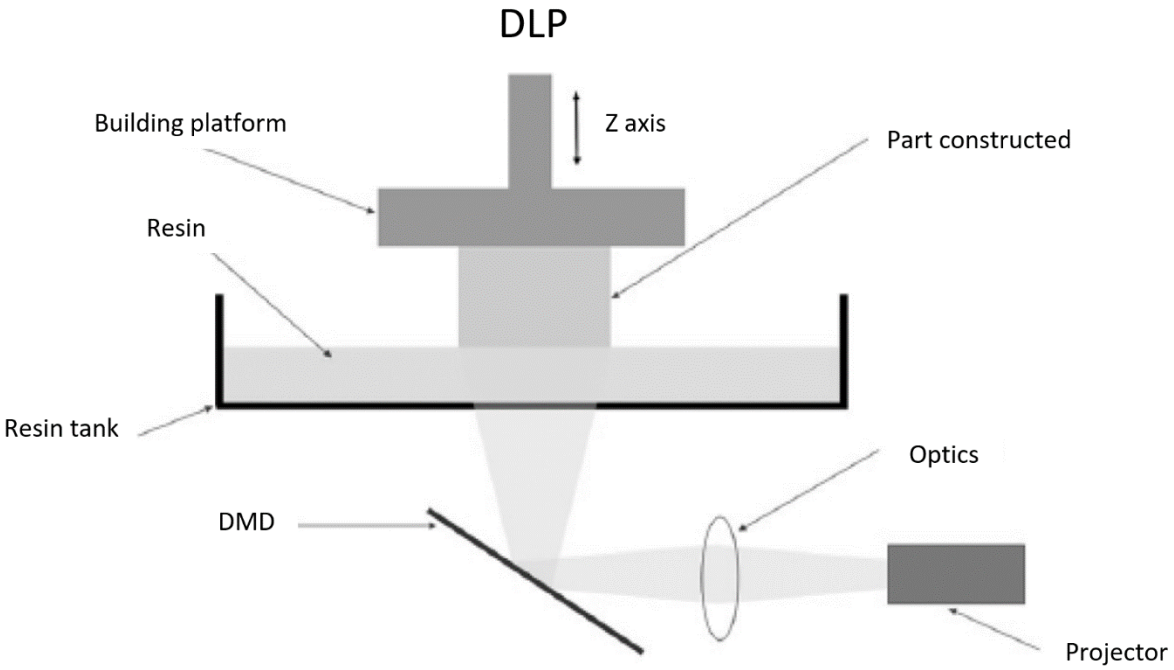

Figure 10. The principle of DLP technique (Taormina et al. 2018, p. 152).

Figure 10 shows basic principle of DLP. Projector flashes the light and the DMD creates the photo of the layer, by reflecting the desired area of the light to the resin. In between every layer the building platform is raised by the amount of layer height. The resolution of DLP process in xy-plane is dependent of the pixels. In the case of DLP, pixel corresponds to small mirrors at the digital micromirror device. The z-axis resolution is dependent on layer height. (All3DP 2018; Formlabs 2019a; Kickstarter 2019; Liqcreate 2019; Taormina et al. 2018, p. 151–154.)

The other similar and relatively new process to DLP process is utilizing LED matrix to produce the UV light. And instead of DMD technique, it uses liquid crystal display (LCD) to create the image which is exposed to the resin. This technique can be also called mask stereolithography (MSLA) or more commonly LCD based 3D printing. This technique belongs to subprocess of vat photopolymerization by controlled area light source. Figure 11

illustrates the basic components and basic idea of LCD based 3D printer. (All3DP 2018; EN ISO 17296-2 2016, pp. 7–12; Formlabs 2019a; Kickstarter 2019; Liqcreate 2019.)

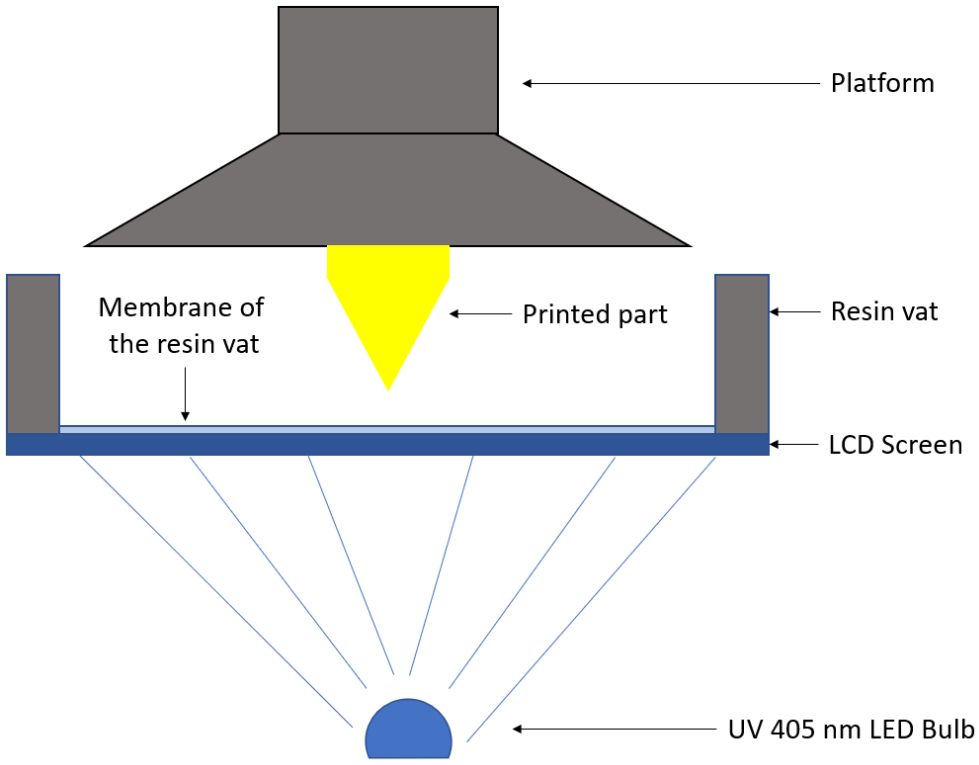

Figure 11. The principle of LCD based 3D printer (Modified from 3DERS 2016).

As it can be seen from the figure 11, the main components in the LCD based 3D printer are the light source, LED, and the LCD screen. The light source can be also a LED matrix and optical collimator can be used to achieve collimated light to the LCD and resin. The membrane of the resin vat is transparent membrane which allows UV light to transmit without affecting the light beams. (All3DP 2018; Kickstarter 2019; Liqcreate 2019.) Within this thesis literature research, it was not found scientific research done considering about LCD based 3D printing, therefore some commercial references were used to clarify the technique.

3.1 Standardized terminology in polymer 3D printing

Standard SFS-EN ISO/ASTM 52900:2017 determines the differences between single-step and multi-step additive manufacturing processes. ISO/ASTM 52900:2017 standard is a terminology standard. Vat photopolymerization is described as a single-step process, if the final part does not require curing. However, there is almost always a need for curing to

achieve desired mechanical properties of final part and to ensure that the part is fully polymerized. Therefore, it has to be considered as a multi-step process. The support removal and cleaning of the part is included into definition of single-step process. Figure 12 shows how the multi-step process is determined. (SFS-EN ISO/ASTM 52900 2017, pp. 6–20.)

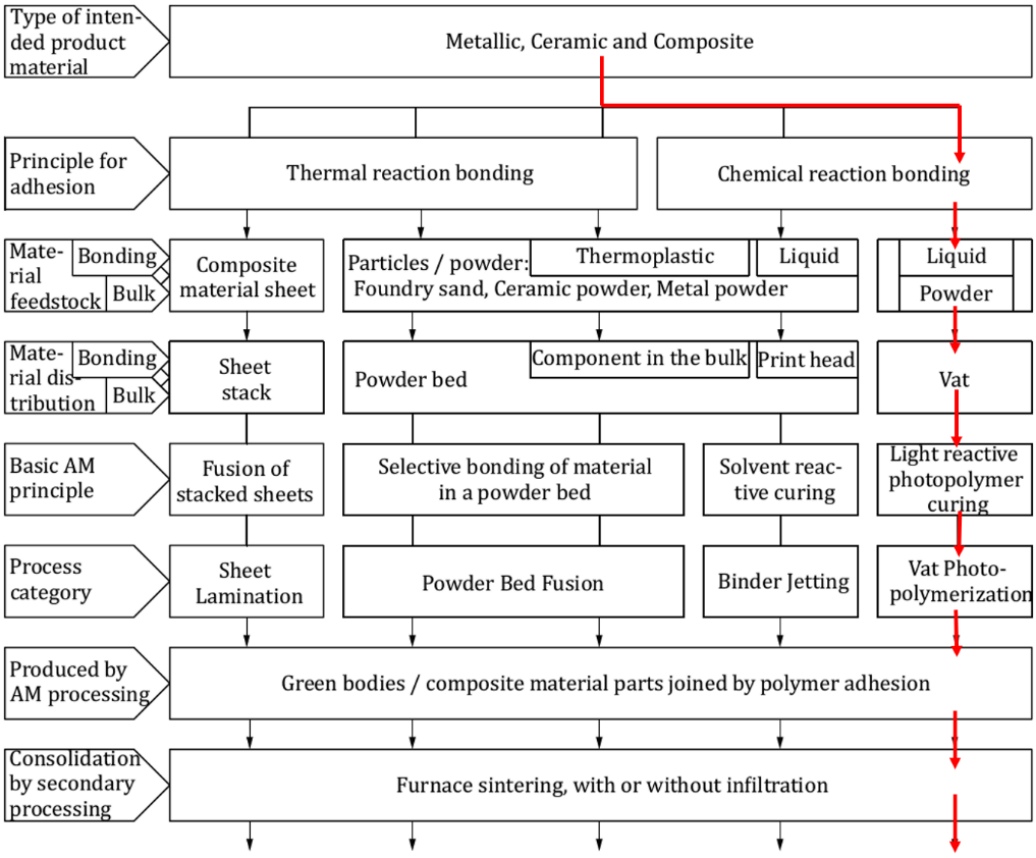

Figure 12. The determination of multi-step process (Modified from SFS-EN ISO/ASTM 52900 2017, p 20).

It can be noticed from the figure 12 that polymers are not mentioned in material box, but the same path (marked with red arrows) is valid for the polymer printing as well. The defining factor for multi-step process is that if some post processing is needed to achieve desired mechanical properties for the part. For example, the key thing in vat photopolymerization to achieve desired mechanical properties is curing of final part. While in single step process (see figure 13) the curing can be left out. (EN ISO/ASTM 52900 2017, pp. 6–20.)

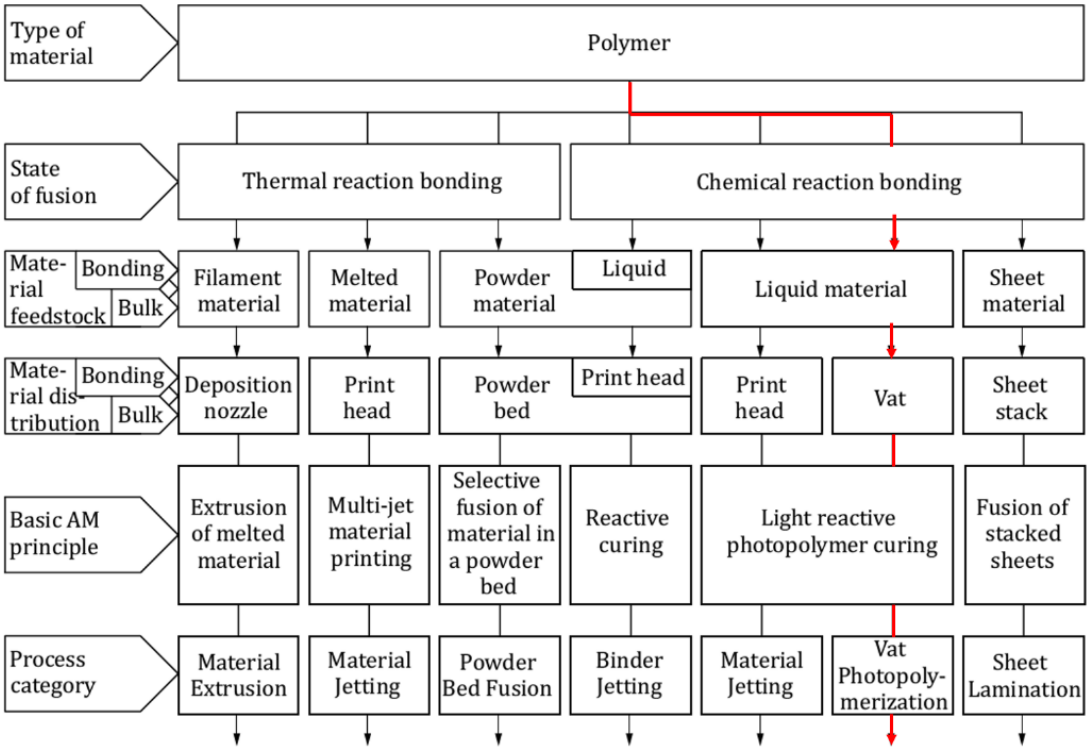

Figure 13. The determination of single-step process (Modified from SFS-EN ISO/ASTM 52900 2017, p 19).

As it can be seen from the figure 13, there is no step for post processing. The path ends in vat photopolymerization, otherwise the steps are the same as in multi-step process. If two completely different work stages are needed to achieve desired properties, it has to be considered as multi-step process. (EN ISO/ASTM 52900 2017, pp. 6–20.) The standard EN ISO/ASTM 52900 is not further explained in this thesis since it is not the main part of the thesis. However, it is necessary to be aware of this standard when additive manufacturing or 3D printing is discussed.

3.2 Print quality in vat photopolymerization

Printing quality plays an important role when prints are evaluated or when printer itself is evaluated. Therefor printing quality should be determined according the application and quality need of this application. Printing quality in vat photopolymerization is often determined in three different ways; visual evaluation, dimensional accuracy and surface roughness. Sometimes mechanical properties of printed part are the most important when defining quality and then other methods are disregarded. (Formlabs 2020.)

No accurate determination for printing quality in vat photopolymerization was found when literature review was carried out. Due to that, it was concentrated into methods that are used to evaluate the printing quality in different researches. It was found that surface roughness is often used as a measurement for printing quality. Surface roughness is often used since it has numerical value, which is easily comparable. For example, Davoudinejad, Pedersen, & Tosello (2017), Fiorenza et al. (2018), Osman et al. (2017) and Arnold et al. (2019) were using surface roughness as an evaluation factor for printing quality. All of these authors were comparing in their studies printed objects according to different surface roughness values. Davoudinejad et al. (2017) also reminds that the printing quality is a sum of the whole process chain from the part designing until the post curing. And all the phases of the process should be optimized in order to get good printing resolution.

4 PARAMETERS IN VAT PHOTOPOLYMERIZATION

Generally, there are considerably large number of parameters among all the additive manufacturing processes affecting the result of the printing. These parameters can be classified in several ways. The classification is done in order to easier the controllability of the sets of parameters. Table 1 shows how Stavropoulos & Foteinopoulos (2018) made the classification for vat photopolymerization according to findings of other studies; how parameters can be classified according the key performance indicator (KPI) studied.

Table 1. Classification of the process parameters of vat photopolymerization according the key performance indicator (KPI) (Modified from Stavropoulos & Foteinopoulos 2018, p. 4).

KPI	**Process parameter** (Variable)
Strain	Temperature
Part shrinkage	Thermal compensation, amorphous / crystalline polymer, mould material, cooling conditions
Deformation compensation	
Dimensional Accuracy	Layer thickness, part position on the platform, shrinkage compensation, retraction, hatch spacing, alternate hatching, blade gap, stagger weave
Cure depth	Penetration depth of UV radiation, scattering coefficient
Etching, deposition, lithography mechanics	Surface type, material, shape
Tool Strength, ejection forces, decision about the quality of a tool according to the previous two	
Separation force	Pulling-up speed, others
Strength of parts	Layer thickness, orientation, hatch spacing
Tensile, flexural and impact strength	Layer thickness, orientation, hatch spacing
Part strength (tensile, impact, flexural)	Layer thickness, post-curing and orientation

Table 1 continues. Classification of the process parameters of vat photopolymerization according the key performance indicator (KPI) (Modified from Stavropoulos & Foteinopoulos 2018, p. 4).

KPI	**Process parameter** (Variable)
Tensile strength, crystallographic orientation-density analysis	Layer thickness, orientation, hatch spacing
Energy distribution of a single pixel	Different types of stereolithography processes

Parameters are classified in table 1 according to their effect on the one or few final characteristics of the printed product. Stavropoulos & Foteinopoulos (2018) made this classification based on the results of the studies they found. It was separated the KPI factors and affecting parameters from the found studies, and then listed these findings. Another way to classify the parameters is presented in figure 14.

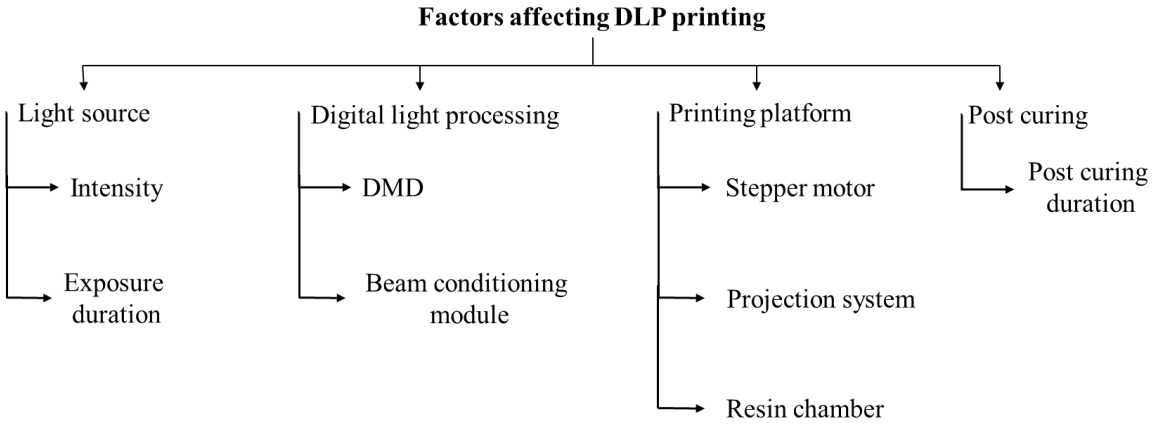

Figure 14. Parameters affecting to DLP print process (Modified from Waheed et al. 2016, p. 2003).

As it can be seen from figure 14, Waheed et al. (2016) classified parameters according the machine functions. This kind of classification is not considering the material characteristics nor the process functions. However, Waheed et al. (2016) were determining that DLP printers can be evaluated by the characteristics of the printed object. These characteristics were surface roughness and dimensional accuracy, which are dependent on object

orientation, layer thickness, resin properties and building style. (Waheed et al. 2016, p. 2003.)

Cause and effect diagram, also known as Ishikawa diagram or fish bone diagram, of DLP, was searched from literature during this thesis, but no scientific nor commercial publications regarding Ishikawa diagram of DLP were found. Basic principle of the Ishikawa diagram is to find causes and effects of the process. One possible reason for the lack of diagrams is that there is no research done about the Ishikawa diagram and parameters in context of DLP. Other possible reason is that DLP printing is still more common in commercial processes than in scientific processes. However, there is all the time emerging new possible applications for DLP technology and furthermore research. Ishikawa diagrams for vat photopolymerization were also searched from literature in general in this thesis, to be able to find information in creating diagram for LCD based resin 3D printing process at the experimental part of the thesis. Just one article considering Ishikawa diagram of SLA was found and this Ishikawa diagram is shown in figure 15. (Martinez-Marquez et al. 2018, p. 24.)

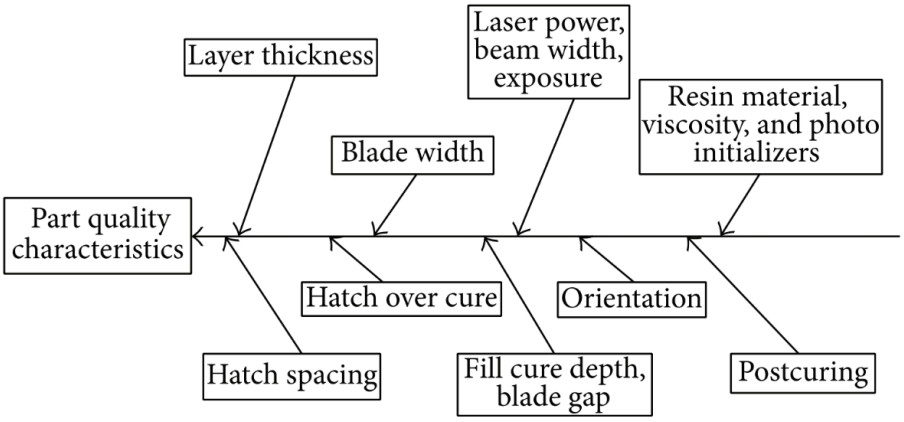

Figure 15. Cause and effect diagram of SLA process parameters (Gowda, Udayagiri & Narendra 2014, p. 3).

Figure 15 shows causes which are resulting the part quality characteristics. In case of the DLP, the causes mean the parameters which are affecting the quality characteristics, such as; dimensional and geometrical accuracy. Parameters are not classified in diagram into to the certain groups, they are just mentioned. The parameters (causes) considering laser can

be changed to consider UV light and irradiation parameters. Otherwise the parameters are valid for the LCD based resin 3D printing. (Gowda, Udayagiri & Narendra 2014, p. 2–3.)

In this thesis, the parameters are classified as following; machine parameters, process parameters, and material parameters. This classification is based on summary of causes of non-conformity to the quality of custom 3D printed bone implants introduced Martinez-Marquez et al. (2018). They classified the causes (parameters) into four categories: method, machine, materials and people. Method class included factors related to the design and manufacturing process. Machine class included the machine and tools used in the process. Material class consists of everything that is considering materials. People class contained the humanity factors. (Martinez-Marquez et al. 2018, pp. 28–29.)

Furthermore, the parameters with metal PBF (Powder Bed Fusion) technique at VTT (Technical Research Centre of Finland), are divided roughly in three categories: process parameters, machine and environment parameters and material parameters. Process parameters are basically the laser parameters (scanning speed, focal point size, power etc.). Machine and environmental parameters are including for example shielding gas flow, build plate (material, pre-heating) and oxygen level inside the chamber. Material parameters are including all the parameters considering material, for example shielding gas properties and particle size of the powder. (Reijonen 2020.)

It is defined in this thesis, that machine parameters include all the parameters that can be adjusted in the machine or in the machine software, for example the light intensity. Process parameters are defined to be the parameters that can be modified in the CAD and slicer software (software that creates the slices of the part and prepares the print file), including the part building orientation, build plate movements and support settings. Material parameters are defined to include all the issues considering materials. Based on this classification, the parameters are introduced and discussed how they are affecting to the print quality.

4.1 Machine parameters

The main components to make photopolymerization happen in right places and right time, are UV light source, UV light and LCD. The UV light is produced with the LED array which

sends UV light with certain wavelength corresponding with wavelength of need of photopolymerization reaction. Usually wavelength used is either 385 nm or 405 nm with LCD photo masked 3D printing in dental applications. (Dreve 2020; Detax 2020; DeltaMed 2020; Whip Mix. 2020.) Printing quality is also depended on the beam of UV light, how coherent the wavelength is and how perpendicular the direction of the light is when it reaches the LCD. The more perpendicular the direction of the light in relation to surface of LCD, the better the printing quality is, because then there is no diffuse radiation which could cure the resin from undesired places. Light with these kinds of properties can be achieved with different kind of optical collimators, which are not discussed in this thesis in order to maintain the limitations of the thesis. (Teng & Ke 2013, pp.21445–21447, 21455.)

According to Wang et al. (2017), the LCD photomask printer cannot reach the theoretical resolution of the pixel size of LCD because of the light diffraction. It can be concluded that LCD determines the xy-resolution mostly but in reality, the resolution is few micrometers worse than theoretical resolution of LCD screen, but it can be improved with perpendicular light beams. It has to be noted that the pixel is always square shaped, so when enough small circular shapes are printed, they become squares. xy-resolution is also determining the voxel size, which can also be considered as a factor for resolution. Voxel is a pixel size but in three dimensions. (Wang et al. 2017, pp. 156-161; Langnau 2018; Mohamed et al. 2019, pp. 1–4.)

The membrane of the resin vat and building plate movement in Z-direction (figure 11) are affecting to printing quality as well. The cured layer will attach to previous layer but also to vat membrane which creates separation forces when the build plate is lifted. If the separation forces are increasing too much, they lead to manufacturing defects, such as delamination and holes in solid printed parts. The separation forces are dependent on the pull-up speed and acceleration of build plate, material viscosity and printing geometry. The complicated thing is that all these factors are affecting to separation force differently and for example the printing geometry affect to separation forces remains widely unknown. (Pan et al. 2017, pp. 353–359; Gritsenko et al. 2017, pp. 151–152, 156.) Movements of the build plate and geometry of a part are considered as process parameters in this thesis, but they are closely connected to machine parameters. This is due to fact that material of the vat membrane can either easier or difficult the separation. Geometry is considered as a process parameter from the point of view that with the building orientation it can be affected to each layer geometry.

Other features that can be considered as machine parameters are; building area and -volume and material of the build plate. However, these are not discussed in this thesis, since these features do not have a significant effect to printing quality.

4.2 Process parameters

One of the most critical process parameters is building orientation, since it determines for example the amount of supports needed. The building orientation is determined often by part geometry, especially with the dental applications because there are often surfaces that have to be dimensionally accurate, so no support structures are allowed to attach there. Building orientation affects to dimensional accuracy so tight fittings can be ensured with optimized orientation. According to Osman, Alharbi, & Wismeijer (2017), 135 degrees build angle results the best surface quality when dental restorations are printed as shown in figure 16.

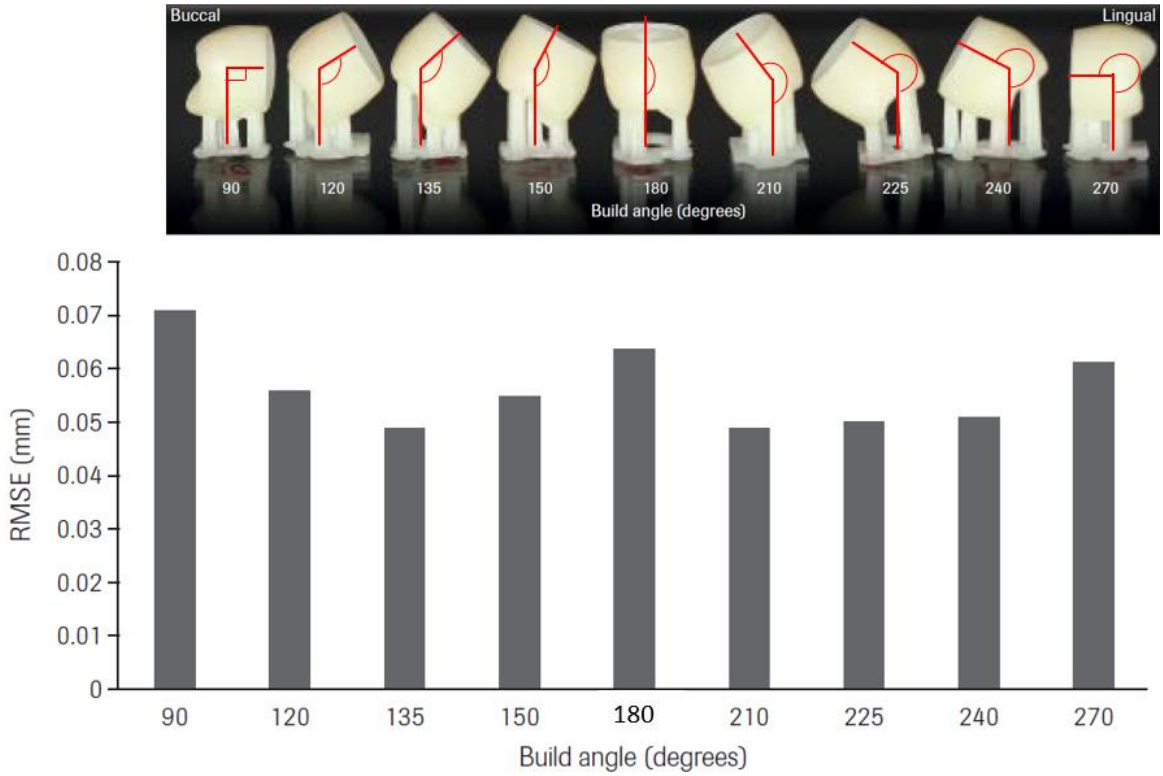

Figure 16. Variation in RMSE (root mean square deviation) of surface quality of final print as function of build angle (Modified from Osman, Alharbi, & Wismeijer 2017, p. 183, 185).

Figure 16 shows RMSE (root mean square deviation) of surface quality of final print as function of build angle. Build angle here means direction of part in relation to print direction. Build angles are illustrated into figure 16. Figure 16 illustrates that when this angle is 90

degrees, there are largest amount of variation in surface roughness i.e. this direction results worst surface quality. Same phenomena can be noted with build angle of 180 degrees and 270 degrees. Best surface quality i.e. smallest deviation in surface roughness can be achieved when build angle 135 degrees is used. This is due to fact that this angle has the most self-supporting geometry through the building process which results less overhangs. It can be concluded that build angle of 135 degrees should be preferred to achieve dimensionally accurate prints. In this case the surface quality is related to the dimensional accuracy because tight fittings are discussed. Deviation in the surface roughness of dental restorations is corresponding the degree of fitting which is considered as dimensional accuracy. (Osman, Alharbi, & Wismeijer 2017, pp. 182–187.)

Exposure time is one of the most critical parameters in DLP printing process. According to Guerra et al. (2019), layer thickness depends on resin components and composition, light intensity and exposure time. Since the resin composition and light intensity are considered as constants in this thesis, only remaining variable is exposure time. Exposure time is the time that resin is exposed under the UV light for every layer. Exposure time is a critical parameter since it determines the number of photons transferred to material to initiate the photopolymerization process. Exposure time plays key role in adhesion of the new layer to the previous one. If exposure time is too long, it overcures the layer so that the next layer will not attach to it. Too long exposure time produces overgrowth of layers which results dimensionally inaccurate prints. On the other hand, if exposure time is too short, layers will not stick together because the polymerization rate is not high enough, and the object will not build properly. Polymerization rate, in this context, means how well the resin is cured. (Ibrahim, Sa'ude & Ibrahim 2017, pp. 11–13; Guerra et al. 2019, pp. 155–156.) Ibrahim at al. (2017) showed that the physical and mechanical properties of the printed part in DLP are mainly depended on layer thickness and exposure time. It can be concluded that these two parameters are always dependent on each other because the longer exposure time there is, the deeper the curing proceeds.

For example, layer thickness has a huge effect to shape of small holes. Gong et al. (2015) researched the effect of layer thickness to the shape of flow channel. The effect is shown in figure 17.

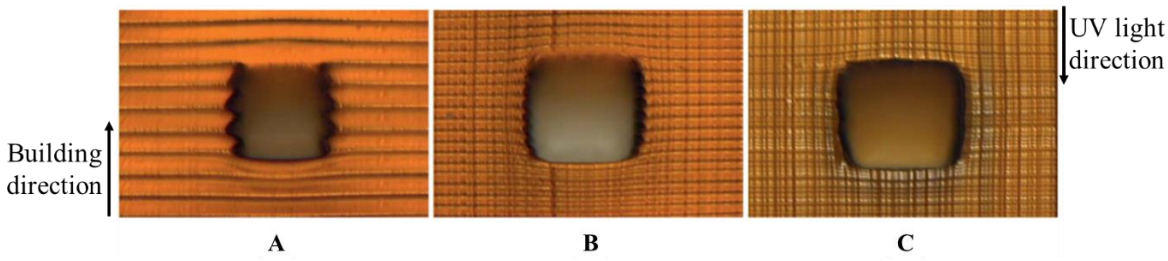

Figure 17. Effect of layer thickness to the shape of a flow channel, height of 200 µm. Layer thicknesses of A) 50 µm, B) 25 µm and C) 10 µm. (Modified from Gong et al. 2015, p. 106628.)

As it can be seen from the figure 17 A, layer thickness of 50 µm causes jutting layers into flow channel and this can be seen as saw-edged shape. According to Gong et al. (2015, pp. 106628–106629) this is due to the fact that top surface of one built layer receives larger amount of UV light than back surface of one built layer. And this causes uneven polymerization of one layer and is seen as saw-edged shape. Sometimes in case of large layer thickness and small size of a hole, hole is often overgrown. Term overgrown means here that hole is not open, or the diameter of the hole is smaller in reality than in CAD model. Figure 17 B represents the shape of hole when the layer thickness is 25 µm and as it can be noted surface is relatively smooth. Saw-edged effect can be detected here but it is not that remarkable anymore. As layer thickness of 10 µm is used (see Figure 17 C), quality of surface is better and saw-edged effect cannot be seen with visual inspection. It has to be noted, that there will be always saw-edged shape because layer by layer building mechanism, but this phenomenon can be reduced with thinner layers. (Gong et al. 2015, p. 106628–106631.)

Layers of the part are divided into three groups. Classification is done between the layers according the height of the part where the layer is located. Simplified classification is presented in figure 18.

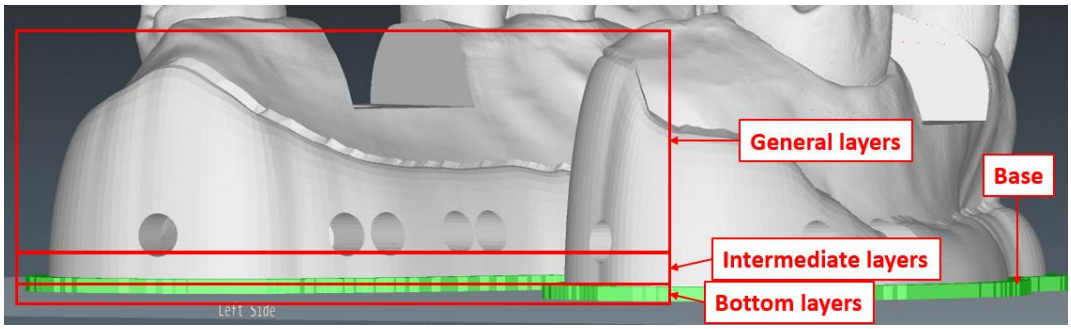

Figure 18. Simplified classification of the layers of the part.

As presented in figure 18, first layers to be printed are called bottom layers, then next ten layers are called intermediate layers and rest of the layers of the part are called general layers. First layers of the print are usually exposed longer times, approximately ten times more than following layers and the layer thickness (with the first layers) is half of the layer thickness that is used. This is done to ensure that the first layers are attached to building plate properly and to ensure that printing process will be successful. The movement of the building plate is remarkably slower in the first layers, because faster movement might damage the build process. This is why first layers can be also called bottom layers. Build plate movement is the movement that build plate is doing during the printing process. Build plate moves always in between the layers few millimeters upwards and then downwards so that the layer height is left in between the print and membrane of the resin vat. The purpose is to ensure the adhesion to each other of the first layers, since when the building plate is lifted, the first layers have to detach from the membrane of the vat carefully. The detaching has large forces applied. Depending on a slicer software, there can be used transition layers or intermediate layers and specified parameters for these, few to ten layers. Usually the parameters in transition layers or intermediate layers are the same as in other layers, but the movement of the build plate is slower. With specified parameters for the transition or intermediate layers the proper base can be ensured. Base here means the first layers that are creating the area where the rest of the part is built. (Amerlabs 2018; 3Dresyns 2020.)

Movement of the build plate is critical to ensure the success of the printing process. This build plate movement is creating the separation force of cured layer, when the new layer (with the whole part) is lifted up from the vat membrane. (Lin et al. 2018, pp. 429–430; 432.) Separation mechanism is showed in figure 19.

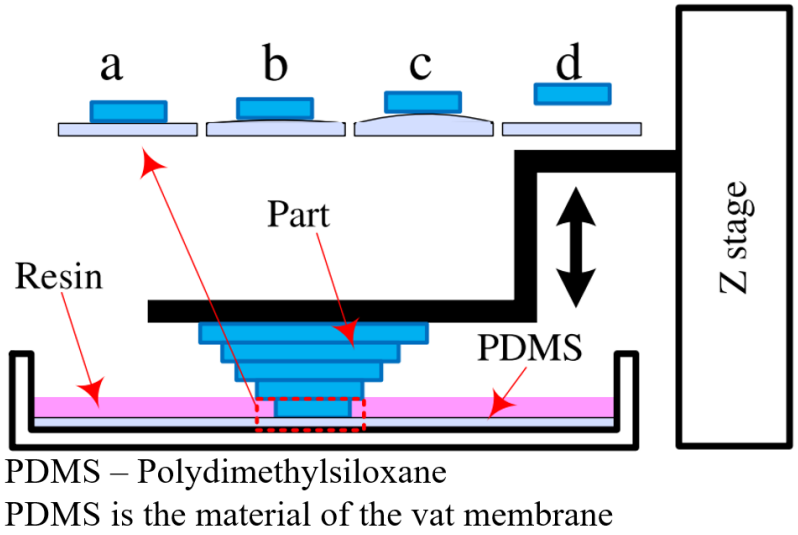

Figure 19. The separation process of part and vat membrane divided into steps a-d (Modified from Liravi, Das & Zhou 2015, p. 136).

Figure 19 shows simplified example of the separation process. At step a, the layer is cured between the part and membrane (PDMS - Polydimethylsiloxane) of the vat. In figure 19 the membrane of the vat is called by its material, PDMS (Polydimethylsiloxane) but it can be considered as any other vat membrane material. At step b, the separation process is started, and the part is started to lift upwards. At step c, the separation force increases as it can be seen from the expansion of the membrane. At step d, the separation process is finished, and the build plate can return down, and same chain is repeated. Z-stage is presenting the movement of z-axis, which is the movement of the build plate. (Liravi, Das & Zhou 2015, p. 136.)

The separation force is created by the build plate acceleration in direction of z-axis, but it is also dependent on the geometry of the previous layers. Acceleration in z-direction is always printer specific. Beside the separation force, the lifting distance have to be set high enough to ensure that the printed part will detach from the vat membrane. Since the membrane is always a bit elastic, the lifting distance has to be set so that it ensures the separation of the part from the membrane, otherwise it will result accumulating material at the bottom of the vat which is ruining the print. (Lin et al. 2018, pp. 429–430; 432.)

There is a lot of research and analysis done about separation forces, however as Pan et al. (2017, p. 354) concluded that according the previous studies there is still controversial

information about the effect of layer geometry to the separation force. Yet they found in their study (Pan et al. 2017) that the more porous the geometry is the greater the separation force is, which is due to fact that then there is larger effective separation area even though the cured layer area remains same. It can be concluded that there is complicated and partly unknown connection with layer geometry and separation force, and it should be examined more. One outcome is that the separation force cannot be controlled directly, but it can be adjusted with other parameters as build plate movements and part geometry. The build orientation of the part also affects to the separation force.

Support structures are one key thing to achieve a successful print. There were few commercial references found from the resin manufacturers, slicer software manufacturers and 3D printer manufacturers. These references were used to examine support structures as a process parameter. In this thesis supports are considered as a constant factor because the optimization of support structures would be independent topic for another study. The main idea and features of the support structures that need to be observed in resin 3D printing are discussed.

Mainly support structures are needed in bottom up resin 3D printing, when there are overhangs or bridges, the geometry is wanted to ensure at the bottom of the part and to prevent the separation forces to break weak spots at the part. Bridges and overhangs can be illustrated with letters Y, H and T, shown in the figure 20. (Amerlabs 2019; 3D Hubs 2020; Chitubox 2020.)

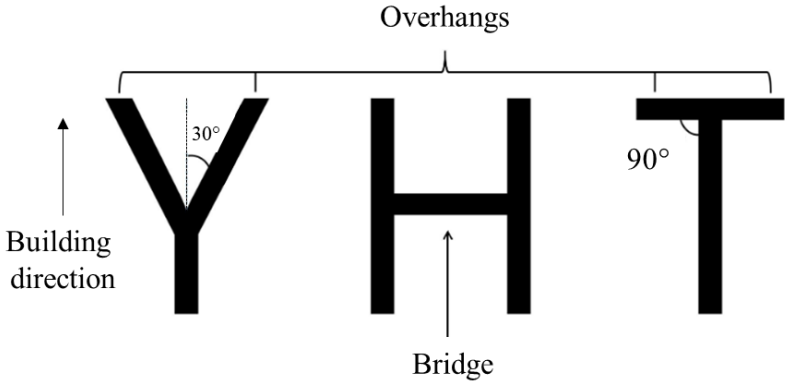

Figure 20. Overhangs and bridges illustrated, at Y-letter the 30 degree angle can be printed without support structures but at the T-letter the 90 degree angles must be supported (Modified from Chitubox 2020).

Figure 20 illustrates the overhangs and bridges. Overhangs are the areas that are literally hanging over the part structure over 45 degree angle, see letter T at the figure 20. In the figure 20 the letter Y could be printed without supports but the letter T must be supported. Bridges are geometries that are horizontally inside the structure of the part, as the connector in the letter H. When the print job is planned and sliced, it must be ensured that there are no so-called islands. (Chitubox 2020; Amerlabs 2019; 3D Hubs 2020.) Island illustrated in figure 21.

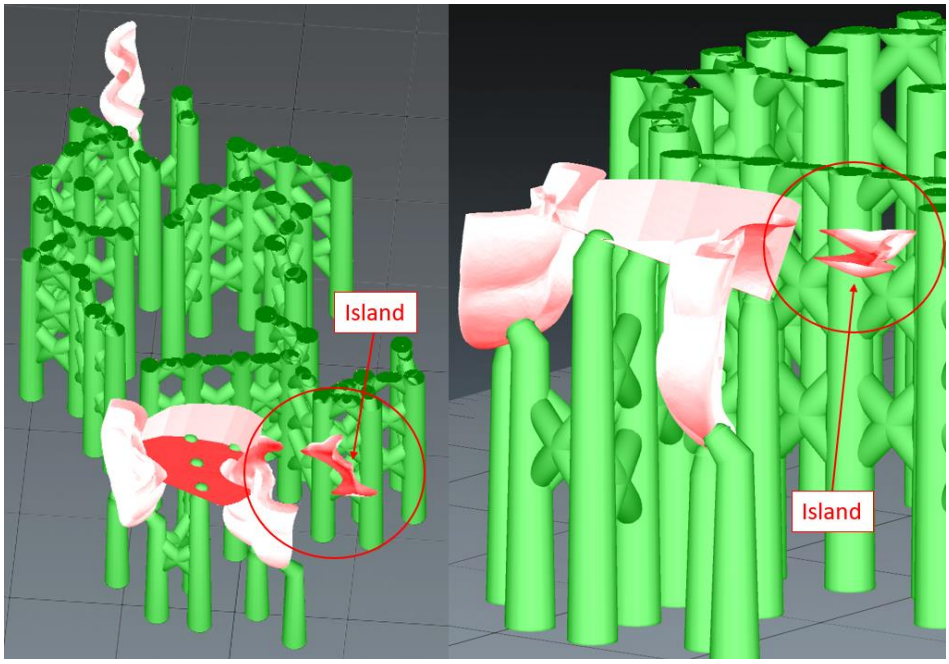

Figure 21. An example of unsupported area (island) building on top of anything.

As figure 21 represents, islands are areas that are forming out of nothing, in other words they are not connected to the part itself and they do not have support structure underneath but are just floating on top of nothing. Usually these areas are relatively small and hard to detect, but anyhow these areas have to be supported to get the print job successful. (Chitubox 2020; Amerlabs 2019; 3D Hubs 2020.)

The part cannot be placed directly on top of build plate when the detailed geometry at the bottom of the part is critical. The lifting of the part is necessary, because the first layers have longer exposure times. Longer exposure creates overgrown layers and ruins the dimensional accuracy. The density of the supports affects a lot to success rate of the print. It can be said that the more is better, because usually in polymer printing the supports are easily removable.

On the other hand, additional material is used for the supports, which creates more costs for the printed part. This results that the amount of supports should be optimized to get a best possible outcome. (Amerlabs 2019; 3D Hubs 2020; Chitubox 2020.)

4.3 Material parameters

Material parameters are discussed shortly in this thesis and only a basic idea of photopolymerization is introduced. The material has a standard composition by a third party and will not be discussed with more details.

In vat photopolymerization, the UV light starts the photopolymerization chain reaction, which forms the layer and further the actual object. Typical resin is mainly composed of monomers, oligomers, photoinitiators and photoabsorbers. The photoinitiators define the wavelength that photopolymerization reaction starts. The wavelength can be in region of the UV light (190–400 nm), visible light (400–700 nm) or infrared light, IR, (700–1000 nm). Creo C5 utilizes wavelength of 405 nm. Figure 22 presents the basic idea of the photopolymerization. (Bagheri & Jin 2019, pp. 598–599; Bertana et al. 2019, pp. 1–2, 7–11; Wu et al. 2019, p. 6153; Zhang & Xio 2018, pp. 1530–1531, 1533.)

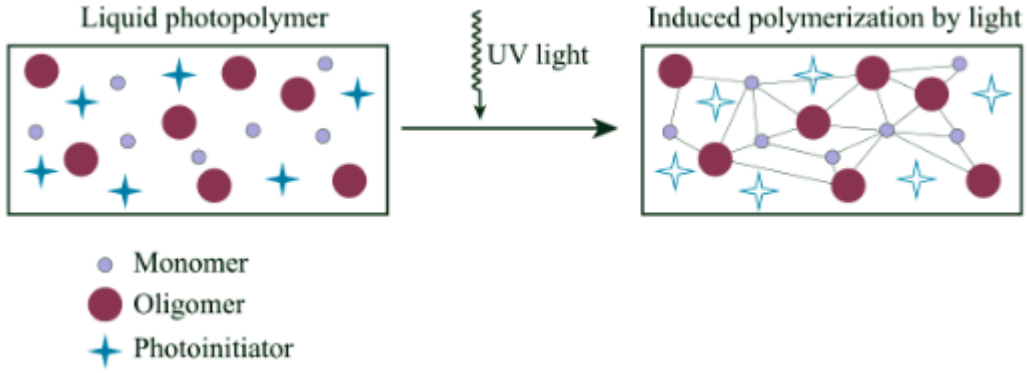

Figure 22. Schematic picture of photopolymerization (Welover 2019).

Figure 22 simplifies how UV light affects photoinitiator molecules. The photoinitiator creates radical ion when UV light reaches the resin and hits the photoinitiator. Radical ion starts the radical polymerization mechanism. Oligomers and monomers polymerize by linking into longer polymer chains during radical mechanism. As the polymer chains expand, a hardened layer is formed. Resin 3D printing utilizes mainly radical mechanism which

occurs only when polymer is exposed to UV light. Another mechanism available, is cation polymerization mechanism. The main difference between these two mechanisms is: radical mechanism occurs only when polymer is exposed to UV light while cation mechanism continues polymerization after the exposition. 3D printing resins are mainly utilizing the radical mechanism. (Bertana et al. 2019, pp. 1–2, 7–11; Sjöberg 2020; Zhang & Xio 2018, p. 1533.)

Although the resin is composed mainly of oligomers, monomers and photoinitiators, there can be added other chemicals to achieve for example some material properties. Pigment can be also added to achieve certain color for the material. But it has been noticed that dark resins have most likely lower Young's modulus since the UV light penetrates deeper with the transparent resins than dark resins. Deeper penetration allows the higher degree of curing. However, it has to be remembered that added chemicals might create problems with biocompatibility and toxicity, when dental and medical applications are discussed. Biocompatibility describes the property of the material being compatible with living tissue. Biocompatible materials do not produce immunological or toxic response when exposed to body or bodily fluids. Therefore, adding chemicals to improve material properties has to be considered carefully. (Bertana et al. 2019, pp. 1–2, 7–11; Sjöberg 2020; Zhang & Xio 2018, p. 1533.)

The resolution of z-axis is many times dependent on the resin, because the resolution is determined as a layer height which results from curing depth. Curing depth can be modified with the light absorbing additives. Absorbing additives reduce the undesired effects related to scattered light. These undesired effects include overgrown layers and dimensional inaccuracy, because of scattered light. However, in order to have a successful DLP printing process, absorption spectrum has to be matched for both the photoinitiator and absorber with the light source spectrum. Usually resins are manufactured for certain wavelength area and the printers are using the wavelengths inside or close to that area. (Gong et al. 2015, pp. 106621–106623; Lingon 2017, pp. 10217–10218.) In general, it exists many different photoinitiators that are reacting with different wavelengths. This thesis concentrates only into ones that can be used with the wavelength of 405 nm.

According Lin et al. (2020, p. 352) if the viscosity of the resin is too high, it creates voids or missing layers during printing. Sa et al. (2019 p. 3310) presented also that successful printing requires fluidity, but also rapid solidification. In order to achieve fluidity, reactive diluents can be added. These diluents are not discussed in this thesis. But it is important to understand how viscosity can have an effect to print quality. Especially in DLP 3D printing, the viscosity of the resin affects to lifting process of the built part between the layers. When viscosity is lower, it enables higher printing speeds because the resin flows faster underneath the previous layer. Parameters affecting to resin flow become more important when wide surfaces are printed. (Ho et al. 2015, pp. 3627; Tumbelston et al. 2015, pp. 1351–1352.)

One important parameter which is relating directly to the material properties but is not classified into that, is layer thickness. This parameter is also known as voxel depth. Schematic view of voxel, depth critical overcure depth, and cure depth is presented in figure 23. (Guerra et al. 2019, pp. 155–156.)

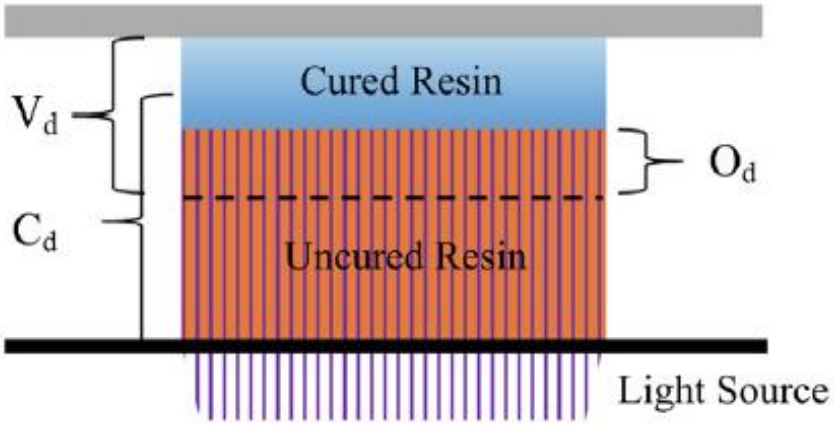

Figure 23. Photocrosslink-based 3D printing scheme, critical overcure depth (O_d) ensures the attachment of the layers. V_d is a voxel depth and C_d is a cure depth. (Guerra et al. 2019, p. 156.)

In the figure 23, V_d is a voxel depth, O_d is a critical overcure depth and C_d is a cure depth. At the macro level every layer needs to be a bit overcured, when measured geometrically not chemically, in order to attach new layer to the previous one. Previous layer should contain at least a bit uncured resin so that the new layer of resin can attach to it by photopolymerization reaction.

5 DIFFERENT PARAMETER OPTIMIZATION PROCESSES

Optimized parameter should be used to achieve printed parts with good quality. Testing and optimizing of each parameter is unreasonable amount of work. Several optimization processes are created to reduce and make the amount of optimization work more reasonable, one example is Taguchi method. These methods are not created to serve the needs of 3D printing industry but to optimize any process in order to achieve better and more stable quality.

Optimization of 3D printing process and parameters have been widely researched. Abdollahi et al. (2018, p. 2) opened the term optimization: "Optimization using statistical design of experiments algorithms can be effective when the selected search space already contains the parameters necessary to achieve good print fidelity. However, adapting these optimization methods for 3D printing of experimental materials, where prior information on the system is often unavailable, can prove difficult." However, articles dealing with optimization processes were considered as useful tools while the parameter optimization process for Planmeca was created. In this section various findings from the literature are presented to show how parameter optimization can be done in digital light processing 3D printing.

5.1 Design of experiments

Design of experiments (DOE) is an efficient and systematic part of research to understand and find connections how process and object parameters affect to final product characteristics. DOE process can be used as a tool to find specific information about importance of a specific variables and their effect in maximizing the properties of the product. The goal of the design of experiments is to provide required information of the process with the minimum amount of experiments. DOE is used among the industry since with minimum amount of experiments it is cheaper to carry out needed experiments and, in that way, to boost processes in companies. (Wanger, Mount & Giles 2014, pp. 291–293). The design of experiments process is usually divided into five steps (Wanger, Mount & Giles 2014, pp. 291):

1. define/name the problem,
2. plan the experiment,

3. execute the experiment,
4. analyze the data and
5. report the results.

This division is made to facilitate the structuring of the process and the time consumption can be tracked afterwards easier. This might be sometimes important for companies to detect and estimate the expenses for the process. (Wanger, Mount & Giles 2014, pp. 291–295.)

Among the industry, there are several different methods for process optimization. In the conventional experimental method, each parameter is studied at the time and is popularly known as fractional design of experiments or as Rao et al. (2008) determined it as OVAT "one variable at a time". With statistical method and well-planned execution, the optimization can be done by far more efficient. This method is widely known as a partial fractional design. The problem is that there are no general guidelines for any application to use a partial fractional design -method. Therefore Dr. Genichi Taguchi formed a set of general guidelines for experiments that cover many applications. (Rao et al. 2008, pp. 510–511.)

In order to understand Taguchi Method, it is necessary to know few terms and their definitions. These terms are widely used among different statistical methods as well:

- response,
- factor,
- level.

Response is a characteristic that is researched, observed or desired to improve. One or more responses can be selected, but the more there are responses the more complicated DOE process becomes. Factor is an independent (without effect directly to other factor) or influencing (has an impact to other factor when changed) and it is the one that is studied, how change of a factor affects to response. More commonly factor is known as a parameter. Amount of levels is chosen for every factor, which means that how many different values factors are receiving. In other words, how many times one parameter is variated. (Rao et al. 2008, pp. 510–512.)

According to Reijonen (2020), the key thing to succeeded DOE process is that the response and factors are determined carefully. It is recommended to choose only one main response or if more responses are required, they should have similar goal and clear order of importance to keep the process simple enough. As an example, the response is often determined as degree of density of the print at VTT (Technical Research Centre of Finland) with new materials. Other similar goal could be that the printed object has desired geometry. The print density, in metal AM, determines quite well if the new material is reasonable to print or not. Machine and environment parameters are tried to keep as constant as possible to remain the DOE process simple enough. The difficulty is that once the main parameters are detected, determined and optimized, and then some other parameter is varied – there is no knowledge does it affect and how does it affect to some of the main parameters. One critical question is how the "second class" parameters should be optimized. Second class parameter are the parameters that are not considered as important for the desired response. Deviation into main parameters and second-class parameters is necessary because there are so many parameters present that all of them cannot be included into first round test matrix. This "second-class parameter" optimization depends on, what is wanted to achieve, and that goal should be set to be in a harmony with the wanted response (for example printing quality). Reijonen remains that too optimized parameters do not allow batch-to-batch variability of materials. Which means that over-optimized parameters, in worst case, are working only with the current material batch. (Reijonen 2020.)

5.2 The Taguchi Method in 3D printing

According Namjung et al. (2019), Guerra et al. (2019) and Griffiths et al. (2016), it is recommended to use Taguchi method as a DOE in order to reduce the number of experiments in 3D printing. In order to use Taguchi method, it is necessary to carry out systematic analysis of the parameters. In this analysis, parameters and their effect to printing quality should be identified. Namjung et al. (2019, p. 162) created steps involved in DOE for their study, but those steps can be applied also in other studies to develop a constant and standardized DOE process. Steps are shown in figure 24.

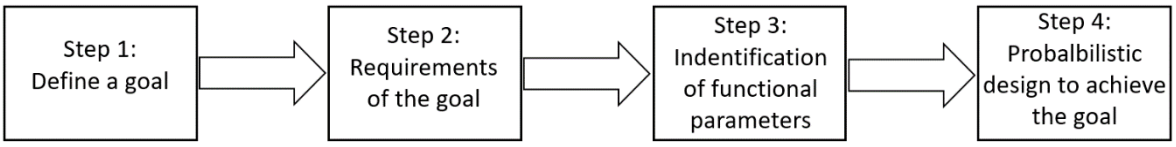

Figure 24. Steps to develop constant DOE (Modified from Namjung et al. 2019, p. 162).

As it can be observed from the figure 24, there are four steps for determining DOE. Step 1 is to define a goal, which can be for example "to create high quality 3D printed parts". Step 2 defines the concrete factor or several factors which determine how the quality is measured (response). It is important to determine measurable values for quality factors. For example, surface roughness can be determined as a quality factor and measured with the root mean squared error (RMSE). Step 3 is the most critical step, since the affecting parameters has to be identified. Step 3 may take more time than the other steps and success of the Taguchi method completely depends on identification the problem and critical parameters. All the parameters affecting to the goal (chosen in step 1) must be listed. From all the listed parameters, the most critical ones (factors) are chosen with the pre-determined criteria. Each identified parameter is set to have certain level of values (levels). Step 4 includes the formation of orthogonal array to determine the experiments. (Namjung et al. 2019, p. 162–164; Rao et al. 2008, pp. 516–519.)

Namjung et al. (2019) chose five critical parameters in order to control surface roughness. For those five parameters, they determined three levels (values). This requirement meets with the Taguchi orthogonal array $L_{27}(3^{13})$, which has five factors with three levels (The University of York, 2004). Orthogonal array is shown in table 2.

Table 2. Taguchi orthogonal array $L_{27}(3^{13})$ for the experiments where PI is photoinitiator, PA is photo-absorber and O initial oxygen concentration (Modified from Namjung et al. 2019, p. 162).

Simulation No.	Factors				
	(PI) %	(PA) %	(O) %	Layer Thickness (µm)	Curing Time (s)
1	1	0.05	10	100	2
2	1	0.05	10	100	3
3	1	0.05	10	100	4
4	1	0.1	15	80	2
5	1	0.1	15	80	3
6	1	0.1	15	80	4
7	1	0.15	21	50	2
8	1	0.15	21	50	3
9	1	0.15	21	50	4
10	2	0.05	15	50	2
11	2	0.05	15	50	3
12	2	0.05	15	50	4
13	2	0.1	21	100	2
14	2	0.1	21	100	3
15	2	0.1	21	100	4
16	2	0.15	10	80	2
17	2	0.15	10	80	3
18	2	0.15	10	80	4
19	3	0.05	21	80	2
20	3	0.05	21	80	3
21	3	0.05	21	80	4
22	3	0.1	10	50	2
23	3	0.1	10	50	3
24	3	0.1	10	50	4
25	3	0.15	15	100	2
26	3	0.15	15	100	3
27	3	0.15	15	100	4

In the table 2 PI is photoinitiator, PA is photo-absorber, O initial oxygen concentration and simulation in this case means the same as experiment. Thicker lines in table are clarifying to separate the three levels from each other. As it can be seen from the table 1, the total amount of the experiments is 27. If these five parameters (named factors in the table) with the three different levels (values of each parameter), would have tested traditionally, it would have resulted 243 (3^5) possible combinations of parameters which means 243 experiments/runs. (Rao et al. 2008, pp. 516–519; Namjung et al. 2019, p. 162–164.)

The idea of reduced amount of experiments in Taguchi method is based on a good understanding of simple and complex results of different parameters affecting the process and quality with possibly low amount of experiments. Minimum number of experiments is based on the orthogonal array properties, for example each pair of columns and each combination of levels appears equal number of times. In this way the pair-wise balancing property can be maintained, effects of the factors can be balanced and a relative value (representing the effects) can be given to effects of a level and then compared with the other levels. (Rao et al. 2008, p. 511.)

5.3 Non-scientific parameter optimization processes

Hobbyist and companies have developed several different parameters optimization processes for vat photopolymerization. These references are not considered as scientific references. However, some information of these references was found useful and were applied in the experimental part. According to Autodesk (Welover 2019), exposure time can be determined with one simple and quick test print. The main idea of this is to create one-layer print which is divided into smaller squares, see the figure 25. (Welover 2019.)

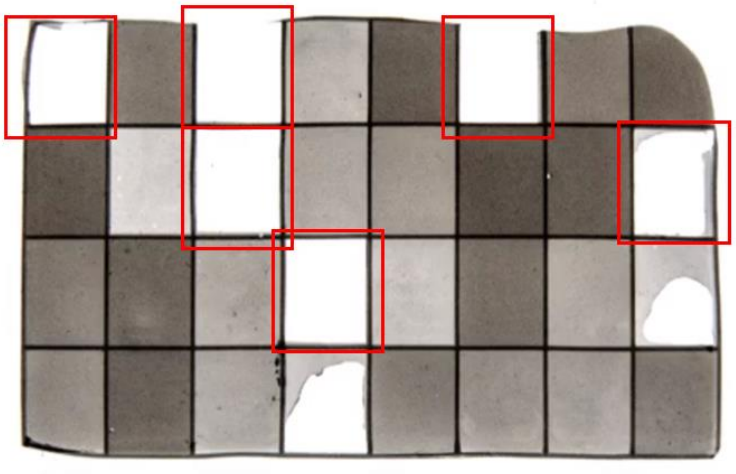

Figure 25. The test print for determining the exposure time, which has been divided into smaller squares (Modified from Welover 2019).

As figure 25 shows, the print file was created so that each square is exposed to different exposure energies. Some squares are not even cured (the totally white ones marked with additional squares). And some of the squares are darker which means that those ones are thicker. This is because squares have different thicknesses due to different exposure times.

After printing the layer thickness of each squares was measured. Exposure dose (in unit of mJ/ cm^2) can be then plotted as function of layer thickness (in unit of mm), see the figure 26.

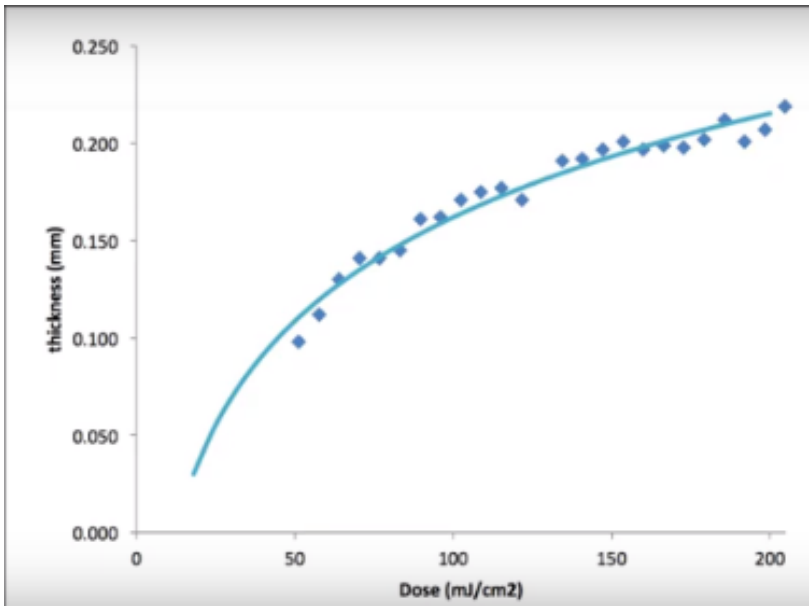

Figure 26. Exposure dose as function of layer thickness (Welover 2019).

According the curve (figure 26), exposure times (t_E) can be calculated for each layer thickness since the irradiance is known, which results a theoretical exposure time. Exposure time can be calculated (Welover 2019):

$$t_E = \frac{E_D}{E_I} \quad (1)$$

In equation 1, the E_D is an exposure dose and E_I is an irradiance. Theoretical time is discussed since the dose in real case is not uniform through the whole layer, because more light energy is bound to the resin at the bottom of the vat. Therefore, the dosage is higher at the bottom of the vat and it decreases through the layer towards previous layer interface. For example, the dose is 45 mJ/cm^2 for layer thickness of 100 micrometers (see figure 26), which results the exposure time theoretically about the 2.25 seconds. This 2.25 second is only a minimum time which the resin requires to cure the layer. Because the uneven dose through the layer, the exposure time is usually 20-40% higher. (Welover 2019.)

Another similar quick and easy way to find approximate exposure time is developed by Anycubic and is designed for Anycubic Photon -printer. The basic idea is to find indicative exposure time by printing a single print which has multiple exposure times. The printed exposure finder object is shown in figure 27. (GitHub 2020.)

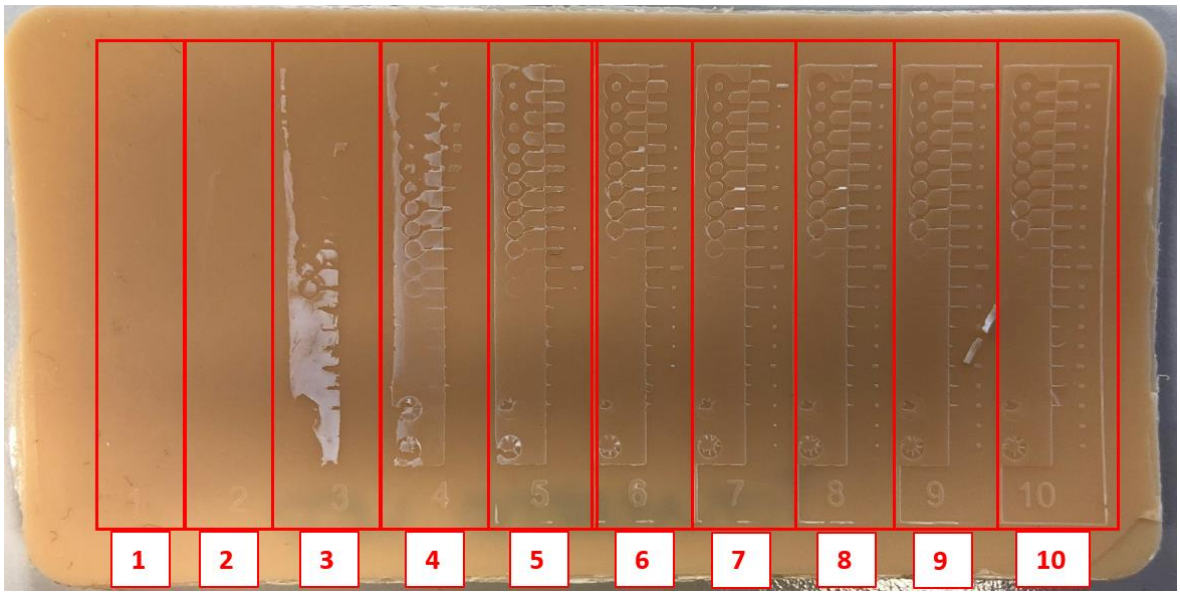

Figure 27. Anycubic Photon quick exposure time finder print printed at Planmeca with Creo C5.

From the figure 27 can be seen that there are 10 columns (from 1 to 10, marked with boxes) and each one of them has different exposure times. It can be noted that columns one and two have not even attached to the print so those can be considered as fatal failure. Columns from three to five have attached poorly. Columns from six to ten are attached properly. The right exposure time is at number seven. Each column has certain features that should be observed when the exposure time is searched. These features are shown in figure 28. (GitHub 2020.)

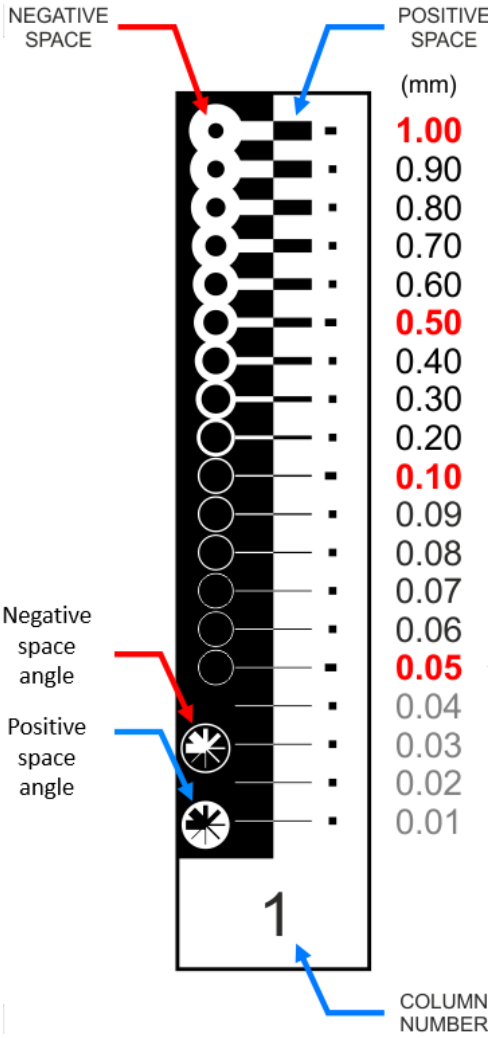

Figure 28. Exposure time finder test print features that should be observed (Modified from GitHub 2020).

As figure 28 illustrates, the geometry contains both extruded (positive space) and removed (negative space) features. The idea is to find the column that has the best print quality in both, positive and negative space. The clogging of spaces is the sing of over exposure. It can be concluded that the right exposure time is at the column with the best details. This test is also depended on the resolution of the printer, because the sizes of the negative and positive spaces are from 1 mm to 0.01 mm. For example, Anycubic Photon has maximum resolution of 0.045 mm, which means that the smallest geometries are not even built. (GitHub 2020.) At the figure 27, the column that has details with best quality is column number seven. That column has the most no clogged circles and the negative and positive space angle areas have printed out and not collapsed nor clogged.

6 AIM AND PURPOSE OF EXPERIMENTAL PART

Purpose of the experimental part was to utilize the information and knowledge collected at the literature part to create the parameter optimization process for Planmeca. The goal was to determine a standardized, documented, repeatable, and traceable procedure for parameter optimization process so that the same process can be repeated with needed dental 3D printing materials. The goal was achieved with the help of literature findings and by applying them into practice.

The experimental part utilized key literature findings. The exposure time finder test print was printed first to find the approximate exposure time. Then Taguchi method was utilized to optimize parameters for the printing process in two phases. Results and analysis chapter was concentrating into presenting the results of the experiments with figures and analysis. In discussion chapter the main results were gathered and discussed. Exposure times are marked within the text in parentheses after each experiment number, if it is considered necessary.

Experimental part was divided into two categories:

1. Testing the created optimization process.
2. Validation round of the created optimization process.

This division was created to easier the discussion of two separate optimization process rounds for two separate materials. First the created optimization process was tested, and the process was validated at the second category.

Previous two categories were divided further into three different parts:

1. Part I: Finding preliminary parameters.
2. Part II: Preliminary parameter test series.
3. Part III: Actual test series.

The categories were divided into three parts to easier and to clarify the discussion of different test series and parts of the experimental part. The division into three parts was separating the optimization process into smaller complexes.

6.2 Limitations of the experimental part

In this thesis, machine parameters were considered as a constant to reduce the number of variables but also because Creo C5 had mechanics and certain machine settings that could not be changed. These settings and mechanics were for example LED properties, light intensity, collimation solution of the UV light and cooling unit. Even though by changing or upgrading some previously listed things, the printing quality could be improved, they were not changed to remain test matrix simpler.

Target of the optimization process was to create a process which resulted parameters that were producing 3D printed object with desired characteristics. However, the parameter set this process produced, had to be tested with actual dental application to ensure the functionality. This thesis does not discuss about the possible modifications of the parameters according the results that dental application produces.

7 EXPERIMENTAL SETUP

The tests were executed at the product development laboratory of Planmeca, at Helsinki, Finland. Only one specific printer was used to ensure the comparability of the results. The slicer software used was Planmeca Creo C5 Studio, version of 2.04.00.01.

7.1 3D printer

The Creo C5 3D printer used (figure 29) was equivalent to customer printer, which meant that it was not modified for product development purpose. The printer was produced in Helsinki, Finland, and it had software version 1.1.0.23.R. Serial number of the printer was CVMA407849. The printer had been running 31 hours before the tests with total amount of 65 runs.

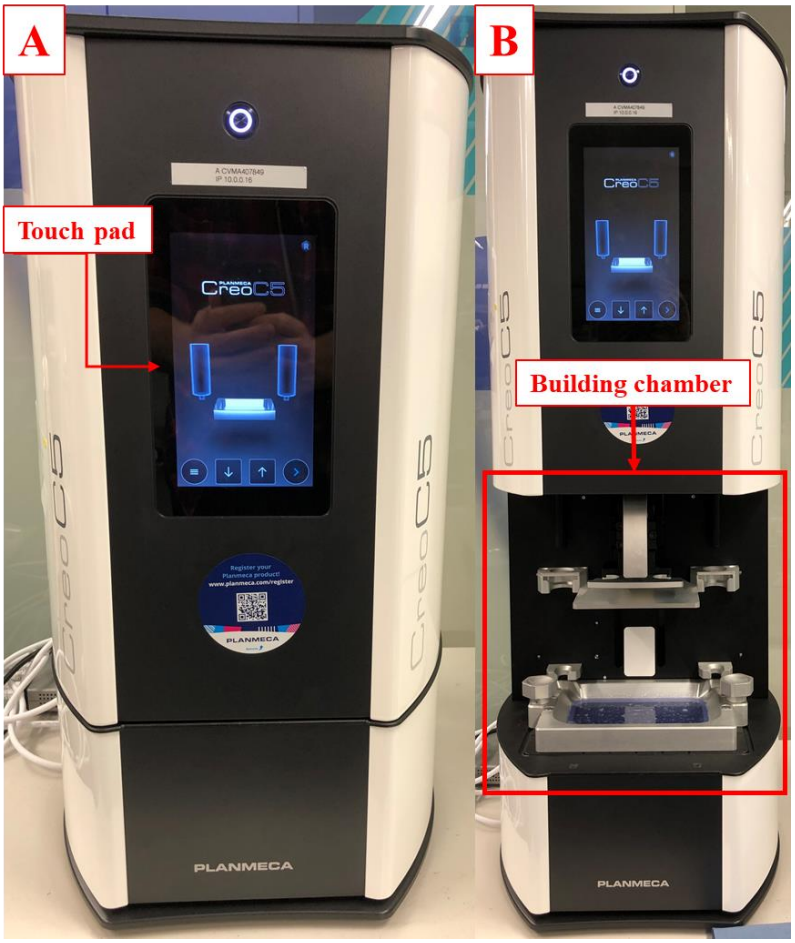

Figure 29. Creo C5 resin printer, on left side (A) printer is closed as during printing and on the right (B) the printer is opened for operations.

As shown in the figure 29, the printer had two modes; front cover closed (A) or open (B). When any operational things needed to be done, for example change of resin vat, the front cover had to be open. The front cover was closed during printing and while the printer was not used. The resin could be stored in the vat inside the printer if the front cover was closed. As seen from the figure 29 there was touch pad at the front cover which was used to operate the printer. The building chamber is presented in the figure 30.

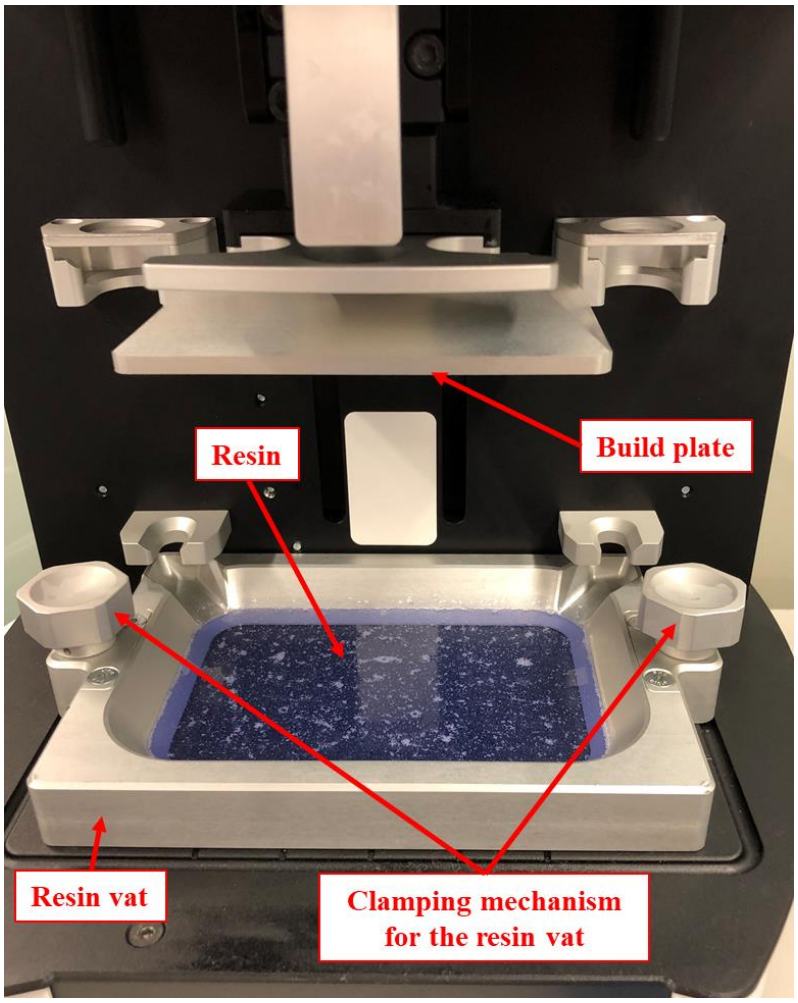

Figure 30. Enlarged figure of the building chamber of Creo C5 and the main components inside.

As it can be seen from the figure 30, the main components inside the building chamber were build plate, resin vat and clamping mechanism for the resin vat. In the figure 30 the vat was filled with transparent Detax Freeprint Ortho resin. The white pigments seen in the resin were air bubbles that had generated while shaking the resin bottle for 2 min intensively, before poured into the vat.

Creo C5 is an LCD-photomask resin 3D printer, which means that the LCD generates the photo of each layer to the bottom of the vat. The schematic figure of the Creo C5 principle and main components are presented in figure 31.

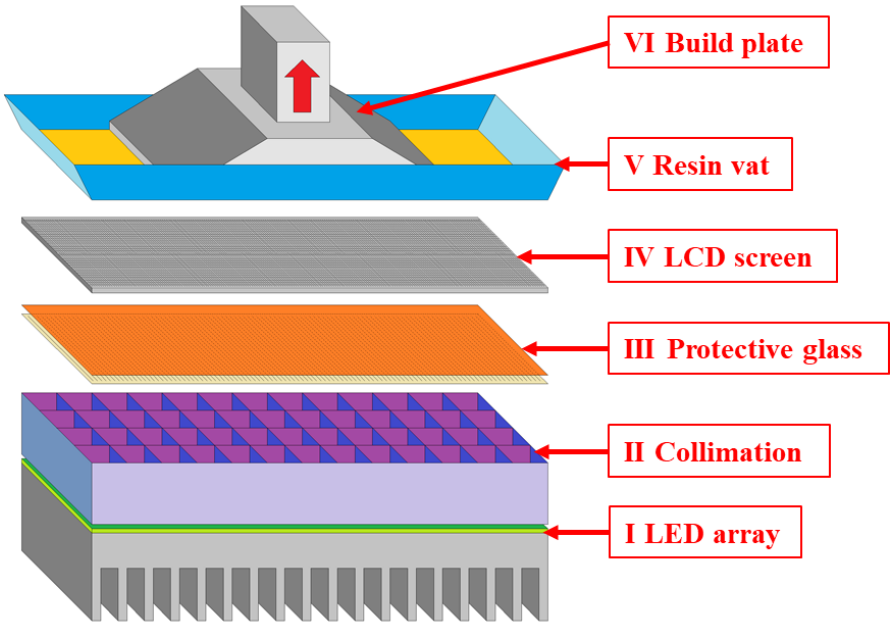

Figure 31. Schematic figure of the Creo C5 components and technique (Luukkanen 2019).

Figure 31 presents main components of the Creo C5. The LED array is attached to the jig at the bottom of the figure 31. Number II is the collimation solution which ensures that the rays of the LED reaches the bottom of the LCD as perpendicular as possible. Number III presents a protective glass which is protecting the LCD screen from below. Number IV is the LCD screen itself and number V is the resin vat, filled with resin. Number VI is the build plate which moves up and down, in z-direction.

7.2 Material

The material for the experimental part was Freeprint Ortho of Detax. The material is designed for DLP printers of 405 nm wavelength. This means that the material has photoinitiators that react to 405 nm wavelength. Freeprint ortho is used mainly for printing surgical guides and orthodontic bases. Detax promises that Freeprint Ortho is autoclavable which was the reason why Freeprint Ortho was chosen for the experimental part. At the moment Planmeca does not offer material which could be autoclaved. Autoclaving is widely used sterilization method in hospitals to sterilize components.

Freeprint ortho has medical device classification of IIa, which means that it can be used intraorally and in contact with blood circuit from 60 min up to 30 days (Regulation (EU) 2017/745 of the European Parliament And of the Council 2017). The level of medical device classification depends on many things. With 3D printed parts the medical device classification is mainly determined according biocompatibility of the printed part and for how long it will be in touch with human body and what kind of contact it is. As a conclusion, 3D printed parts follow the medical device regulations and classifications, and clear guidelines for the workflow are indicated in the Instructions For Use (IFU) documents. However, the surveillance of the execution of these guidelines in practice for the time is insufficient and incomplete. (Sjöberg 2020.)

Saremco Print Crowntec was chosen as a material for validation round. This material is also a dental 3D printing material used for permanent crowns, inlays and onlays, but also for temporary crowns, bridges and artificial teeth.

7.3 Used post treatment equipment

The test prints were washed with the BioSonic UC50DB ultrasound washer, shown in figure 32. Water was used to fill up the washer. The classes were filled with Emplura propanol-2, which has purity of 99,5%.

Figure 32. BioSonic UC50DB ultrasound washer filled with water and classes, for dirty and clean wash, filled with Emplura Propanol-2.

As seen from the figure 32, there are two classes (dirty wash and clean wash) inside the ultrasound washer. The division for dirty and clean wash was made in order to get cleaner parts after washing. The test prints were washed first 6min inside the dirty wash and then dried with compressed air. Then test prints were washed for 6min inside the clean wash and afterwards dried with compressed air.

7.4 Used measurement equipment

Measurement tools used in this thesis were either digital micrometer or slide gauge, shown in the figure 33.

Figure 33. Measurement tools, above (A) digital micrometer Micromar 40 EWR(i) from Mahr and below (B) slide gauge MarCal 16 ER from Mahr.

Figure 33 shows the digital micrometer (A) which was used when more detailed measurements were needed and slide gauge (B) when larger measurements were measured. Measurement equipment were calibrated before executing the tests.

7.5 Test samples

Printing geometry for the experimental part was created in this thesis. The parts were modelled with OnShape, which is internet-based CAD-software. The geometries of the parts were based on the observations of the earlier printing results, but also general overview of different test prints used among hobbyists and different researches. CAD-models of the test parts can be seen in the figure 34.

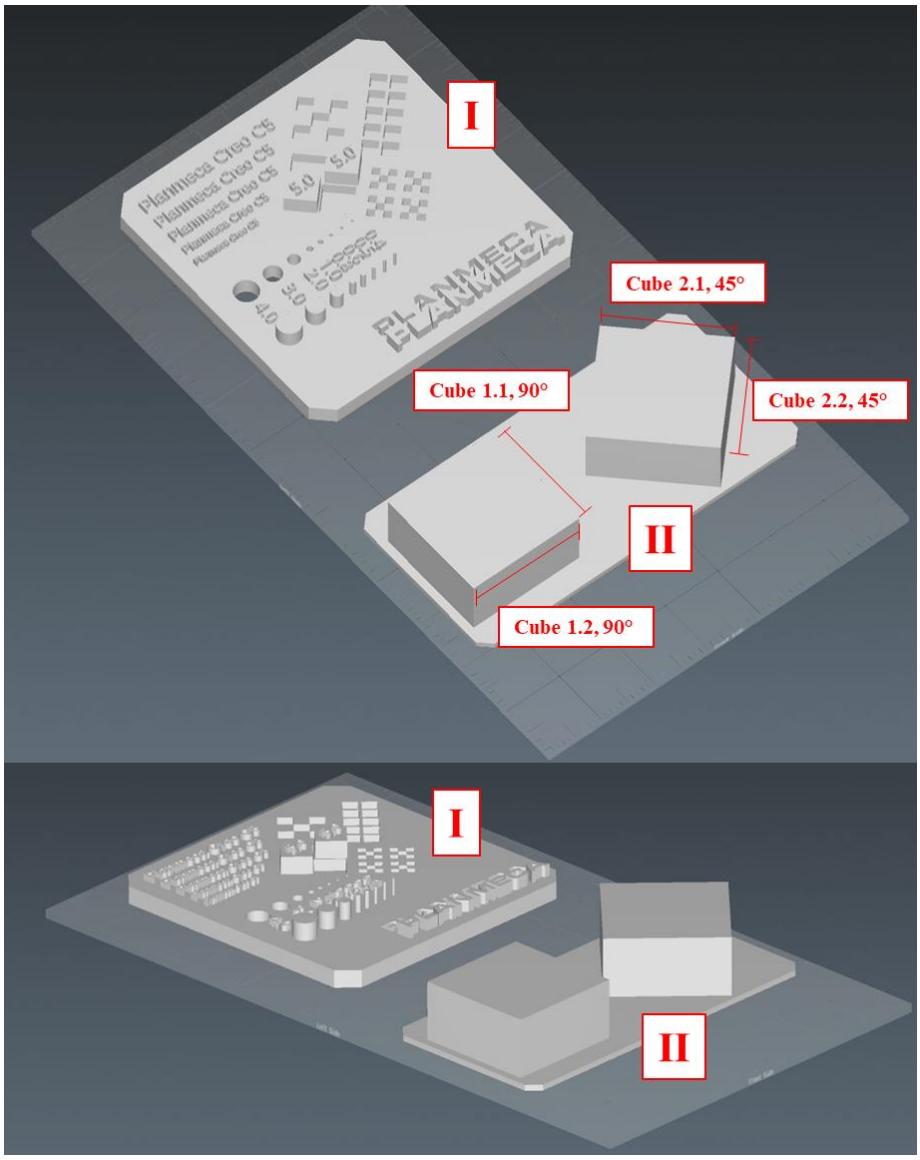

Figure 34. Test print geometries imported to the Planmeca Creo C5 Studio Expert, two separate parts: Planmeca test plate (I) and 20 mm measurement cubes (II) and cube sides numbered according the measurement locations.

As seen from the figure 34 the test print included two separate parts, which were called; Planmeca test plate (I) and 20 x 20 x 10 mm measurement cubes (II). The Planmeca test plate included small and detailed geometries. These geometries were designed to evaluate printing quality. The cubes engraved to Planmeca test plate were added for evaluation of the sharpness of the prints. Different sizes of texts and pillars were added for evaluation of how small and detailed geometry printer can produce. The measurement cubes were for dimensional accuracy test, each side of the cubes was measured. There was not added the base plate that Studio software was suggesting but the base plate for the measurement cubes was created already in the CAD-software. The thickness of the base plate was 1 mm.

8 EXPERIMENTAL PROCEDURE

Taguchi method was utilized to optimize parameters in the experimental part. Utilization of the method based on the findings from the literature review, Namjung et al. (2019), Guerra et al. (2019) and Griffiths et al. (2016) were utilizing Taguchi method for parameter optimization. Initial values for the build plate movements (speed up, speed down and lift distance) were based on the current parameters of the materials that Planmeca has set to market. The exposure time was approximated according to a simple test. These steps and methods are discussed in this paragraph. The experimental procedure is summarized in figure 35.

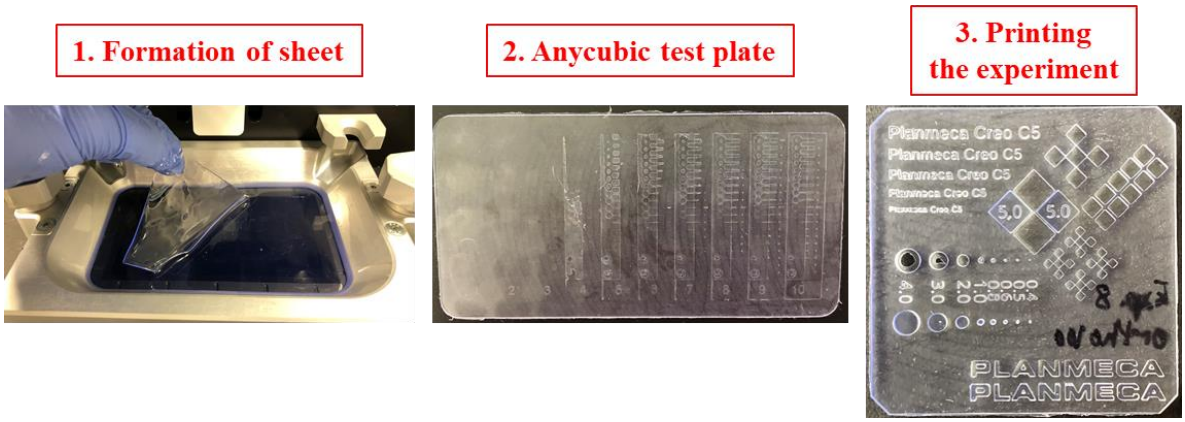

Figure 35. The experimental procedure summarized.

As figure 35 simplifies the experimental procedure, there were three different prints that were printed. First the sheet was cured at the bottom of the vat, then Anycubic test plate was printed and the experiments were printed when optimization rounds were executed. A large part of the experimental part based on the previous knowledge gained by testing and learning method, which was critical to be able to plan and execute the experimental part.

8.1 Planning of the experiments

According the four steps, created by Namjung et al. (2019, p. 162) (figure 24), first step of planning was to determine the response (goal) of the experiment. The response was chosen to be visually successful and dimensionally accurate prints. Visually successful print was determined (step 2) in in internal printing quality guide of Planmeca, as: “Print is visually

successful when the wanted geometry from the CAD-model has been printed without defects". There were certain steps how this could be observed, and these steps were explained with the results. Dimensional accuracy was achieved when the measurements of the cubes were within the tolerance of ± 100 µm.

Based on the chosen response, the process parameters affecting to visually successful and dimensionally accurate prints were identified (step 3). Identification based on the previous knowledge; which process parameters are affecting the most to geometry of the printed part. Identified process parameters were build plate movement, exposure time, build orientation, layer thickness or voxel depth, classification of layers, part geometry, separation force and support structure settings. The most critical process parameters were chosen to be build plate movements (speed up, speed down and lift distance), and exposure time. These process parameters were chosen as the most critical ones because they are affecting the most to the geometry of the prints. They have always an absolute numerical value which can be easily varied and because of closed system in Creo C5, customers cannot change these parameters. Layer thickness was determined to be constant, 100 µm. Layer thickness of 100 µm is widely used with variable materials in Creo C5 printer and constant layer thickness results simpler test matrix. However, lower layer thickness is required to maintain the accuracy of the print in some dental applications with certain materials. Layer thickness can be modified before the tests (in this case), but it should not be a variable in test matrix. Support structure settings and build orientation were not chosen as critical parameters, because they were considered as second-class parameters, based on the knowledge gained from Reijonen (2020). Successful print has to be achieved before optimizing the building orientation or support settings.

The test matrix was chosen (step 4) based on the knowledge that four factors were varied with three levels. Corresponding matrix was Taguchi orthogonal array $L_9(3^4)$ (The University of York 2004). The amount of test prints could be kept reasonable with this orthogonal array and the test results were easier to handle, because there were not more than nine prints in each test round. The factors were varied with three different levels (values) to get the perspective how change of each factor (to lower and higher) change the response. The complete Taguchi orthogonal array $L_9(3^4)$ is shown in table 3.

Table 3. Taguchi orthogonal array $L_9(3^4)$.

	Parameter			
Experiment number	Speed Up	Speed down	Lift distance	Exposure time
x.1	a	a	a	a
x.2	a	b	b	b
x.3	a	c	c	c
x.4	b	a	b	c
x.5	b	b	c	a
x.6	b	c	a	b
x.7	c	a	c	b
x.8	c	b	a	c
x.9	c	c	b	a

Table 3 shows how the Taguchi orthogonal array was formed and how the parameters were varied inside the array. The array was utilized as a base for every material when the test rounds were planned. Levels (a, b, c) were replaced with different values. Letter x before the experiment number represents the number of test round. The parameter optimization process was divided into three parts after the planning. These parts are illustrated in the figure 36.

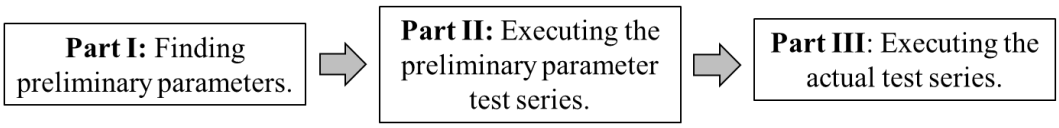

Figure 36. Simplified work flow of the experimental part.

As figure 36 summarizes, the first part included finding the preliminary parameters (especially exposure time) for the chosen material. In second part (preliminary parameter test series) the chosen parameters were varied and tested to achieve the response. Third part based on the results from the second part, best parameter set from the preliminary parameter test series was chosen for the actual test series. Method for the actual test series varied either only exposure time or executed similar multivariable test with three levels, as in the preliminary test series.

8.2 Finding of preliminary parameters for the test prints

The first part of the parameter optimization process was to determine preliminary parameters to be able to print parts without significant defects. Preliminary parameter finding was based on the Anycubic test plate, which was introduced in the literature review. However, exposure time for the bottom layers had to be found before printing Anycubic test plate.

Exposure time for the bottom layers was determined with a simple test. Bottom of the vat was exposed with UV light, LCD screen fully opened. Resin was cured (exposed to UV light) for 30 seconds, and thin sheet was formed at the bottom of the vat. The sheet was removed from the bottom of the vat as shown in figure 37.

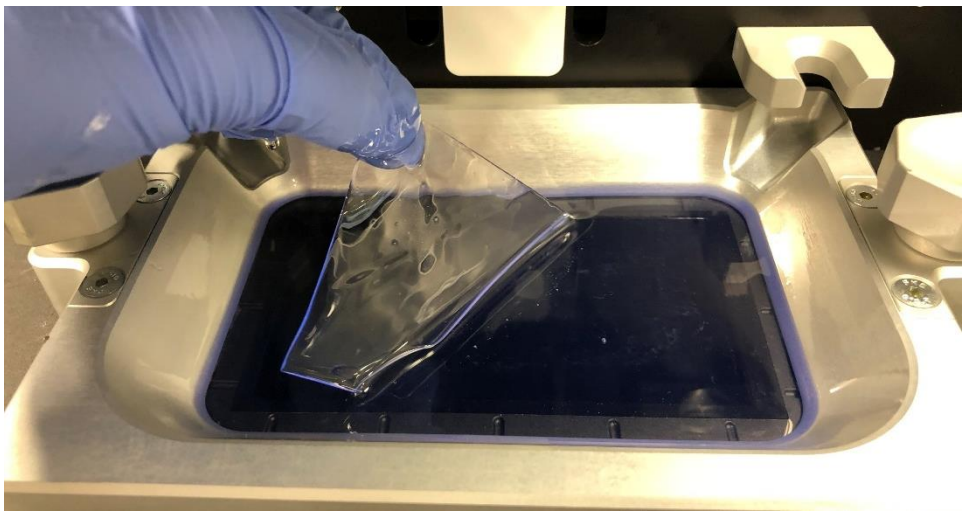

Figure 37. Peeling the sheet from the bottom of the vat.

The figure 37 represents how the sheet was peeled from the bottom of the vat and that the sheet was exactly same shape as LCD screen in xy-plane. After peeling, sheet was washed with Emplura propanol-2 for 6 min + 6 min and dried in between and after, with compressed air. The sheet was measured with micrometer from six different locations after washing. Locations of the measurements (numbers 1-6) are shown in figure 38.

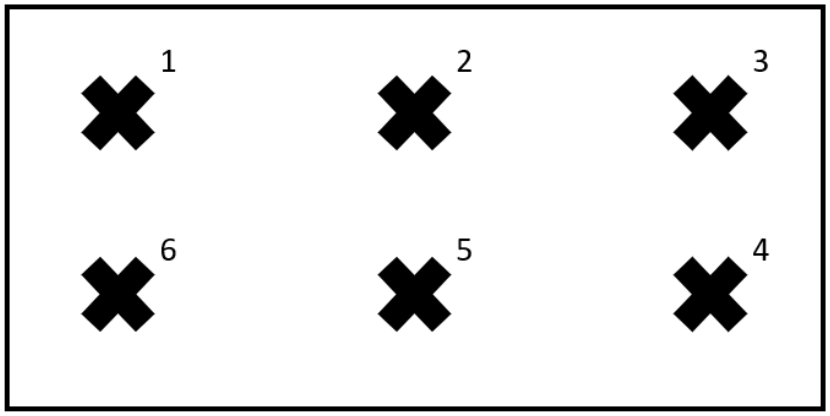

Figure 38. Numbered measurement locations of the sheet.

Arithmetic mean for the thickness was calculated based on the measurements from the locations shown in figure 38. Calculated mean was utilized to calculate the exposure time for the bottom layers ($t_{E,B}$):

$$t_{E,B} = \left[\left(\frac{100}{\bar{X}}\right) \cdot t_{E1}\right] \cdot 10 \qquad (2)$$

In equation 2, $t_{E,B}$ is the exposure time of bottom layers, $\bar{X}$ is an arithmetic mean for the thickness and t_{E1} is the exposure time which is used to cure the sheet to the bottom of the vat. Equation 2 utilizes the idea that curing thickness is increasing linearly with the exposure time, which means that if the exposure time is doubled the curing thickness is also doubled. However, it was recognized that linearity is not the case in reality, but as Welover (2019) showed, the relation is above the linear curve (see figure 26) which means that thickness is increasing more rapidly than exposure time. Calculations of the exposure time for bottom layers can be found from appendix V.

Based on the measurements and calculations of exposure time for bottom layers (appendix V), the print file for Anycubic test plate was created, and the part was printed. The printing file was created with Planmeca Creo C5 Studio, but the g-code was modified before printing to adjust different exposure times for each column. Part of the g-code and photos of the layers 11, 16 and 20 are shown in figure 39.

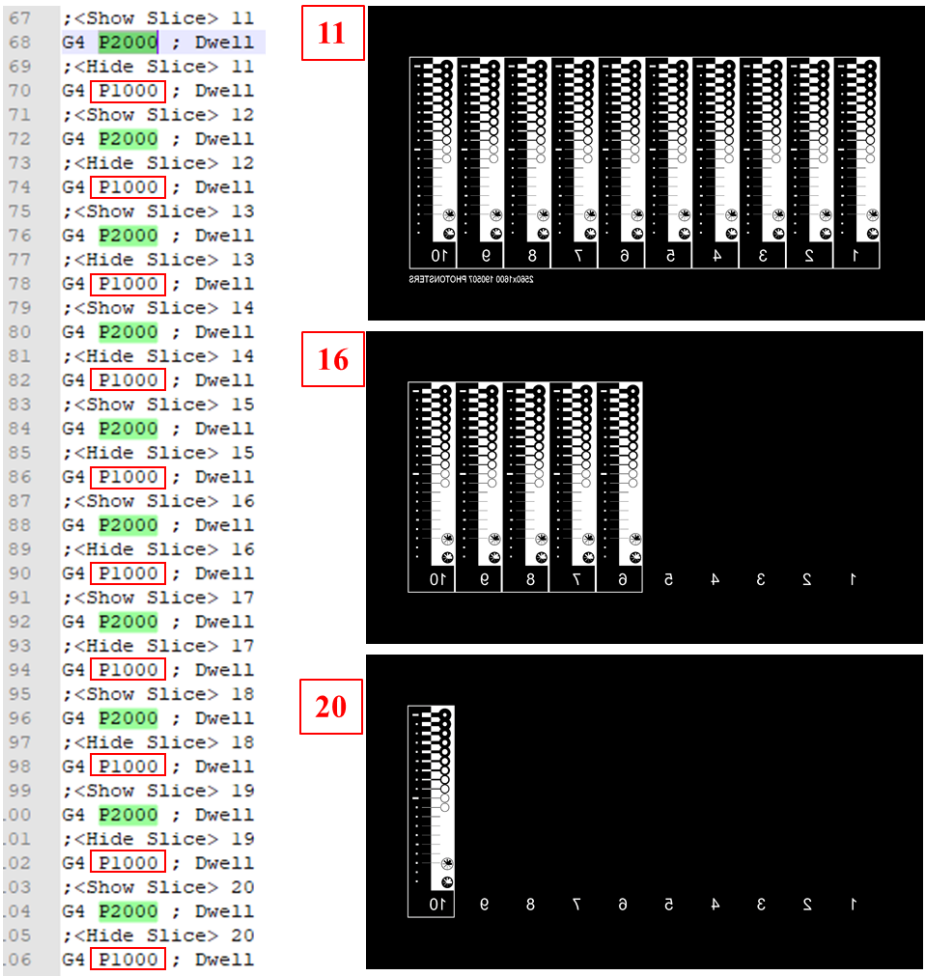

Figure 39. Part of the g-code which determines the exposure time for each column and photos of the layers 11, 16 and 20.

Figure 39 (g-code) shows exposure times highlighted for each layer. Only one 100 µm layer was printed which had all the 10 columns separately. However, different figures (figure 39, numbers 11, 16 and 20) are discussed as layers because in g-code they can be seen as separate layers. The exposure times are in milliseconds. Command G4 (in the g-code) stands for dwelling and P serves as a parameter for commands, which in this case is time (milliseconds). Command "G4 P2000" tells the stepper motor to stay still for 2 second at the current location. Embedded software of the Creo C5 processes the printing file (created with Creo C5 Studio) before the printing. The software controls the stepper motor of the build plate according the g-code during the printing and xy-geometry of each layer is created with the figures of the layers. In addition, software controls UV light source and LCD screen with the help of separate electronic control system. In figure 39, times marked with boxes are the times in between the layers. Figure 39 shows the figures of the layers 11, 16 and 20. As seen

from the figure, layer 11 has all ten columns while layer 16 has columns 6, 7, 8, 9 and 10. Layer 20 has only column number 10, which receive 20 seconds of exposure (each layer has 2 second exposure time). Corresponding exposure times for each layer can be found, from the g-code, under the text ";<Show slice> xx", where xx is the number of the layer. The exposure times can be adjusted by modifying these times.

The plan was to set the exposure time for each layer as one second, so that the exposure time for the columns would variate from one second to ten seconds with one second steps. If there were no attached columns after one second steps, second try was done with steps of two second, as in figure 39. Preliminary exposure time was varied in the test matrix after it was found. The variation based on the steps of exposure time used in Anycubic test plate. The variation of two seconds was used if steps of one second were used in Anycubic test plate. On the other hand, the exposure time was varied with four seconds in the test matrix, if steps of two seconds were used in Anycubic test plate. This was based on the fact that when the steps are larger, the optimal exposure time is in the wider range. Therefore, variation of four seconds gave more information about effect of exposure time to quality characteristics of the print. Variation of the exposure time was always done higher and lower, to find the effect of exposure time more clearly. The parameters were varied with three levels (a, b, c) according table 4.

Table 4. Values for the Taguchi orthogonal array $L_9(3^4)$.

	Value		
Parameter	**a**	**b**	**c**
Speed up [mm/min]	v_{u1}	v_{u2}	v_{u3}
Speed down [mm/min]	v_{d1}	v_{d2}	v_{d3}
Lift distance [mm]	z_1	z_2	z_3
Exposure time [sec]	t_1	t_2	t_3

Table 4 illustrates how the parameters were variated. Table 4 is used to simplify the presentation of varied parameters with varied values. Values are placed into Taguchi orthogonal array. Complete arrays can be found from appendices I and III with the values filled in the arrays. After the execution of each test series, the experiments were evaluated according the evaluation matrix, shown in table 5.

Table 5. An example of the structure of the evaluation matrix.

Experiment	**Text**	**Pillars**	**Cubes** [± 100 µm]	**Sharp Shapes**	**General inspection**	**Overall**
x.1	NOT OK	NOT OK	NOT OK	OK	NOT OK	1
x.2	OK	NOT OK	NOT OK	OK	NOT OK	2
x.3	OK	NOT OK	OK	OK	OK	4
x.4	OK	OK	OK	OK	OK	5
x.5	NOT OK	NOT OK	NOT OK	OK	NOT OK	1
x.6	OK	NOT OK	OK	OK	NOT OK	3
x.7	OK	OK	NOT OK	OK	OK	4
x.8	OK	NOT OK	OK	OK	OK	4
x.9	NOT OK	NOT OK	NOT OK	NOT OK	NOT OK	0

Table 5 illustrates the evaluation matrix and how the overall grade formed for each experiment. Every evaluation class was evaluated either OK or NOT OK, and OK resulted one point while NOT OK resulted zero points. Overall grade is the total number of points from each class. Visual evaluation had four separate sections which were evaluated. Measurement cubes were measured and evaluated depending whether they were within the tolerance (OK) or not (NOT OK). Altogether these five separate evaluation points resulted overall grade which determined if the print was accepted for further consideration or not.

8.3 Execution of the experiment series of Freeprint Ortho

The execution of the parameter optimization process was divided into three parts which are explained and discussed in this paragraph. Also, every test round can be divided into five steps: choosing the parameter set based on the results from previous series, creating and planning the test matrix, printing the test series of experiments, analyzing the results and documenting the results. Similar deviation for the DOE process was introduced by Wanger, Mount & Giles (2014, pp. 291).

8.3.1 Execution of the finding preliminary test parameters

Preliminary parameter finding was executed according the plan. The sheet was cured to the bottom of the vat and peeled off to measure and calculate the theoretical exposure time for 100 µm layer thickness. Measurements and calculations are shown in appendix V, table 8.

According the calculations, theoretical exposure time resulted 150 seconds for the bottom layers and 15 seconds for transition layers. These theoretical times were used as exposure times in the Anycubic test plate to create the base for the exposure time finder test. The Anycubic test plate print file was created and printed according the plan. Exposure time was varied with steps of one second first and second print file with steps of two seconds. This was done because after first print it was noticed that the exposure time was more than 10 seconds.

8.3.2 Execution of the preliminary parameter test series

Taguchi orthogonal array was formed based on the found preliminary exposure time and previous knowledge of the other critical parameters. Variation of the parameters was done according the table 6.

Table 6. Values for the Taguchi orthogonal array L9(3^4) for the preliminary parameter test series test matrix of Detax Freeprint Ortho.

	Value		
Parameter	**a**	**b**	**c**
Speed Up [mm/min]	100	200	300
Speed Down [mm/min]	200	300	400
Lift Distance [mm]	6	7	8
Exposure time [sec]	12	16	20

Parameters seen in table 6 were placed into Taguchi orthogonal array according the letter (a, b or c) and the test matrix was formed. Taguchi orthogonal array can be seen in appendix I, table 1. Experiments were printed according the test matrix and no modifications were made in between the prints.

8.3.3 Execution of the actual test series

Actual test series included the comparison of two ways to optimize parameters. Comparison was done because it was not possible to define which way would have been more reasonable before testing. Both test series were executed and compared to make the decision based on facts. First Taguchi orthogonal array was created to have second optimization round for all the critical parameters. Starting values were based on the findings of the preliminary

parameter test series and fast printing time was pursued. Variation of the parameters is shown in table 7.

Table 7. Values for the Taguchi orthogonal array L9(3^4) for the actual test series test matrix of Detax Freeprint Ortho.

	Value		
Parameter	**a**	**b**	**c**
Speed Up [mm/min]	400	500	600
Speed Down [mm/min]	300	400	500
Lift Distance [mm]	6	5	4
Exposure time [sec]	19	18	17

In table 7 the lift distance and exposure times are reduced and build plate movement speeds are increased to decrease printing times. Another way to optimize parameters in the actual test series concentrated to optimize exposure time only. Exposure time was considered as the most critical parameter, so it was important to find optimal exposure time. On the other hand, the results from the preliminary parameter test series were already good and it was not found critical defects caused by other parameters, thus it was considered critical to find minimum exposure time. Variation of the exposure times is shown in table 8.

Table 8. Exposure time variation for the second test round of Detax Freeprint Ortho.

	2.2.1	2.2.2	2.2.3	2.2.4	2.2.5	2.2.6	2.2.7	2.2.8	2.2.9
Exposure time [sec]	19.5	19	18.5	18	17.5	17	16.5	16	15.5

As seen from the table 8, the exposure time was varied with 0.5 second steps. Experiment numbers are in the form of 2.2.x, which tells that it was actual test series (2), only exposure time was varied (2), and the last number (x) describes the experiment number. The goal was to find a limit, when the exposure time was too low, and the print failed. When the limit was known the optimized minimum exposure time could be used. Other parameters for the test matrix were taken from the experiment 1.8 of preliminary parameter test series.

8.4 Execution of the validation test series

The material used for validation round was called Crowntec from Saremco print. The preliminary parameter finding was done according the same plan as with Freeprint Ortho. The sheet was cured to the bottom of the vat and peeled off to measure and calculate the theoretical exposure time for 100 µm layer thickness. Calculations and measurements of the sheet are shown in appendix V, table 9. The calculation according the equation 2 resulted 37 seconds exposure time for the bottom layers (appendix V). For the transition layers (100 µm) it was used 3.7 seconds as an exposure time to create the base for the Anycubic test plate. However, 3.7 seconds was discovered too low, because 3,7 seconds resulted unclear test plate which could not be interpreted, shown in figure 40.

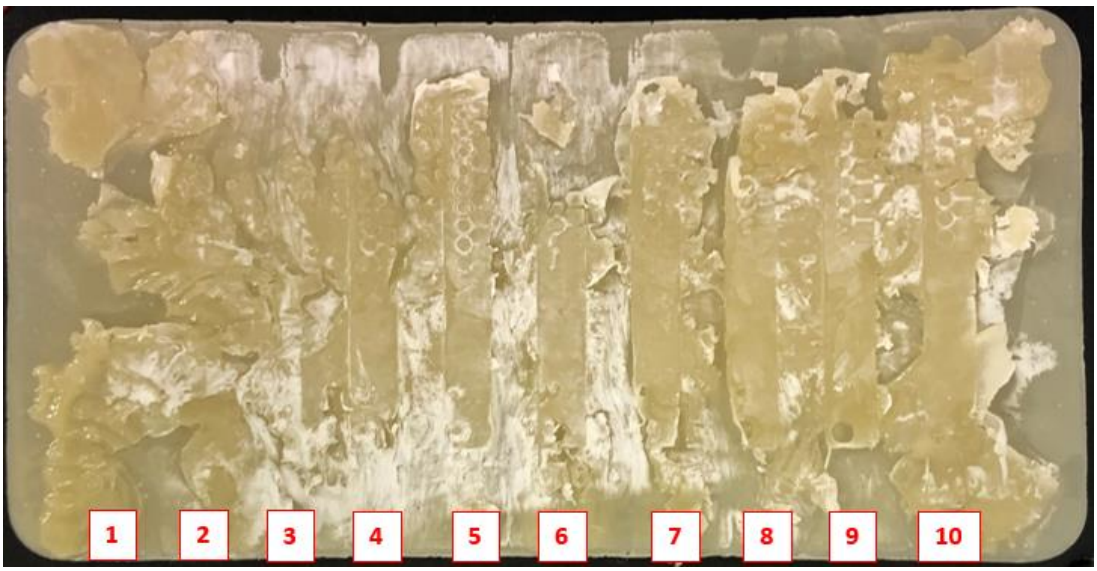

Figure 40. Anycubic test plate with the exposure time of 3,7 seconds for the transition layers (100 µm).

As seen from the figure 40, the test plate was not well formed, and it was so unclear that it could not be interpreted. Due to failure, the exposure time was increased from 3.7 seconds up to 8 seconds. The Anycubic test plate was formed by increasing the exposure time. However, the Anycubic test plate had to be printed third time because it was observed that the preliminary exposure time was over 10 seconds. It was found with the two second steps that preliminary exposure time was 14 seconds which was then varied as planned. Parameters for the test matrix of preliminary parameter test series of Saremco Print Crowntec can be found from the table 9.

Table 9. Values for the Taguchi orthogonal array L9(3^4) for the test matrix of preliminary parameter test series of Saremco Print Crowntec.

	Value		
Parameter	**a**	**b**	**c**
Speed Up [mm/min]	100	150	200
Speed Down [mm/min]	100	150	200
Lift Distance [mm]	6	7	8
Exposure time [sec]	10	14	18

Values seen in the table 9 were placed into Taguchi orthogonal array *L9(3^4)*, which is shown in the appendix III, table 5. Slow built plate movements were chosen because it was found during literature review that high viscosity of the resin affects to printing process. According Lin et al. (2020, p. 352), Sa et al. (2019 p. 3310), Ho et al. (2015, pp. 3627) and Tumbelston et al. (2015, pp. 1351–1352) high viscosity resins requires slower printing speeds to ensure the flow of the resin underneath the part but also it may affect the lifting process negatively.

Only exposure time was decided to variate for the actual test series, based on the results from the preliminary parameter test series. Exposure time was found critical with Crowntec material and there were not found remarkable differences in results between build plate movements. The variation of the exposure time is shown in table 10.

Table 10. Exposure time variation for the actual test series of Saremco Print Crowntec.

	2.1	2.2	2.3	2.4	2.5	2.6	2.7	2.8	2.9
Exposure time [sec]	12	11	10	9	8	7	6	5	4

As seen from the table 10, the exposure time varied with one second steps. The plan was to see how reduction of exposure time affects to print quality and whether the dimensional accuracy can be achieved or not. Other parameters (used for the actual test series) were from the experiment 1.9. The exposure time was variated from 12 seconds because it was considered that the optimal exposure time is in between the 14 and 10 seconds.

9 RESULTS AND ANALYSIS

The main result of literature review was that Taguchi method is widely utilized DOE process when 3D printing parameters are optimized. Another surprising result was that there were not many researches done considering the LCD photomask resin 3D printing and no scientific references were found where the study would have concentrated into optimizing support structures for DLP 3D printing. Dental applications and 3D printing are not widely researched area from the technical point of view, even though 3D printing is becoming more popular among the dental applications.

9.1 Results and analysis of Freeprint Ortho

The results are presented and discussed with similar division as before. Preliminary parameter finding results are presented and analyzed first. Then results of preliminary parameter test series are presented and analyzed. And at the last, results of actual test series are presented and analyzed.

9.1.1 Preliminary parameter finding

The parameters for the Freeprint ortho -material can be found from the appendix I, table 1. First the Anycubic test plate was printed with one second steps and the result is shown in the figure 41. The Anycubic test plates are observed according the GitHub (2020) instructions.

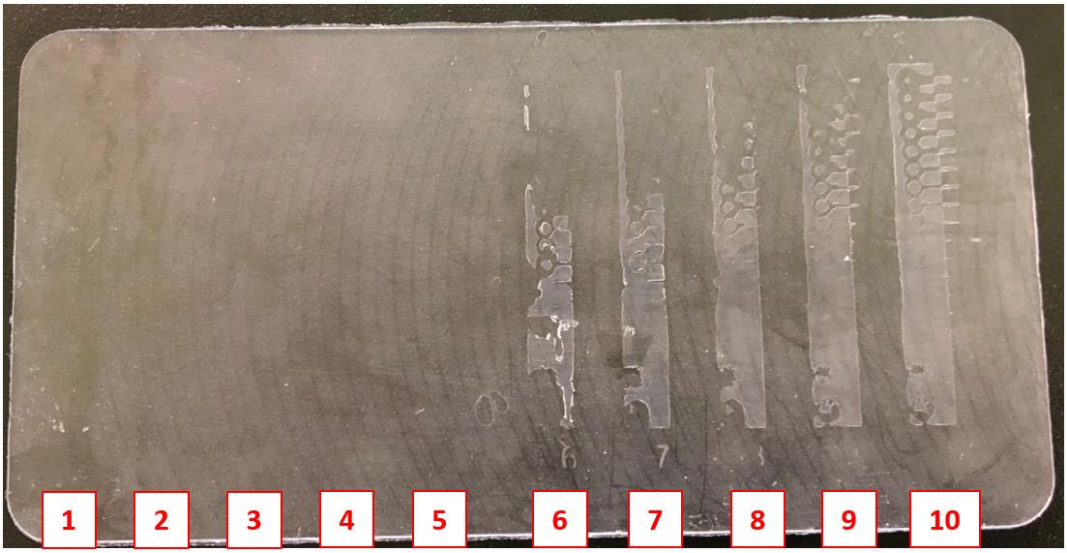

Figure 41. Printed Anycubic test plate with 1 second steps in each column from 1 to 10.

As it can be seen from the figure 41, none of the columns have attached to the base properly. Added numbers are clarifying the places of the columns. Columns from 1 to 5 cannot be even seen at the base, while columns 6 to 10 are poorly attached. Reason for this was the increase of exposure time. Columns from one to five did not receive enough exposure to attach to base and columns from six to ten received only enough to attach poorly to the base. It was concluded that the exposure time for 100 µm is more than 10 seconds. Therefore, the second Anycubic test plate was printed with two second steps, presented in figure 42.

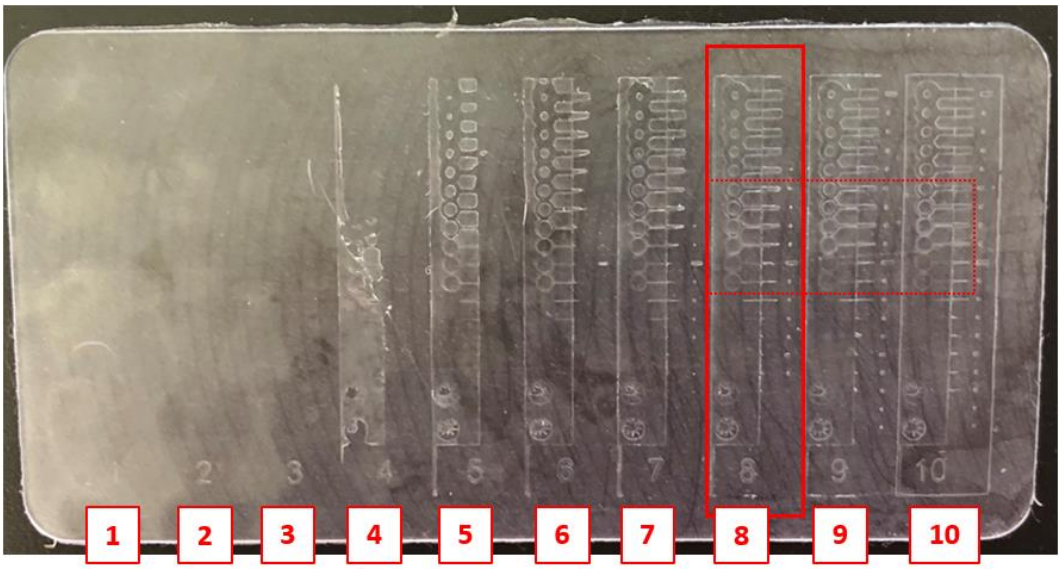

Figure 42. Printed Anycubic test plate with 2 second steps for each column from 1 to 10, number 8 was chosen as the best one and dashed lines are presenting the area of enlarged figure.

As seen in figure 42, columns from seven to ten were attached to base properly which meant that the right preliminary exposure time was around one of them. Columns from one to three (corresponding the exposure time of two to six seconds) were not even attached to the base. Column number eight was considered as having the right preliminary exposure time. Columns seven and six had some problems with the first circles, so those columns were not in the consideration. When checked the negative and positive space angles of the columns 9 and 10, they had not been printed out as well as the negative and positive space angles of number eight. Column number eight was chosen, because it was well-formed in general. The critical point was at the 10th circle (column eight), which was not clogged, as it was at the

column nine and ten. The part of the figure 42 (marked with dashed lines) is enlarged in figure 43.

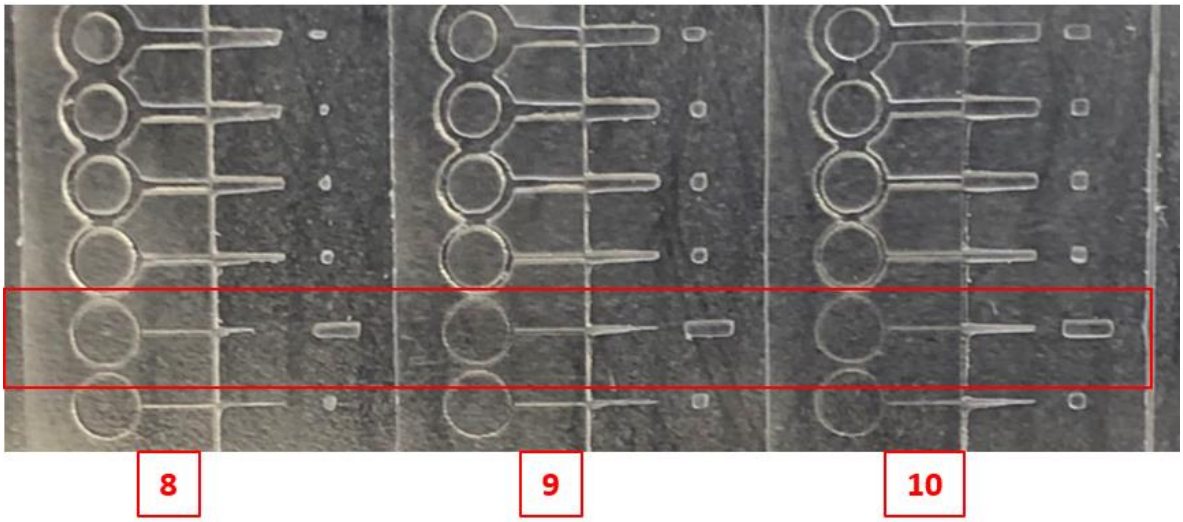

Figure 43. Enlarged figure of the 10th row of the circles of the columns 8, 9 and 10.

As seen from the figure 43, at the row of circles (marked with box), column eight had open negative space while columns nine and ten had clogged negative space. Open negative space can be seen as brighter circle contours at the column eight, compared to columns nine and ten. Based on this observation, it was chosen the exposure time of 16 seconds to be varied in the preliminary parameter test series.

9.1.2 Preliminary parameter test series

Preliminary parameter test series had visually good experiments. Experiments were visually inspected and evaluated according the general visual geometries as OK or NOT OK. Measurement cubes were measured (appendix II, table 4) and evaluated according the measurement. Only prints with grade 5 were accepted for further consideration, because with Ortho material the test results were good. The qualification limit should be always chosen case specific, depending of the quality characteristics of experiments. Evaluation matrix of the preliminary parameter test series shown in table 11.

Table 11. Evaluation matrix of experiments of the preliminary parameter test series, based on visual inspection and dimensional accuracy.

Experiment	**Text**	**Pillars**	**Cubes** [± 100 µm]	**Sharp Shapes**	**General inspection**	**Overall**
1.1	NOT OK	NOT OK	NOT OK	OK	NOT OK	1
1.2	OK	NOT OK	NOT OK	OK	NOT OK	2
1.3	OK	OK	OK	OK	OK	5
1.4	OK	OK	OK	OK	OK	5
1.5	NOT OK	NOT OK	NOT OK	OK	NOT OK	1
1.6	OK	NOT OK	OK	OK	NOT OK	3
1.7	OK	OK	NOT OK	OK	OK	4
1.8	OK	OK	OK	OK	OK	5
1.9	NOT OK	NOT OK	NOT OK	OK	NOT OK	1

Table 11 shows the evaluation matrix of the preliminary parameter test series. Evaluation of the text section was based on the observation of the clarity of the texts, individual letters and their shapes. Pillars were checked if they had been built or not and cubes were measured. Sharp shapes consisted of evaluation of all the detailed shapes of the Planmeca test plate, especially shapes and their sharpness of the engraved cubes. General inspection was executed always first and included rapid observation over the whole print, it was based on the first impression.

Based on the table 11, it can be concluded that there were only three prints that got overall grade of 5. These three prints had similar quality characteristics and each print had exposure time of 20 seconds. On the other hand, there were three prints with the overall grade of 1. All these prints had the exposure time of 12 seconds. It was concluded that 12 seconds was too short exposure time and exposure time of 20 seconds was sufficient but had to be researched if it was possible to shorten. Common defect to all prints was that the bottom layer was overgrown, but it was considered as minor defect which can be optimized later, so it was not observed during the observation of the experiments. In the figure 44 it is presented two prints (experiments 1.1 and 1.8) which had overall grades of 1 and 5.

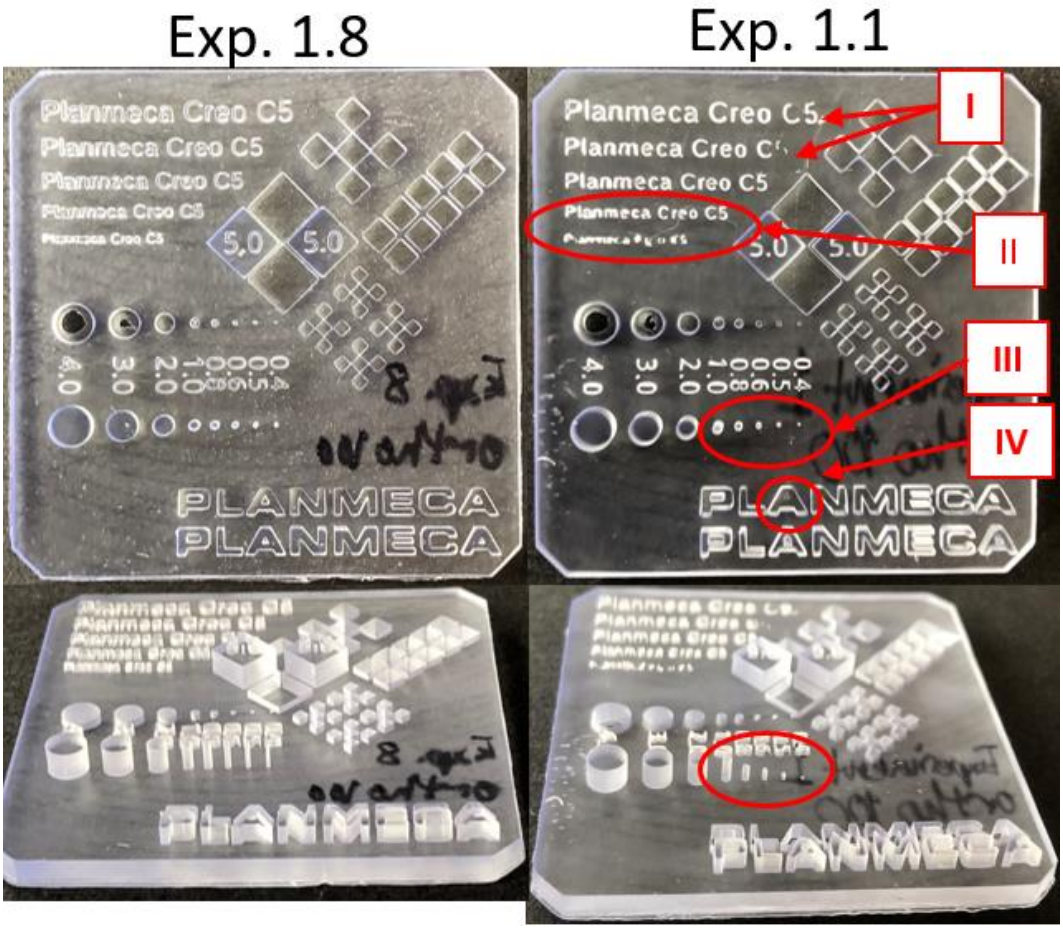

Figure 44. Experiment 1.1 (grade 1) where text has collapsed (number I, II and IV), and pillars are not built properly (III) while experiment 1.8 has passed all the evaluation points (grade 5).

In the figure 44, the difference between the print that had grade 5 (Exp. 1.8) and the print with the grade 1 (Exp. 1.1) can be seen. The evaluation matrix was based on the geometrical characteristics of the printed part, experiment 1.8 had all the geometries built properly and measurement cubes were within the tolerances (shown in appendix II, table 4). There were clogging detected at the smallest font sizes, but they were not considered as a critical defect in the first test round. As seen from the figure 44, experiment 1.1 had several defects (I-IV). The part failed already at the general inspection, thinnest pillars were not built (III), texts were not built properly (I, II and IV) and the smallest font size was unclear and was not attached (II). Planmeca logo at the right bottom had also critical defect at the engraved text, extruded part of the letter A did not build (IV). Experiment numbers 1.3, 1.4 and 1.8 were chosen the best ones of the test round because they had the best quality characteristics according the evaluation matrix. Parameter set of the experiment 1.8 was chosen for further

tests because it had faster printing time than 1.3 and 1.4 (printing times were added to Taguchi arrays and are presented in the appendix I, table 1). In the figure 45, it is presented the enlarged figure of the clogged text and overgrown bottom layer at the experiment 1.8.

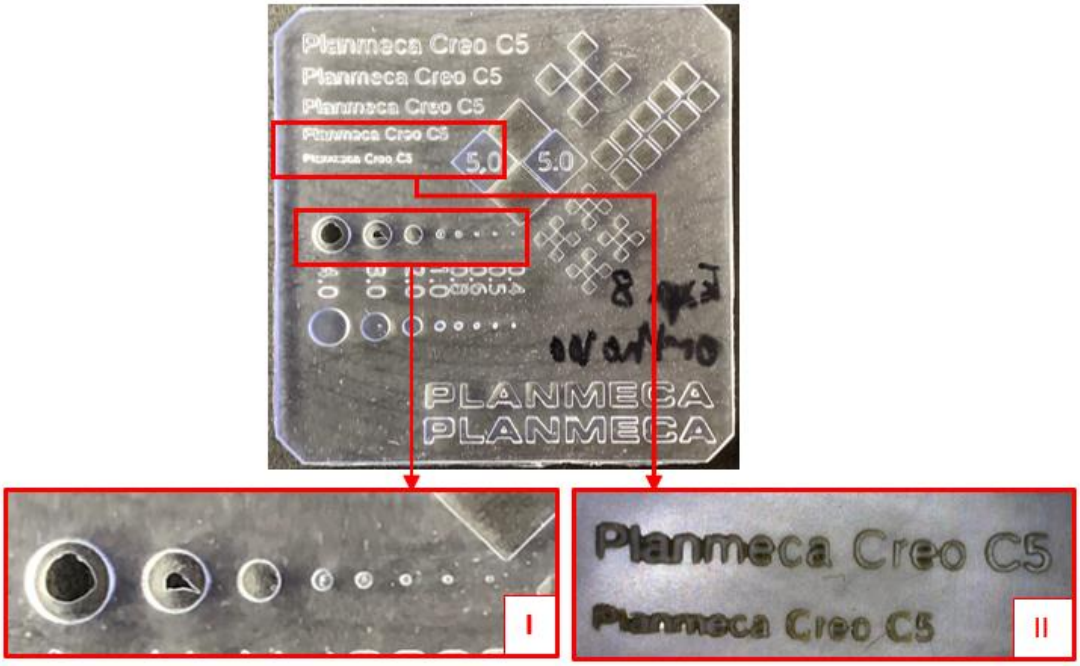

Figure 45. Overgrown bottom layers detected through the holes that should be open (I) and clogged texts (II), experiment 1.8.

As it is seen from the figure 45, the bottom layers had overgrown because they had too long exposure time. The holes (seen in the figure 45, I) should be open at the bottom of the part. However, the exposure time of bottom layers was not critical in terms of the response and could be optimized afterwards. In figure 45, II it is presented the enlarged text where the clogging of the smallest font size could be noticed. It was not considered as critical defect because the measurements of the measurement cubes were within the tolerances, and clearly under the top limit (+100 µm).

9.1.3 Actual test series

Dead pixels were detected after experiment 2.5, which caused some defects to experiment from 2.1 to 2.5, but these defects were ignored when results were observed. Defects that dead pixels caused were mainly holes in the print at the same location where dead pixel appeared at the LCD, shown in figure 46. However, after the LCD was changed these defects disappeared.

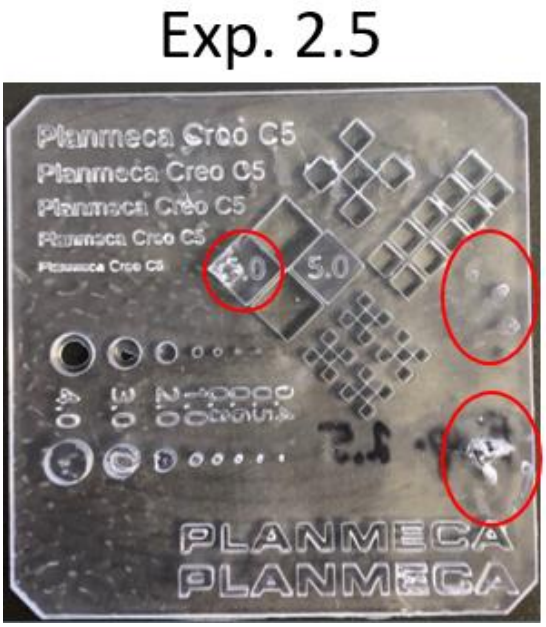

Figure 46. Defects caused by dead pixels at the LCD screen, part of defects marked with circles.

The defects caused by dead or frozen pixels at the LCD screen can be seen in the figure 46 (marked with circles). The actual test series included two ways to optimize parameters. Same evaluation criteria was used as in the preliminary parameter test series. The evaluation matrix can be seen in the table 12 and corresponding printing parameters with printing times in appendix I, table 2.

Table 12. Evaluation matrix of the actual test series based on visual inspection and dimensional accuracy.

Experiment	**Text**	**Pillars**	**Cubes** [± 100 µm]	**Sharp Shapes**	**General inspection**	**Overall**
2.1	NOT OK	OK	OK	OK	NOT OK	3
2.2	NOT OK	OK	OK	OK	OK	4
2.3	NOT OK	OK	OK	OK	OK	4
2.4	NOT OK	OK	OK	OK	OK	4
2.5	NOT OK	OK	OK	OK	OK	4
2.6	OK	OK	OK	OK	OK	5

Table 12 continues. Evaluation matrix of the actual test series based on visual inspection and dimensional accuracy.

Experiment	Text	Pillars	Cubes [± 100 µm]	Sharp Shapes	General inspection	Overall
2.7	OK	OK	NOT OK	OK	OK	4
2.8	OK	OK	OK	OK	OK	5
2.9	NOT OK	OK	OK	OK	OK	4

As seen from the evaluation matrix (table 12), actual test series produced better results than the preliminary parameter test series. Overall there was only one experiment with the grade 3, six experiments with the grade 4 and two experiments with the grade 5. Experiments 2.6 and 2.8 resulted the grade 5 but experiment 2.8 was chosen for further comparison because it had fastest printing time. The comparison of the experiments 2.6 (exposure time of 18 sec) and 2.8 (17 sec) is shown in figure 47.

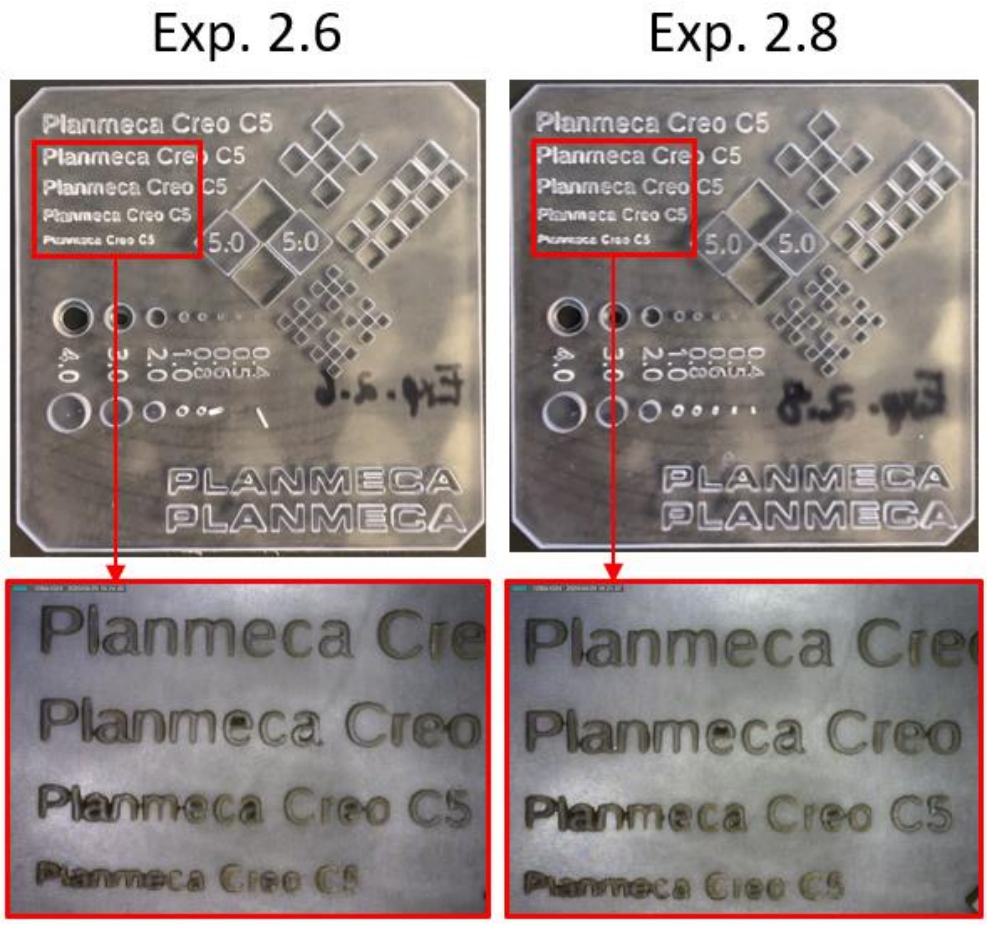

Figure 47. Experiments 2.6 and 2.8 of the actual test series with enlarged figures of the text.

As seen from the figure 47 the test results were quite identical with the experiments 2.6 and 2.8. Measurements of the cubes (appendix II, table 4) were under 20 mm and within the tolerance in both cases. Both experiments had the lift distance of 6 mm which indicated that 6 mm was the minimum lift distance for Ortho (material). Experiment 2.6 had part of the pillars broken, but it was because the print was dropped while it was washed, pillars were perfectly formed when the print was taken out from the printer. Experiment 2.1 (19 sec), which got the worst grade 3, is shown in figure 48.

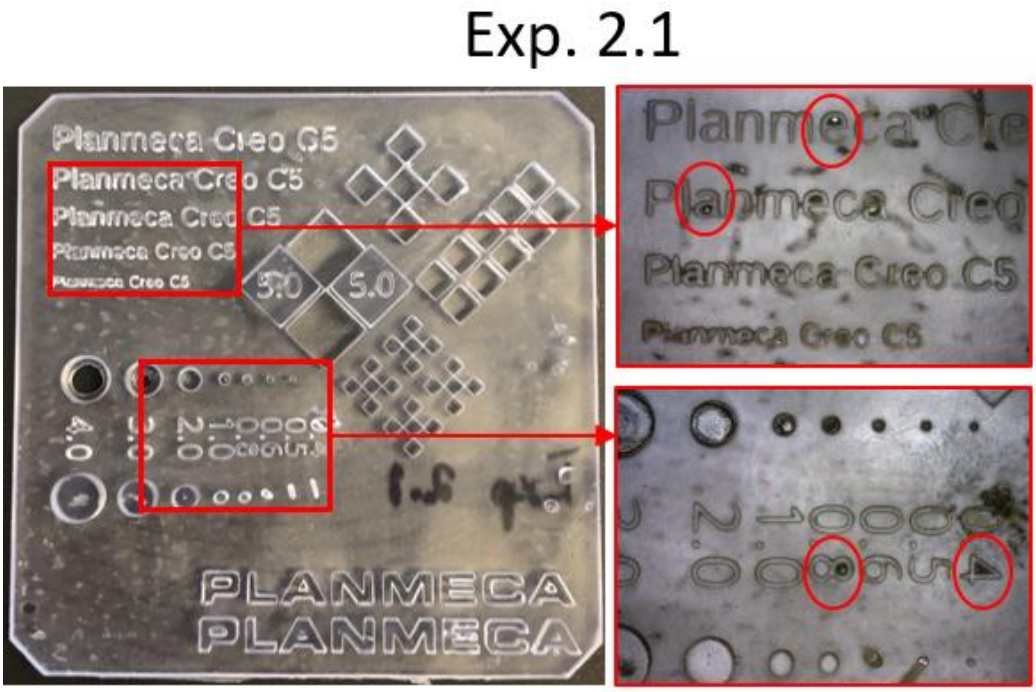

Figure 48. Experiment 2.1 which got overall grade of 3.

As seen from the figure 48, some of the letters in the texts were clogged so that it was hard to read what was written there, unlike at the experiments 2.6 and 2.8. Also, the measurements of the two pillars and holes (0.8 and 0.4), marked with circles had clogged. These aspects resulted that the general inspection was NOT OK.

Other way to approach the optimization round two, was to variate only the exposure time. This was done with 0.5 second steps and altogether nine test prints were made. It was considered that with nine prints enough wide range of exposure times were covered but still the amount of experiments was handled easily. The prints were evaluated with the same

criteria as during preliminary parameter test series. Evaluation matrix is presented in the table 13.

Table 13. Evaluation matrix of the actual test series, where only exposure time was varied, based on visual inspection and dimensional accuracy.

Experiment	**Text**	**Pillars**	**Cubes** [± 100 µm]	**Sharp Shapes**	**General inspection**	**Overall**
2.2.1	OK	NOT OK	OK	OK	OK	4
2.2.2	NOT OK	OK	OK	OK	OK	4
2.2.3	NOT OK	OK	OK	OK	OK	4
2.2.4	OK	OK	OK	OK	OK	5
2.2.5	OK	OK	OK	OK	OK	5
2.2.6	OK	OK	NOT OK	OK	OK	4
2.2.7	OK	OK	NOT OK	OK	OK	4
2.2.8	NOT OK	OK	OK	OK	OK	4
2.2.9	NOT OK	OK	OK	OK	OK	4

As it can be noted from the table 13, two experiments resulted the overall grade of 5 and rest of the prints got overall grade of 4. corresponding parameters can be seen in appendix I, table 3. Best results were achieved with exposure times of 17.5 and 18 seconds. These exposure times were within the same frame as the best results from the multivariable test round (experiment 2.8 – 17 seconds). Experiments of 2.2.4 and 2.2.5 are shown in the figure 49.

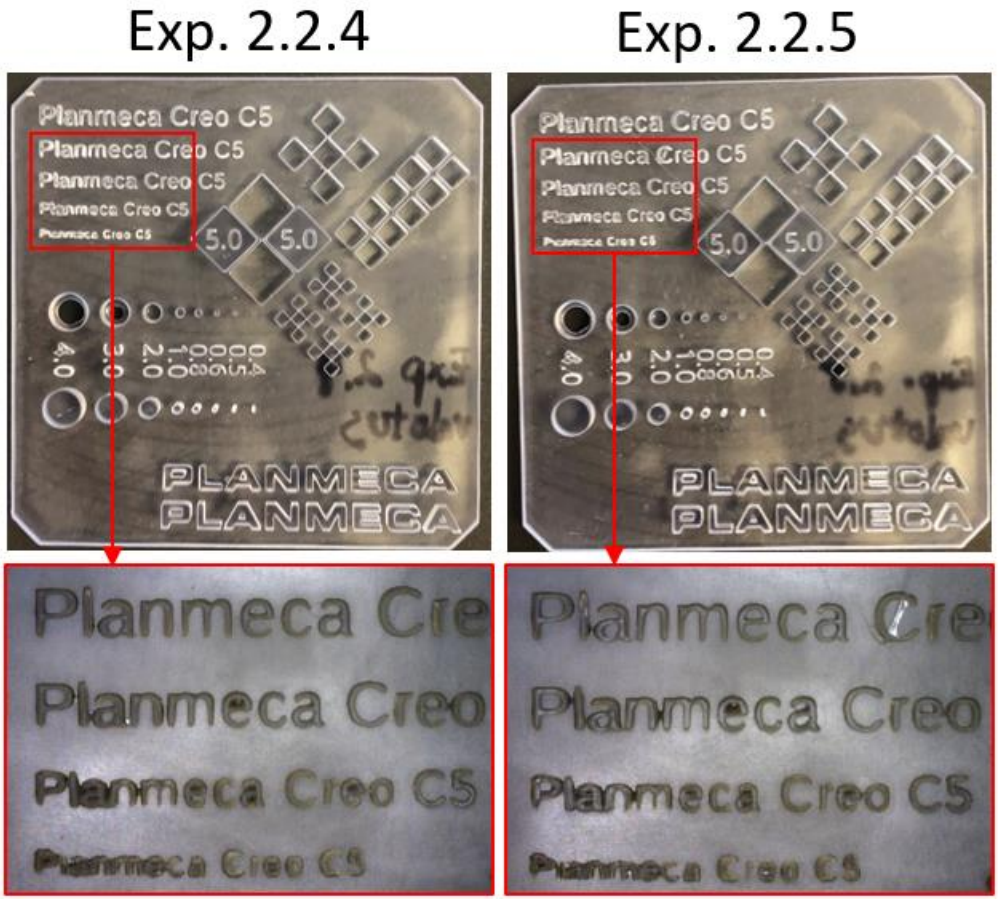

Figure 49. Experiments and enlarged figures of the experiments 2.2.4 and 2.2.5, second test round where only exposure time was varied.

As seen from the figure 49 the detailed texts were built well, and only minor clogging was detected. Both experiments had dimensional accuracy within the tolerances, shown in appendix II, table 4. One minor defect was that the smallest text was not easy to read, but concentrating on that at this point would not had been efficient. Results in overall were good, as it can be seen from the other experiments as well. For example, experiments 2.2.9 (15.5 sec) and 2.2.7 (16.5 sec) shown in figure 50, had grade 4.

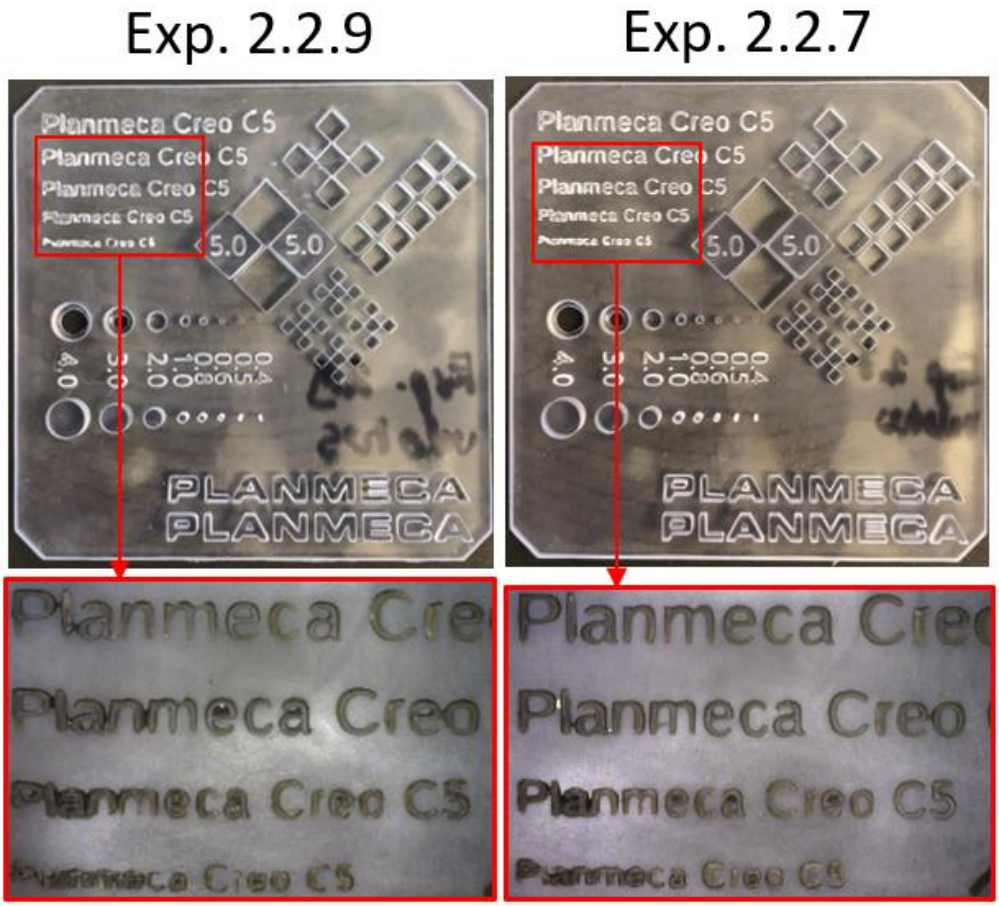

Figure 50. Experiments and enlarged figures of the experiments 2.2.9 and 2.2.7, actual test series where only exposure time was varied.

As it can be observed from the figure 50, experiment 2.2.9 had good quality, but the smallest text was only barely attached to the part why it could not be accepted. On the other hand, experiment 2.2.7 had almost as clear text as experiments 2.2.4 and 2.2.5 but the measurement cubes were not within the tolerances. It was concluded that the minor differences were due to short steps of exposure time variation, only 0.5 second difference between the experiments 2.2.4 and 2.2.5. Short variation made the detection of the defects challenging, while compared to multivariable test round experiments.

When compared the best results of both optimization ways (multivariable and single variable tests), it could be concluded that both ways led to similar result (experiments 2.8 and 2.2.5). Parameters are compared at the table 14.

Table 14. Parameters of the best results from the actual test series with both methods.

Experiment	Speed Up [mm/min]	Speed Down [mm/min]	Lift distance [mm]	Exposure time [sec]	Printing time [sec]
2.2.5	400	300	6	17.5	46
2.8	600	400	6	17	44

As seen from the table 14, there were not big difference in printing times even though experiment 2.8 had faster movements of the build plate and faster exposure time. It could be interpreted that significant decreases in printing times cannot be achieved when there is low number of layers in a printed part. However, because the printing times were wanted to be as fast as possible, the parameter set of the experiment 2.8 was chosen for further consideration and dental application tests.

9.2 Results and analysis of Saremco Print Crowntec

Validation round resulted worse results in terms of printing quality when compared to first test round. The reason was found after the tests were executed, Saremco Print Crowntec -material was designed for wavelength 385 nm, not for 405 nm. However, it was still possible to carry out the optimizing process even though the results in terms of printing quality were not good and materials for 385 nm should not be used with Creo C5.

9.2.1 Preliminary parameter finding

Anycubic test plate was printed first with one second steps, column one received one second of exposure and column ten received ten seconds of exposure. It was noted that the preliminary exposure time was over ten seconds, as shown in figure 51.

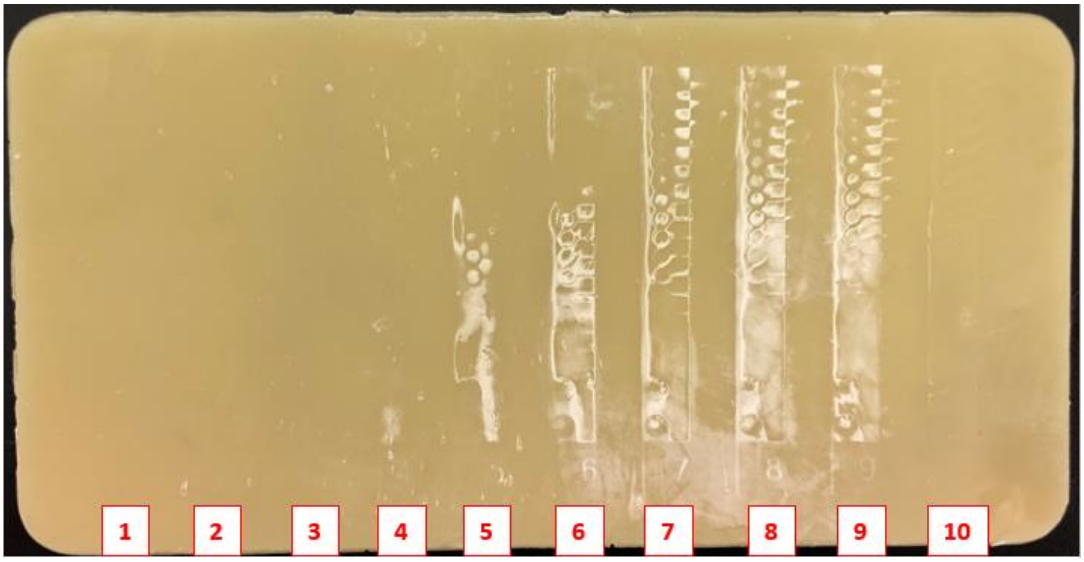

Figure 51. Printed Anycubic test plate with one second steps in each column from one to ten.

It can be seen from the figure 51 that columns from one to four had not attached to the base of the print. Columns from five to nine had attached poorly, but the strange thing was that column number ten, which received ten seconds of exposure, had not attached at all. This phenomenon could not be explained. However, the columns were attached to the base when the test plate was printed with two second steps, as it is shown in the figure 52.

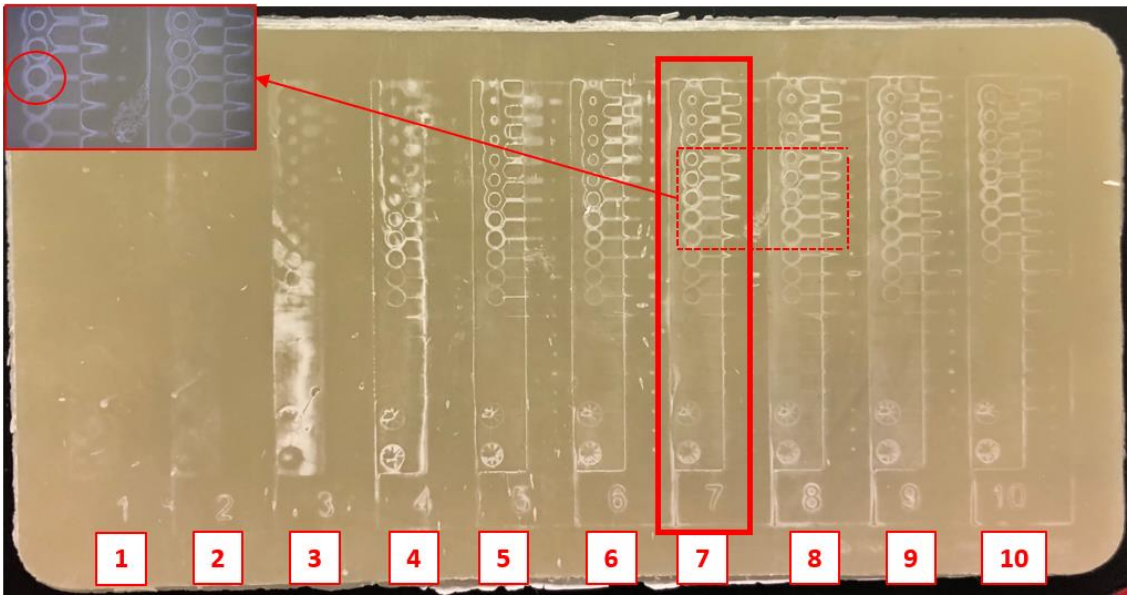

Figure 52. Printed Anycubic test plate with two second steps in each column from two to 20 seconds and enlarged picture of the critical circles.

As seen from the figure 52 enlarged photo, at the column seven the circle was open, but at the column eight it was only partly open. Based on this, it was selected the exposure time of the column seven as the preliminary exposure time. Column seven resulted 17 seconds for the preliminary exposure time, which was then varied up- and downwards.

9.2.2 Preliminary parameter test series

Experiments were visually inspected, and the evaluation matrix was formed after executing all the experiments of the preliminary parameter test series. The visual inspection was executed with the same criteria as with the Freeprint Ortho material, even though the quality was way worse. One thing to consider is that if the evaluation matrix does not result any difference in between the prints, the evaluation criteria should be loosened so that evaluation matrix results difference. By loosening the evaluation criteria, the printing quality characteristics of the experiments can be separated and detected, and further the best parameter set of the test series can be chosen. In general, the results for printing quality were bad. As shown in table 15, there were only three prints that did not got overall grade of 0.

Table 15. Evaluation matrix of the preliminary test series, based on visual inspection and dimensional accuracy.

Experiment	**Text**	**Pillars**	**Cubes** [± 100 µm]	**Sharp Shapes**	**General inspection**	**Overall**
1.1	NOT OK	OK	NOT OK	NOT OK	NOT OK	1
1.2	NOT OK	NOT OK	NOT OK	NOT OK	NOT OK	0
1.3	NOT OK	NOT OK	NOT OK	NOT OK	NOT OK	0
1.4	NOT OK	NOT OK	NOT OK	NOT OK	NOT OK	0
1.5	NOT OK	OK	NOT OK	NOT OK	NOT OK	1
1.6	NOT OK	NOT OK	NOT OK	NOT OK	NOT OK	0
1.7	NOT OK	NOT OK	NOT OK	NOT OK	NOT OK	0
1.8	NOT OK	NOT OK	NOT OK	NOT OK	NOT OK	0
1.9	NOT OK	OK	NOT OK	NOT OK	NOT OK	1

As it can be observed from the table 15, experiments 1.1, 1.5 and 1.9 got overall grade of 1, rest of the experiments got 0. Common for experiments 1.1, 1.5 and 1.9, was the exposure time of 10 seconds (appendix III, table 5). Furthermore, the measurement cubes of these

experiments had the smallest variation in dimensional accuracy (appendix IV, table 7). Pillars of the experiments (1.1, 1.5 and 1.9) were evaluated as OK, because pillars were not overgrown so they were not built together as with experiment 1.8 (18 sec) as shown in figure 53.

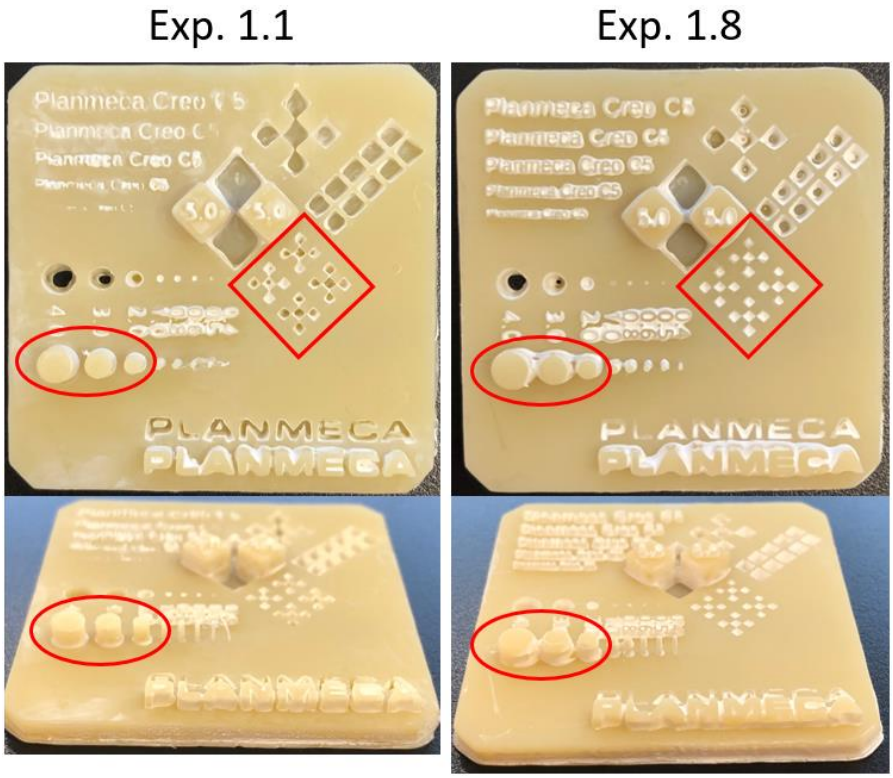

Figure 53. Experiment 1.1 has pillars built separately but at experiment 1.8 pillars have overgrown so that they are built together.

As figure 53 represents, the pillars had overgrown at the experiment 1.8 and when compared to experiment 1.1 the pillars were built separately. It could be noted also that the smallest engraved cubes (marked with boxes) were clogged at the experiment 1.8 while at the experiment 1.1 only four of them were clogged. When compared texts from all of the experiments, experiments (1.1, 1.5 and 1.9) had the best result even though they did not get the grade OK. Effect of exposure time can be seen when texts are observed, when exposure time increased the texts were clogged. Clogging can be detected from the figure 54.

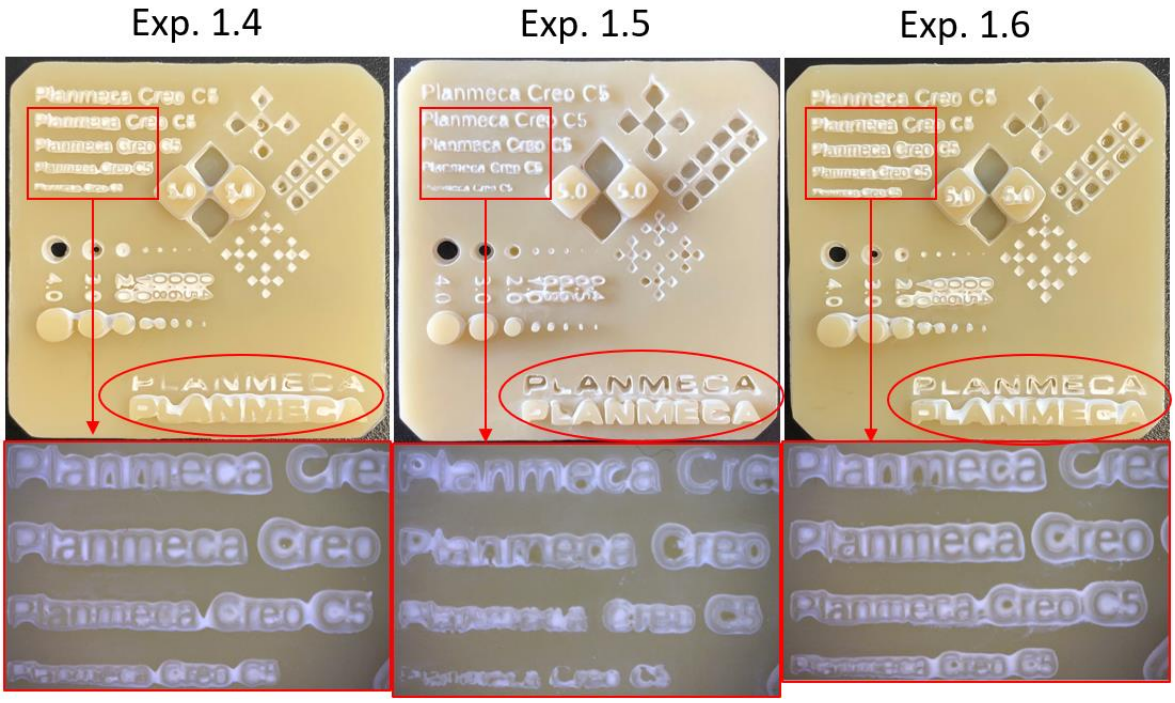

Figure 54. Clogging at the texts is detected with experiments 1.4 and 1.6 while experiment 1.5 has poorly attached text.

As seen from the figure 54, there is the Planmeca logo extruded and engraved at the right bottom corner of each experiment. At the experiments 1.4 (18 sec) and 1.6 (14 sec) the Planmeca logo was clogged in both extruded and engraved styles. Experiments 1.4 and 1.6 had also longer exposure time. At the experiment 1.5 (10 sec) the logo was not clogged, yet the text was unclear. When observed the enlarged figures, it was noted that at experiments 1.4 and 1.6 the texts were overgrown so that the letters were not separate but still the texts could be red. When observed experiment 1.5, the texts had not attached to the print, which was indicating of insufficient exposure time. It was considered that the optimal exposure time was in between the 10 seconds and 14 seconds. However, the measurement cubes in every experiment were overgrown which indicated that the exposure time was too long for each experiment. After all, these aspects should not be considered too much, because this resin was designed for 385 nm wavelength not for 405 nm. It was concentrated to follow the process flow.

Parameter set from experiment 1.9 (10 sec) was chosen to be optimized at the actual test series, because it had the shortest printing time. And the quality characteristics were the same as experiment 1.5.

9.2.3 Actual test series

Actual test series concentrated optimizing the exposure time only and other parameters were kept the same as the parameter set of experiment 1.9 had. In other words, it was tried to find the minimum exposure time for Crowntec material, so that the detailed geometries can be still seen. The exposure time was varied from 12 seconds and not from 10 seconds. Based on the results of the preliminary parameter test series, the assumption was that optimal exposure time was in between the 10 seconds and 14 seconds. Evaluation matrix of the actual test series is shown in table 16. All the experiments were still evaluated with same criteria as before.

Table 16. Evaluation matrix of actual test series based on visual inspection and dimensional accuracy.

Experiment	**Text**	**Pillars**	**Cubes** [± 100 µm]	**Sharp Shapes**	**General inspection**	**Overall**
2.1	NOT OK	OK	NOT OK	NOT OK	NOT OK	1
2.2	NOT OK	OK	NOT OK	NOT OK	NOT OK	1
2.3	NOT OK	OK	NOT OK	NOT OK	NOT OK	1
2.4	NOT OK	OK	NOT OK	NOT OK	NOT OK	1
2.5	NOT OK	NOT OK	NOT OK	NOT OK	NOT OK	0
2.6	NOT OK	NOT OK	NOT OK	NOT OK	NOT OK	0
2.7	NOT OK	NOT OK	NOT OK	NOT OK	NOT OK	0

As table 16 shows, experiments from 2.1 (12 sec) to 2.4 (9 sec) had the grade 1 which indicated that the minimum exposure time was with the parameter set of experiment 2.4 (9 sec). Corresponding parameters can be seen in the appendix III, table 6. Effect of decrease in exposure time is shown in figure 55.

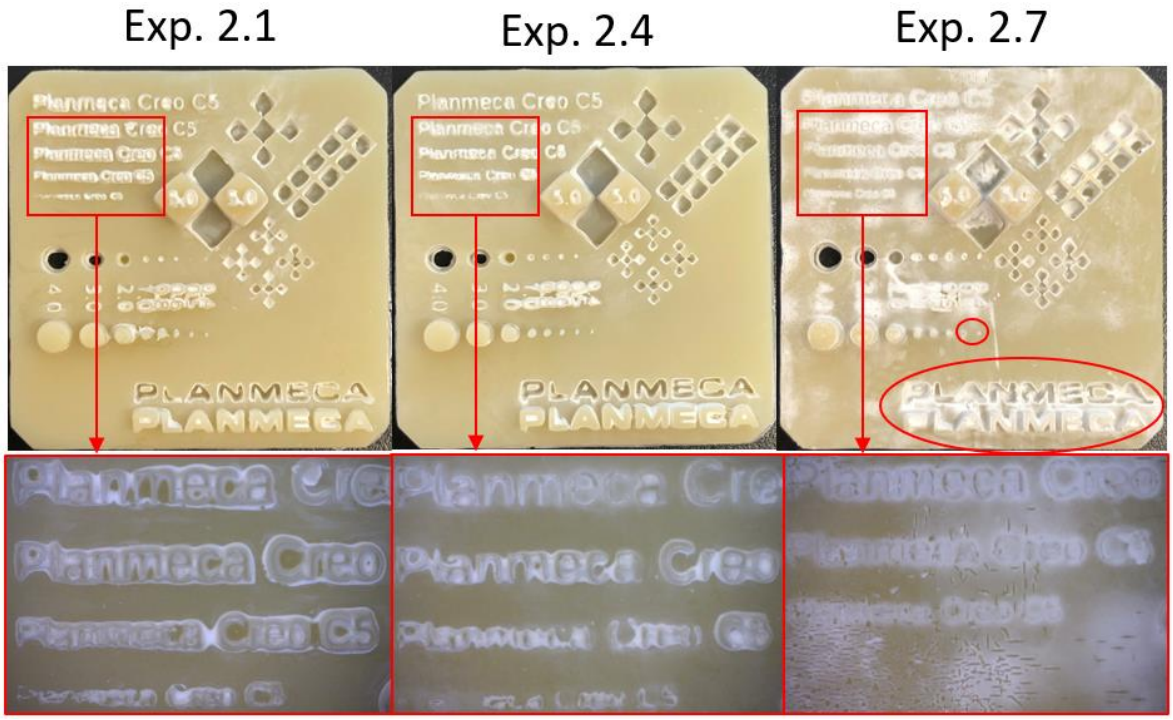

Figure 55. Experiments 2.1, 2.4 and 2.7 compared how well the texts have printed, experiment 2.7 had also missing pillars and Planmeca text is missing some characters.

As it can be observed from the enlarged figures of the figure 55, when exposure time was decreasing the texts were no longer attached to the part. Experiment 2.1 had exposure time of 12 seconds and the text was attached to the part, but it was overgrown. Experiment 2.4 had exposure time of 9 seconds and the mid-size text was only partly attached to the part, but the smallest font size was not attached to the part. Experiment 2.7 had exposure time of 6 seconds and there was no text attached to the part. Experiment 2.7 had collapsed pillars and Planmeca logo had not built properly, there were missing some characters of the engraved logo. However, parameter set of the experiment 2.4 was chosen for further examination. Parameter set can be seen in the table 17.

Table 17. Parameter set for further examination.

Experiment	**Speed Up [mm/min]**	**Speed Down [mm/min]**	**Lift distance [mm]**	**Exposure time [sec]**	**Printing time [sec]**
2.4	200	200	7	9	30

In the table 17 it is presented the parameters for Saremco Print Crowntec material which were result from the optimization process developed in this thesis.

10 DISCUSSION

In this paragraph main results are discussed and presented using graphs, flow chart and fish bone diagram. The relation between the critical parameters and printing time was examined without forgetting the printing quality. It was noticed that printing time could be reduced when the best results of the preliminary parameter test series and actual test series were compared. Figure 56 represents the effect of optimization process to exposure time and build plate movements. Shorter exposure time and higher speed of build plate were resulting faster printing times.

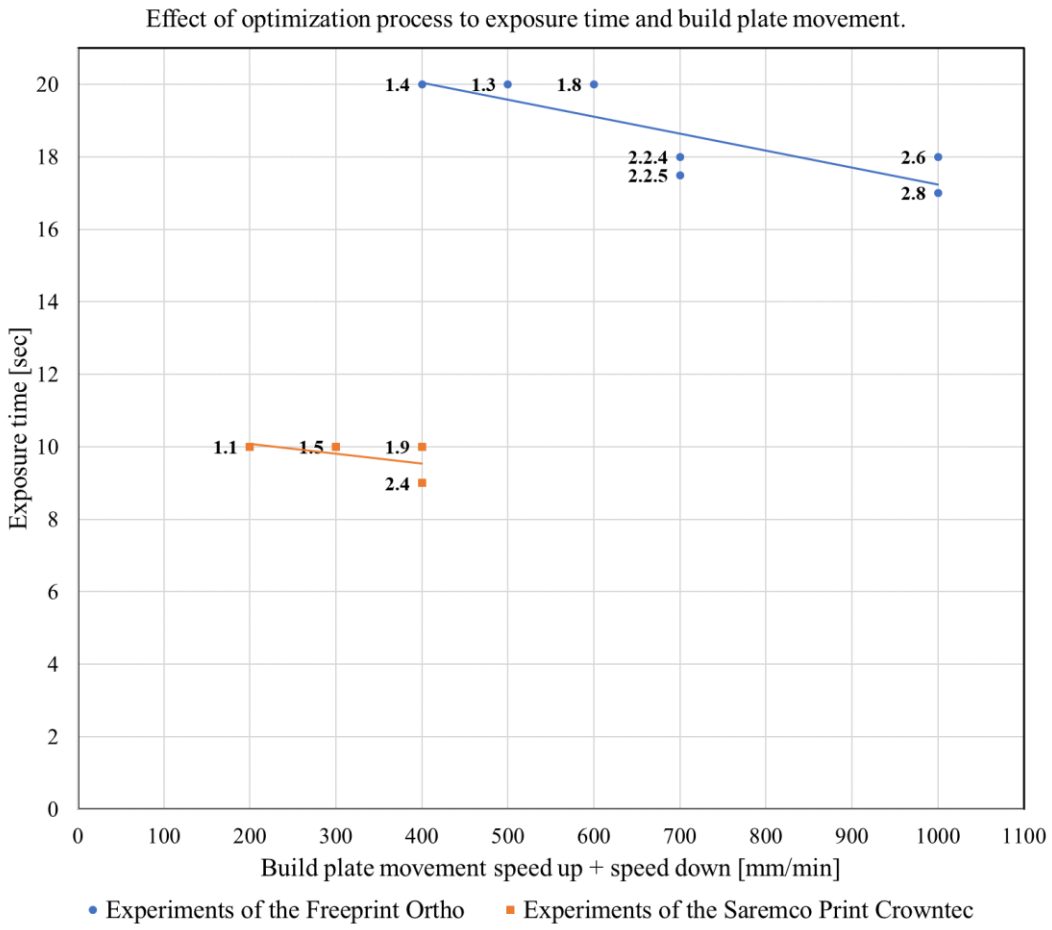

Figure 56. Effect of combined build plate movements (speed up and speed down) and exposure time to printing when optimization process is carried out with accepted prints.

It can be observed form the figure 56 that with optimization process the printing times were reduced. Data points were corresponding the experiment numbers and at the x-axis the

speeds of the build plate movements were summed. The curves represented the downward trend of printing times when optimization was executed in terms of printing quality. Faster printing times were pursued in this case, but the main response was to maintain printing quality at high level, which is why the decreases in printing times were not remarkable. Printing time was decreased 13,7% with Ortho material, from 51 minutes (experiment 1.8) down to 44 minutes (experiment 2.8), printing times can be seen at the appendices I and III. Optimization did not result as large decrease with Crowntec material, because the material was not suitable for Creo C5. Anyhow, the printing time was decreased 6,25%, from 32 minutes (experiment 1.9) to 30 minutes (experiment 2.4) over the optimization rounds. It is essential to remember that reduction of printing times was executed with two test series, which resulted only 18 experiments. All the critical parameters could be optimized. Relation between the exposure time and dimensional accuracy was found, which was critical information in terms of dimensional accuracy. Relation shown in figure 57.

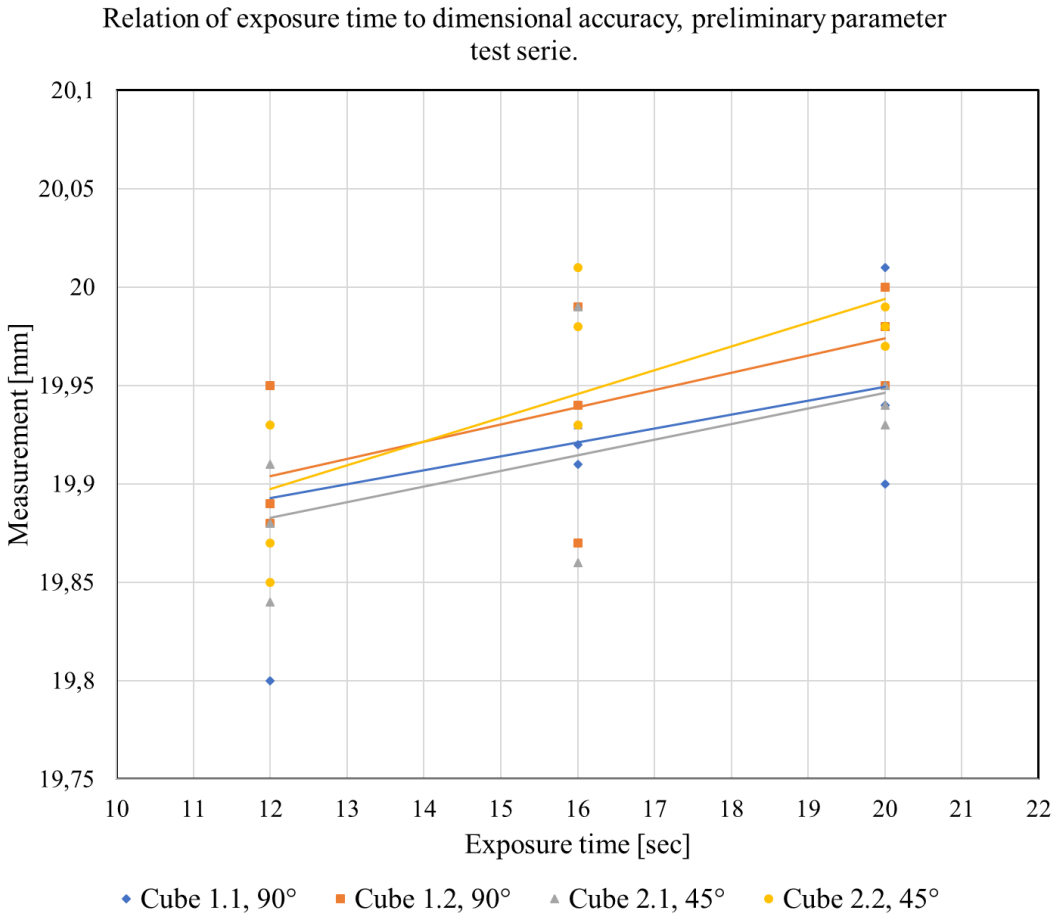

Figure 57. Exposure time vs. dimensional accuracy of the Freeprint Ortho during the preliminary parameter test series.

As it can be noted from the figure 57, the measurements of the cubes increased when exposure times increased as well. In figure 57 the increase of exposure time can be seen also as an improving factor for dimensional accuracy, because measurements are within thinner range. This might due to more constant layer build, which means that layers were built properly and there were not remarkable saw-edged side at the cubes. When exposure time was 20 seconds, the measurements were within 0.11 micrometers, but when the exposure time was 12 and 16 seconds, the measurements were within 0.15 micrometers. The large variation of the measurements was due to large variation in exposure times. When compared measurements and variation of the preliminary parameter test series to measurements and variation of the actual test series, the difference can be detected from the figure 58.

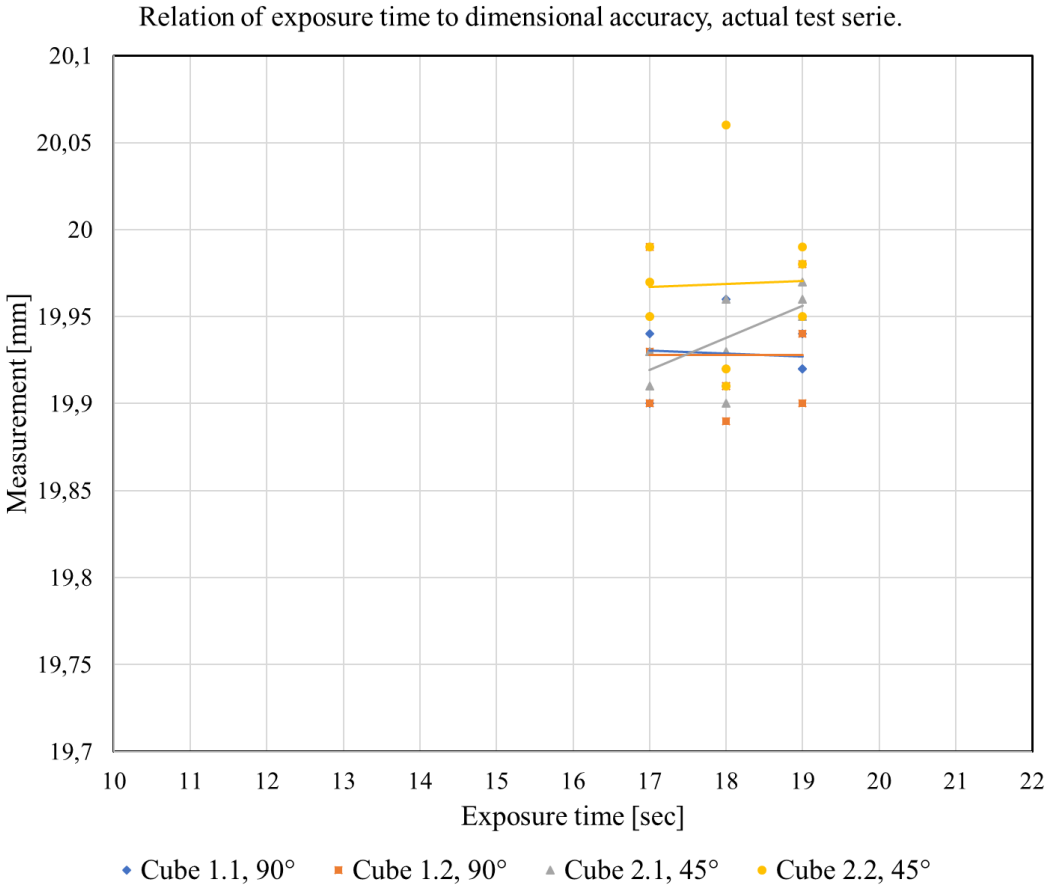

Figure 58. Exposure time vs. dimensional accuracy of the Freeprint Ortho during the actual test series.

As it can be observed from the figure 58, the deviation between the measurements was less than in the preliminary parameter test series. This was because the right exposure time was

close by varied times and the exposure time was varied with shorter steps than in the preliminary parameter test series. Exposure times of 17 and 19 seconds resulted deviation of 0.09 µm and 18 seconds resulted deviation of 0.07 µm, if the anomalous measurement with cube 2.2, 45° was ignored, if not, the deviation was 0.17 µm between the longest and shortest dimension. Figure 58 also shows (in general) how the slope of the curve was more controlled when exposure times were varied with shorter steps. On the other hand, the deviation of the measurements was harder to detect because the differences were smaller, and it was used slide gauge which caused inaccuracy in measurements.

Two sub-questions of the main research question were dealing with critical parameters in DLP printing and the critical parameters with Creo C5. Fishbone diagram (figure 59) was created to clarify which parameters are affecting to printing quality in Creo C5 printer.

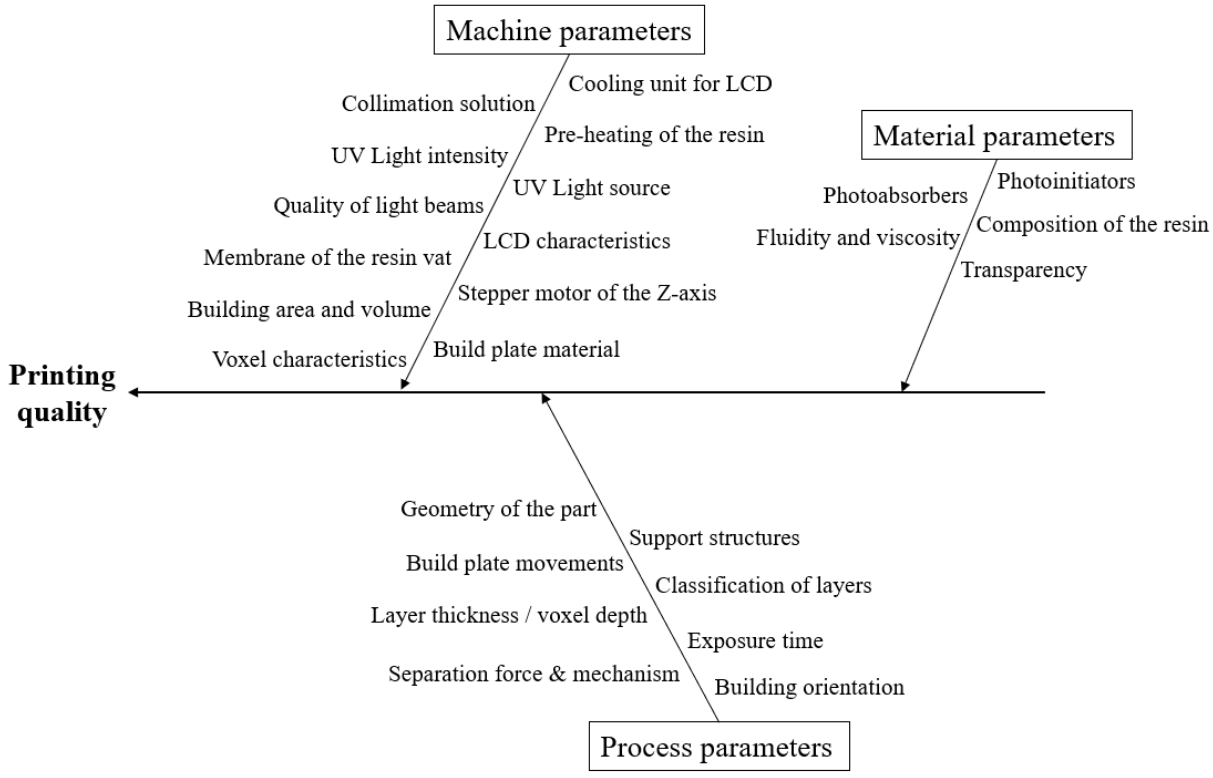

Figure 59. Fish bone diagram, parameters that are affecting to printing quality with Creo C5.

Parameters affecting to printing quality with Creo C5 printer are presented in the figure 59 as fish bone diagram. All the affecting parameters to printing quality were listed into the

diagram. Some of the listed parameters could be dived further into sub-parameters, like UV Light source. UV Light source as a parameter included the power of the individual LED, what kind of lenses had been used, what was the wavelength of light source and how the LEDs had been placed at the array. In this thesis it was concentrated in process parameters and variation of the chosen critical process parameters. Exposure time was considered as the most important individual process parameter, because it had an effect to dimensional accuracy but also to cure depth, layer thickness and geometrical characteristics. The fish bone diagram was not considering post curing as a parameter affecting to the quality characteristics of the printed part, even though it has an effect. The main research question was considering about the steps of successful parameter optimization process for Planmeca. These steps were created according the executed printing tests and the flow chart of the whole process is presented in figure 60.

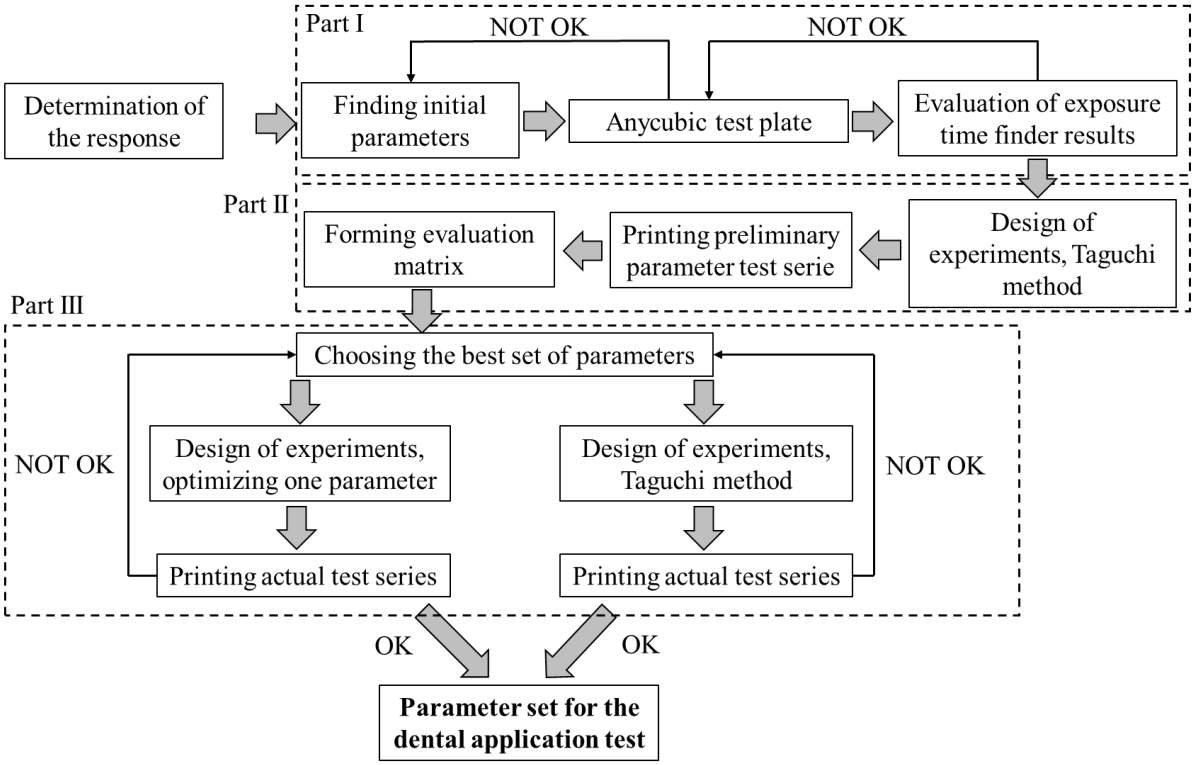

Figure 60. Flow chart for parameter optimization process created in this thesis.

The figure 60 answered to main research question, which was: What are the steps for successful parameter optimization process for Planmeca? Every box in the flow chart can be considered as a one step. However, to simplify the chart, complexes marked with dashed lines (called part I, II and III) can be considered also as one step. First step was to choose

the response based on the material that was researched. Part I consisted of the preliminary parameter finding actions. In part I it was possible to go backwards if the found preliminary parameters were not resulting desired quality, as it was done in this thesis. In part II preliminary parameter test series was executed and the experiments were evaluated. Preliminary test series was considered as a constant round, there was no possibility to modify the parameters and re-execute the test series. Re-executing might have caused purposeless optimizing which was not efficient at this point of the process. Part III included two possibilities for optimization, by executing a multivariable test as during the preliminary parameter test series or concentrating only into exposure time optimization. Both ways were tested in this thesis and they resulted similar results. It is also worth of noting that the method can be changed, if it is noticed that the chosen method is not working. One possible way is to carry out the same test series twice, inside the part III. Altogether, the outcome of the part III was considered as the set of parameters for the dental application printing test. Further optimization can be done with the dental application test print, methods and DOE processes discussed in this thesis can be utilized.

One goal of the thesis was to determine traceable procedure for optimization. It was tracked, that executing part I took one working day, including the creation of the printing files. Executing parts II and III took two working days, including the formation of test matrix and printing files. Experiments were evaluated always after the whole test round to ensure the same evaluation criteria for each print. The evaluation of each test round took half a day. As a remark, the re-execution of the part III, in other words another test round, has to be considered as two days of execution and half a day of evaluation. As a summary, the optimization process takes 7 seven days, if no extra test rounds are required.

11 ERROR ESTIMATION

Error estimation in this thesis concentrated on two used references in the literature review, the measurements of the cubes, and material choice for the validation round. Literature review was executed with some non-scientific references when parameter optimization processes were searched. References GitHub 2020 and Welover 2019 are not scientific references but were based on the information and knowledge that hobbyist and companies have gained when using DLP printers. As showed in experimental part, some information from these references were useful.

The measurements of the measurement cubes might have had some error because slide gauge was used as a measurement tool and measurements were taken by free hands. Also, the overgrown layers might have caused dimensional inaccuracy, because the measurements varied depending whether the measurement tool hit the bottom or top of the side of the cube which was saw-edged.

The material used in validation round was not optimized for 405 nm wavelength, but for 385 nm. This caused some problems with the printing quality, which was very poor. This fact was identified after the evaluation of the second test round, the printing quality was not improved. Later the fact was confirmed from the material manufacturer that the used version of Crowntec, was not optimized for printers using 405 nm wavelength. Wrong type of material was probably affecting negatively to measurement cubes also, because there was wide variation and the tolerance was not achieved.

12 CONCLUSION

The aim of the thesis was to determine a standardized, documented, repeatable and traceable procedure for parameter optimization process so that the same process can be repeated with needed dental 3D printing materials at Planmeca. The process was planned and created based on the findings of the literature research. The planned process was executed with Freeprint Ortho material, and the process was validated with Saremco Crowntec material to ensure the functionality of the process. The research problem was provided a solution with the optimization process developed in the experimental part of this thesis.

The main result from the literature review was that Taguchi method is widely utilized design of experiments (DOE) process when 3D printing parameters are optimized. With Taguchi method (multivariable DOE) the number of experiments could be decreased when compared to traditional fractional design of experiments. The number of experiments in the experimental part could be decreased from 81 (3^4) (fractional DOE) down to only 9 experiments per test round (Taguchi method). The literature review also resulted other essential results about the DOE process and one of them was the importance of choosing the response and identification of the critical parameters. According the literature review identification of the critical parameters is the key issue for a successful DOE process. These identified critical parameters for Creo C5 were build plate movement (speed up, speed down and lift distance) and exposure time. Parameters were classified into three groups based on the findings from the literature review and the interview of Reijonen (2020). The classification eases the handling of the parameters as larger complexes. Parameters were classified as follows: process, machine and material parameters. Furthermore, the literature review resulted that the most important parameters for resin 3D printing were layer thickness, exposure time, resin composition, UV light characteristics, voxel size and build angle with support structure settings.

The experimental part concentrated on creating the standardized, documented, repeatable and traceable procedure for optimization the critical parameters for Creo C5. The process was created, and the standardized and repeatable steps are represented at the conclusions, figure 59. The experiments were manufactured with Creo C5 photomask resin 3D printer.

Documentation was done during the test rounds and the first draft of document template was created for Planmeca for documentation of the upcoming optimization processes. Traceability for the process was ensured by keeping a record of how long it took to complete each step. Altogether it was tracked that the optimization of the critical parameters took 7 working days. But this result has to be re-considered case-specific always, because new materials might bring new obstacles in terms of printing.

The experimental part showed that the created process worked, and it can be used with various materials. Preliminary exposure time could be determined with one simple test which turned out to be an effective way of finding preliminary exposure time. Determined preliminary exposure time was a bit too long in every case, but the optimization process ensured that the exposure time was optimized. Taguchi orthogonal array $L_9(3^4)$ was used as a test matrix, which resulted the 9 experiments per test series. Experiments were visually evaluated according the four different classes and measurement cubes were measured to evaluate the dimensional accuracy. The initial exposure time calculation for Anycubic test plate was not proven to be completely accurate, because it had to be modified in validation round. It might be due to material, which was not suitable for the printer. However, the calculation method should be researched more.

Preliminary parameter test series of Freeprint Ortho resulted three experiments which got the grade 5, each of them had exposure time of 20 seconds. Parameter set of the experiment 1.8 was chosen to be varied in the actual test series because it had the fastest printing time of the succeeded prints. In actual test series critical parameters were varied in two different ways. First it was executed another Taguchi multivariable test round, another way was variating the exposure time only. The exposure time was varied with nine different values, to find optimal exposure time. Both ways resulted similar results, there were two succeeded prints from both ways that got grade 5. Faster printing times were favored so it was chosen the parameter sets with faster printing times for comparison. Finally, it was chosen the parameter set of the experiment 2.8 to be used for dental application test print.

Validation round proved the functionality of the created process, even though the printing quality was not at good level. The process resulted better printing quality and printing times could be decreased. The parameter set that validation round resulted, was not considered as

optimized set of parameters in terms of chosen response, but the optimization process improved printing quality. Poor results in terms of printing quality were based on the material, which was optimized for different wavelength of UV light.

13 FURTHER STUDIES

The optimization process of the critical parameters for Creo C5 was created at the experimental part. However, there were certain phenomena which were limited out form this thesis and were not discussed nor studied. These phenomena are providing topics for upcoming researches. Suggested topics for further studies are listed below:

- Research of optimal building angle and maximum overhang area for dental applications with Creo C5.
- Optimization of support structures and amount of support structures for LCD photomask 3D printing.
- Study of the applied separation forces in vat photopolymerization.
- Effect of build angle and part geometry to the separation forces.
- Study of the optimal separation process for Creo C5.
- Effect of light intensity to exposure time and printing quality.

LIST OF REFERENCES

Abdollahi, S., Davis, A., Miller, J. & Feinberg, A. 2018. Expert-guided optimization for 3D printing of soft and liquid materials. PLoS ONE, Vol. 13, Iss. 4, pp. 1-19.

All3DP. 2018. LCD vs DLP – Resin 3D Printing Technologies Compared. [Web document]. [Referred 22.11.2019]. Available: https://all3dp.com/2/lcd-vs-dlp-3d-printing-technologies-compared/

All3DP. 2019. 2019 Dental 3D Printing Guide: All You Need to Know. [Web document]. [Referred 23.12.2019]. Available: https://all3dp.com/2/dental-3d-printing-all-you-need-to-know/

Amerlabs. 2018. Key things to know before calibrating resin 3D printer. [Web document]. Updated 16.3.2018. [Referred 6.3.2020]. Available: https://ameralabs.com/blog/key-things-calibrating-resin-3d-printer/

Amerlabs. 2019. 6 Key Principles of 3D Printing Supports that Work. [Web document]. Updated 16.5.2019. [Referred 6.3.2020]. Available: https://ameralabs.com/blog/6-tips-3d-printing-supports/

Anderson, P. 2017. Clinical Applications of 3D Printing. Spine, Vol. 42, pp. 30-31.

Arnold C., Monsees, D., Hey, J. & Schweyen, R. 2019. Surface Quality of 3D-Printed Models as a Function of Various Printing Parameters. Materials, Vol. 12, pp. 1-15.

Bagheri, A. & Jin, J. 2019. Photopolymerization in 3D printing. ACS Applied Polymer Materials, Vol. 1, pp. 593-611.

Bertana, V., De Pasquale, G., Ferrero, S., Scaltrito, L., Catania, F., Nicosia, C., Marasso, S.L., Cocuzza, M. & Perrucci, F. 2019. 3D Printing with the Commercial UV-Curable Standard Blend Resin: Optimized Process Parameters towards the Fabrication of Tiny Functional Parts. Polymers, Vol. 11, Iss. 2, pp. 1-14.

Bhargav, A., Sanjairaj, V., Feng, L. W. & YH, J. F. 2018. Applications of additive manufacturing in dentistry: A rewiev. Journal of Biomedical Materials Research, Vol, 106, Iss. 5, pp. 2058-2064.

Chitubox. 2020. A Complete Guide about Support Structures in SLA/DLP/LCD 3D Printing. [Chituboxs website]. [Referred 6.3.2020]. Available: https://www.chitubox.com/article_howto_17839_4_41.html

Davoudinejad, A., Diaz-Perez, L., Quagliotti, D., Pedersen, D., Albajez-García, J., Yagüe-Fabra, J. & Tosello, G. 2018. Additive manufacturing with vat polymerization method for precision polymer micro components production. 15th CIRP Conference on Computer Aided Tolerancing, CIRP CAT 2018. Proceedings of the International Conference, held at Milan, Italy 11-13 June 2018. Pp. 98-102.

Davoudinejad, A., Pedersen, D. & Tosello, G. 2017. Evaluation of polymer micro parts produced by additive manufacturing processes using vat photopolymerization method. Conference: The European Society for Precision Engineering and Nanotechnology. Proceedings of the International Conference, held at Leuven, Belgium October 2017. Pp. 1-3.

DeltaMed. 2020. 3Delta – Light-curing resins for dental 3D-printing. [DeltaMeds website]. [Referred 5.3.2020]. Available: https://www.deltamed.de/en/brand-products/3d-dental/

Detax. 2020. 3D Print. [Detaxs website]. [Referred 5.3.2020]. Available: https://www.detax.de/en/shop/dental/dental-labor-3D-Druck.php

Dreve. 2020. Resins. [Dreves website]. [Referred 5.3.2020]. Available: https://dentamidshop.dreve.de/dentamiden/catalog/category/view/s/resins/id/133/

EN ISO 17296-2. 2016. Additive manufacturing – General principles – Part 2: Overview of process categories and feedstock. Brussels: European Committee for Standardization. 14 p.

EN ISO/ASTM 52900. 2017. Additive manufacturing – General principles – Terminology. Brussels: International Organization for Standardization. 25 p.

Fiorenza, L., Yong, R., Ranjitkar, S., Hughes, T., Quayle, M., McMenamin, P., Kaidonis, J., Townsend, G. & Adams, J. 2018. Technical note: The use of 3D printing in dental anthropology collections. American Journal of Physical Anthropology, Vol. 167, Iss. 2, pp. 400-406.

Formlabs. 2019a. SLA vs. DLP: Compare Resin 3D Printing Technologies (2019 Guide). [Formlabs website]. [Referred 22.11.2019]. Available: https://formlabs.com/blog/3d-printing-technology-comparison-sla-dlp/

Formlabs. 2019b. Digital Dentistry: 5 Ways 3D Printing has Redefined the Dental Industry. [Formalbs website]. [Referred 23.12.2019]. Available: https://dental.formlabs.com/blog/digital-dentistry-dental-3d-printing/

Formlabs. 2020. Understanding Accuracy, Precision and Tolerance in 3D Printing. [Formlabs website]. [Referred 25.2.2020]. Available: https://formlabs.com/blog/understanding-accuracy-precision-tolerance-in-3d-printing/

GitHub. 2020. Anycubic Photon – Files and method to quickly find the best latitude exposure settings for any resin or 405nm UV coating. [GitHubs website]. [Referred 28.2.2020]. Available: https://github.com/altLab/photon-resin-calibration?fbclid=IwAR0QXa4xnSdARWNmwP4GNhezCUsJHSWMZlvBWJWwE8GaD2aprkWlY1bGv4o

Gong, H., Beauchamp, M., Perry, S., Woolley, A. & Nordin, G. 2015. Optical approach to resin formulation for 3D printed microfluidics. RSC Advances. Iss. 129, pp. 106621-106632.

Gowda, R., Udayagiri, C. & Narendra, D. 2014. Studies on the Process Parameters of Rapid Prototyping Technique (Stereolithography) for the Betterment of Part Quality. International Journal of Manufacturing Engineering, Vol 14, pp. 1-11.

Griffiths, C.A., Howarth, J., De Almeida-Rowbotham, G., Rees, A. & Kerton, R. 2016. A design of experiments approach for the optimization of energy and waste the production of parts manufactured by 3D printing. Journal of Cleaner Production, Vol. 139, pp. 74-85.

Gritsenko, D., Yazdi, A., Lin, Y., Hovorka, V., Pan, Y. & Xu, J. 2017. On characterization of separation force for resin replenishment enhancement in 3D printing. Additive Manufacturing, Vol. 17, pp. 151-156.

Guerra, A., Lammel-Lindeman, J., Katko, A., Kleinfehn, A., Rodriguez, C., Catalani, L., Becker, M., Ciurana, J. & Dean, D. 2019. Optimization of photocrosslinkable resin components and 3D printing process parameters. Acta Biomaterialia, Vol. 97, pp. 154-161.

Ho, C., Ng, S., Li, K. & Yoon, Y-J. 2015. 3D printed microfluids for biological applications. Lab on a Chip, Vol.15, Iss. 18, pp. 3627-3637.

Ibrahim, A., Sa'ude, N. & Ibrahim, M. 2017. Optimization of process parameter for digital light processing (DLP) 3D printing. Sixty-second International Conference on Artificial Intelligence and Soft Computing, ICAISC: Proceedings of the International Conference, held at Seoul, South Korea 18-19 April, 2017. Pp. 11-14.

Kickstarter. 2019. SLASH: The Next Level of Affordable Prefessional 3D Printer. [Kickstarter website]. [Referred 25.11.2019]. Available: https://www.kickstarter.com/projects/644653534/slash-the-next-level-of-affordable-professional-3d

Langnau, L. 2018. What is a voxel in 3D printing? [Web document]. Make Parts Fast, A Design World Resources, 2018. Published 7.3.2018. [Referred 5.3.2020]. Available: https://www.makepartsfast.com/what-is-a-voxel-in-3d-printing/

Lin, C-H., Lin, Y-M., Lai, Y-L. & Lee, S-Y. 2020. Mechanical properties, accuracy, and cytotoxicity of UV-polymerized 3D printing resins composed of Bis-EMA, UDMA, and TEGDMA. The Journal of Prosthetic Dentistry, Vol. 123, Iss. 2, pp. 349-354.

Lin, Y., Lin, Y., Zhang, Y. & Yang, C. 2018. Simulating an Intelligent Printing Control for a Digital Light Processing (DLP) 3D Printer. Proceedings of IEEE International Conference of Applied System Invention (ICASI), Chiba, Japan. 13-17.4.2018. Pp. 429-432.

Lingon, SC., Liska, R., Stampfl, J., Gurr, M. & Mulhaupt, R. 2017. Polymers for 3D Printing and Customized Additive Manufacturing. Chemical Reviews, Vol. 117, Iss. 15, pp. 10212-10290.

Liqcreate. 2019. What is the difference between SLA, DLP and LCD 3D-printers? [Liqreate website]. [Referred 22.11.2019]. Available: https://www.liqcreate.com/supportarticles/what-is-the-difference-between-a-sla-dlp-and-lcd-3d-printers/

Liravi, F., Das, S. & Zhou, C. 2015. Separation force analysis and prediction based on cohesive element model for constrained-surface Stereolithography processes. Computer-Aided Design, Vol. 69, pp. 134-142.

Luukkanen, M. 2019. Periaatekuva [private e-mail]. Receivers: Eetu Holstein. Sent. 11.12.2019, 14.54 o'clock. (GMT +0200). Attachment: "CREO_source_B.png"

Lättemaa, E. 2020. Bachelor of Applied Science - Dental Laboratory Technology/Technican. CAD/CAM Product Specialist, Planmeca. Interview, 14.4.2020. Interviewer Eetu Holstein. Notes are occupied by the interviewer.

Martinez-Marquez, D., Mirnajafizadeh, A., Carty, C. & Stewart, R. 2018. Application of quality by design for 3D printed bone protheses and scaffolds. PLoS One, Vol. 13, Iss. 4, pp. 1-47.

Mohamed, M., Kumar, H., Wang, Z., Martin, N., Mills, B. & Kim, K. 2019. Rapid and Inexpensive Fabrication of Multi-Depth Microfluidic Device using High-Resolution LCD Stereolithographic 3D Printing. Manufacturing and Materials Processing, Vol. 3, Iss. 26, pp. 1-11.

Namjung, K., Ishan B., Daehoon, H., Chen, Y. & Howon, L. 2019. Improving Surface Roughness of Additively Manufactured Parts Using a Photopolymerization Model and Multi-Objective Particle Swarm Optimization. Applied Sciences, Vol. 9, Iss. 1, pp. 150-173.

Osman, R., Alharbi, N. & Wismeijer, D. 2017. Build Angle: Does It Influence the Accuracy of 3D-Printed Dental Restorations Using Digital Light-Processing Technology? The International Journal of Prosthodontics, Vol. 30, Iss. 2, pp. 182-188.

Pan, Y., He, H., xu, F. & Feinerman, A. 2017. Study of separation force in constrained surface projection stereolithography. Rapid Prototyping Journal, Vol. 23, Iss. 2, pp. 353-361.

Planmeca. 2020. Company. [Planmeca website]. [Referred 14.4.2020]. Available: https://www.planmeca.com/fi/cadcam/hammasskannaus/planmeca-emerald-s/

Planmeca. 2019. Company. [Planmeca website]. [Referred 27.12.2019]. Available: https://www.planmeca.com/company/

Rao, R.S., Kumar, C.G., Prakasham, R. S. & Hobbs, P.J. 2008. The Taguchi methodology as a statistical tool for biotechnological appliations: A critical appraisal. Biotechnology Journal, Vol. 3, Iss. 4, pp. 510-523.

Regulation (EU) 2017/745 of the European Parliament And of the Council. 2017. Medical devices. Given 5.4.2017. 02017R0745 EN 228 p.

Reijonen, J. 2020. Master of Science (Tech.). Research Scientist, VTT. Skype interview, 30.1.2020. Interviewer Eetu Holstein. Notes are occupied by the interviewer.

Roland. 2020. What is CAD CAM? [Roland's website]. [Referred 9.1.2020]. Available: https://www.rolanddga.com/th-th/products/dental/dwx-series

Sa, L., Kaiwu, L., Shenggui, C., Junzhong, Y., Lin, W. & Li, R. 2019. 3D printing dental composite resins with sustaining antibacterial ability. Journal of Materials Science, Vol. 54, Iss. 4, pp. 3309-3318.

Scopus. 2020a. Analyze search results. [Scopus website]. [Referred 3.2.2020]. Available: https://www-scopus-com.ezproxy.cc.lut.fi/term/analyzer.uri?sid=cad2567357d53f499d02102f76b2c94a&origin=resultslist&src=s&s=TITLE-ABS-KEY%28Resin+3D+printing%29&sort=plf-f&sdt=b&sot=b&sl=32&count=1317&analyzeResults=Analyze+results&txGid=709861fbc46940035a0b5c3b9c426d40

Scopus. 2020b. Analyze search results. [Scopus website]. [Referred 3.2.2020]. Available: https://www-scopus-com.ezproxy.cc.lut.fi/term/analyzer.uri?sid=15f524f8e43d2dc30bb737979c112b92&origin=resultslist&src=s&s=TITLE-ABS-KEY%283D+printing+in+dental+applications%29&sort=plf-f&sdt=b&sot=b&sl=49&count=180&analyzeResults=Analyze+results&txGid=671433b9d353e14225f9e2dae6aba1b6

Shah, P. & Chong, B. S. 2018. 3D imaging, 3D printing and 3D virtual planning in endodontics. Clinical Oral Investigations, Vol. 22, Iss. 2, pp. 641-654.

Sjöberg, P. 2020. Doctor of Science (Tech.). Senior Scientist, Planmeca Oy. Interview, 8.4.2020. Interviewer Eetu Holstein. Notes are occupied by the interviewer.

Stansbury, J. W. & Idacavage, M. J. 2016. 3D printing with polymers: Challenges among expanding options and opportunities. Dental Materials, Vol. 32, Iss. 1, pp. 54-64.

Stavropoulos, P. & Foteinopoulos, P. 2018. Modelling of additive manufacturing processes: a review and classification. Manufacturing Review, Vol. 5, pp. 1-26.

Taloussanomat. 2019. Planmeca Oy. [Taloussanomat website]. [Referred 27.12.2019]. Available: https://www.is.fi/yritys/planmeca-oy/helsinki/0112773-2/

Taormina, G., Sciancalepore, C., Messori, M. & Bondioli, F. 2018. 3D printing processes for photocurable polymeric materials: technologies, materials, and future trends. Journal of Applied Biomaterials & Functional Materials, Vol. 16, Iss. 3, pp. 151-160.

Teng, T. & Ke, J. 2013. A novel optical film to provide a highly collimated planar light source. Optic express, Vol. 21, Iss. 18, pp. 21444-21455.

The University of York. 2004. Department of Mathematics, Orthogonal Arrays (Taguchi Designs). [Web page]. [Referred 23.1.2020]. Available: https://www.york.ac.uk/depts/maths/tables/orthogonal.htm

Tumbelston, J., Shirvanyants, D., Ermoshkin, N., Johnson, A., Kelly, D., Chen, K., Pinschmidt, R., Rolland, J., Ermoshkin A., Samulski, E. & DeSimone, J. 2015. Continuous liquid interface production of 3D objects. Science, Vol. 347, Iss. 6228, pp. 1349-1352.

Waheed, S., Cabot, J., Macdonald, N., Lewis, T., Guijt, R., Paull, B. & Breadmore, M. 2016. 3D printed microfluids devices: enablers and barriers. Lab on a Chip, Vol. 16, Iss 11, pp. 1993-2013.

Wang, Z., Martin, N., Hini, D., Mills, B. & Kim, K. 2017. Rapid Fabrication of Multilayer Microfluid Devices Using the Liquid Crystal Display-Devices Using the Liquid Crystal Display-Based Stereolithography 3D Printing System. 3D Printing and Additive Manufacturing, Vol. 4, pp. 156-164.

Wanger, J., Mount, E. & Giles, H. 2014. [Chapter 25] Design of Experiments. In: Extrusion – The Definitive Processing Guide and Handbook. 2nd Edition. Pp. 291-308.

Welover. 2019. DLP 3D Printing: Understanding Process And Materials Enables You To Prevent Production Problems. [Welover's website]. [Referred 11.12.2019]. Available: https://www.wevolver.com/article/dlp.3d.printing.understanding.process.and.materials.enables.you.to.prevent.production.problems

Whip Mix. 2020. 3D Print Resins. [Whip Mix's website]. [Referred 5.3.2020]. Available: https://whipmix.com/product-category/3d-print-resins/

Wu, D., Zhao, Z., Zhang, Q., Qi, J. & Fang, D. 2019. Mechanics of shape distortion of DLP 3D printed structures during UV post-curing. Soft Matter, Vol. 15, Iss. 30, pp. 6151-6159.

Zhang, J. & Xio, P. 2018. 3D printing of photopolymers. Polymer Chemistry, Iss. 13, pp. 1530-1540.

3DERS. 2016. Illuminate DLP 3D printer hits Kickstarter running with affordable 2K resolution. [3DERS website]. [Referred 25.11.2019]. Available: https://www.3ders.org/articles/20161117-illuminate-dlp-3d-printer-hits-kickstarter-running-with-affordable-2k-resolution.html

3D Hubs. 2020. Supports in 3D Printing: A technology overview. [3D Hubs website]. [Referred 6.3.2020]. Available: https://www.3dhubs.com/knowledge-base/supports-3d-printing-technology-overview/

3Dnatives. 2018. The 3D Printing Dental Market is Booming. [3Dnatives website]. [Referred 23.12.2019]. Available: https://www.3dnatives.com/en/3d-printing-dental-market-170120184/

3Dresyns. 2020. Printing Guidelines: Tuning out 3Dresyns in SLA, DLP & LCD 3D printers. [Web document]. [Referred 6.3.2020]. Available: https://www.3dresyns.com/pages/how-to-fine-tune-3dresyns-for-your-printer

Table 1. Taguchi orthogonal array L9(34) for the preliminary parameter test series of Freeprint Ortho, printing time added to array.

	Parameter				
Experiment number	Speed Up [mm/min]	Speed down [mm/min]	Lift distance [mm]	Exposure time [sec]	**Printing time [min]**
1.1	100	200	6	12	41
1.2	100	300	7	16	49
1.3	100	400	8	20	57
1.4	200	200	7	20	54
1.5	200	300	8	12	39
1.6	200	400	6	16	44
1.7	300	200	8	16	47
1.8	300	300	6	20	51
1.9	300	400	7	12	37

Table 2. Taguchi orthogonal arrays L9(34) for the actual test series of Freeprint Ortho, printing time added to array.

	Parameter				
Experiment number	Speed Up [mm/min]	Speed down [mm/min]	Lift distance [mm]	Exposure time [sec]	**Printing time [min]**
2.1	400	300	6	19	49
2.2	400	400	5	18	45
2.3	400	500	4	17	42
2.4	500	300	5	17	44
2.5	500	400	4	19	46
2.6	500	500	6	18	46
2.7	600	300	4	18	45
2.8	600	400	6	17	44
2.9	600	500	5	19	46

Table 3. Taguchi orthogonal arrays L9(34) for the actual test series of Freeprint Ortho, when only exposure time is varied, printing time added to array.

	Parameter				
Experiment number	Speed Up [mm/min]	Speed down [mm/min]	Lift distance [mm]	Exposure time [sec]	**Printing time [min]**
2.2.1	400	300	6	19.5	50
2.2.2	400	300	6	19	49
2.2.3	400	300	6	18.5	48
2.2.4	400	300	6	18	47
2.2.5	400	300	6	17.5	46
2.2.6	400	300	6	17	45
2.2.7	400	300	6	16.5	44
2.2.8	400	300	6	16	43
2.2.9	400	300	6	15.5	42

Table 4. Measurements of the 20 x 20 mm cubes of Freeprint Ortho.

Experiment - material	**Cube 1.1, 90°**	**Cube 1.2, 90°**	**Cube 2.1, 45°**	**Cube 2.2, 45°**
1.1 - ortho	19.93	19.89	19.84	19.87
1.2 - ortho	19.92	19.99	19.86	19.93
1.3 - ortho	20.01	20	19.94	19.98
1.4 - ortho	19.94	19.98	19.93	19.97
1.5 - ortho	19.95	19.95	19.88	19.85
1.6 - ortho	19.91	19.94	19.93	19.98
1.7 - ortho	19.93	19.87	19.99	20.01
1.8 - ortho	19.9	19.95	19.95	19.99
1.9 - ortho	19.8	19.88	19.91	19.93
2.1 - ortho	19.92	19.98	19.97	19.95
2.2 - ortho	19.92	19.91	19.93	20.06
2.3 - ortho	19.9	19.9	19.93	19.97
2.4 - ortho	19.95	19.93	19.93	19.99
2.5 - ortho	19.94	19.94	19.95	19.99
2.6 - ortho	19.91	19.91	19.96	19.91
2.7 - ortho	19.96	19.89	19.9	19.92
2.8 - ortho	19.94	19.99	19.91	19.95
2.9 - ortho	19.92	19.9	19.96	19.98
2.2.1 - ortho	19.95	19.92	19.91	19.93
2.2.2 - ortho	19.93	19.91	19.93	19.98
2.2.3 - ortho	19.93	19.9	19.93	19.9
2.2.4 - ortho	19.99	19.91	19.99	19.92
2.2.5 - ortho	19.96	19.94	20.03	19.98
2.2.6 - ortho	19.89	19.91	19.9	19.92
2.2.7 - ortho	19.95	19.89	20	19.91
2.2.8 - ortho	19.93	19.96	19.92	19.96
2.2.9 - ortho	19.99	19.99	20	20.06

Table 5. Taguchi orthogonal array L9(34) for the preliminary parameter test series of Saremco Print Crowntec, printing time added to array.

	Parameter				
Experiment number	Speed Up [mm/min]	Speed down [mm/min]	Lift distance [mm]	Exposure time [sec]	**Printing time [min]**
1.1	100	100	6	10	36
1.2	100	150	7	14	43
1.3	100	200	8	18	51
1.4	150	100	7	18	51
1.5	150	150	8	10	35
1.6	150	200	6	14	39
1.7	200	100	8	14	44
1.8	200	150	6	18	46
1.9	200	200	7	10	32

Table 6. Taguchi orthogonal array L9(34) for the actual test series of Saremco Print Crowntec, printing time added to array.

	Parameter				
Experiment number	Speed Up [mm/min]	Speed down [mm/min]	Lift distance [mm]	Exposure time [sec]	**Printing time [min]**
2.1	200	200	7	12	36
2.2	200	200	7	11	34
2.3	200	200	7	10	32
2.4	200	200	7	9	30
2.5	200	200	7	8	28
2.6	200	200	7	7	26
2.7	200	200	7	6	25

Table 7. Measurements of the 20 x 20 mm cubes of Saremco Print Crowntec.

Experiment - material	**Cube 1.1, 90°**	**Cube 1.2, 90°**	**Cube 2.1, 45°**	**Cube 2.2, 45°**
1.1 - crowntec	20.36	20.31	20.36	20.34
1.2 - crowntec	20.75	20.55	20.64	20.7
1.3 - crowntec	20.65	20.83	20.84	20.71
1.4 – crowntec	20.68	20.89	20.69	20.86
1.5 – crowntec	20.43	20.25	20.39	20.43
1.6 – crowntec	20.68	20.82	20.83	20.71
1.7 - crowntec	20.57	20.39	20.51	20.51
1.8 – crowntec	21.06	20.8	20.86	20.94
1.9 – crowntec	20.49	20.31	20.48	20.6
2.1 – crowntec	20.48	20.51	20.68	20.5
2.2 - crowntec	20.48	20.36	20.38	20.54
2.3 – crowntec	20.37	20.29	20.28	20.37
2.4 – crowntec	20.24	20.46	20.39	20.26
2.5 – crowntec	20.22	20.39	20.36	20.33
2.6 – crowntec	20.2	20.26	20.35	20.3
2.7 – crowntec	20.14	20.2	20.15	20.14

Measurements and calculations for the preliminary parameter finding of Detax Freeprint Ortho and Saremco Print Crowntec.

Table 8. Measurements of the sheet of Detax Freeprint Ortho -resin.

	1	**2**	**3**	**4**	**5**	**6**
Measurement [mm]	0.189	0.187	0.2	0.189	0.189	0.187

Exposure time for bottom layers of the Freeprint Ortho:

$$t_{E,B} = \left[\left(\frac{100}{\bar{X}}\right) \cdot t_{E1}\right] \cdot 10$$

$$t_{E,B} = \left[\left(\frac{100}{190.05}\right) \cdot 30\right] \cdot 10$$

$$t_{E,B} = [15{,}79] \cdot 10$$

$$t_{E,B} \approx 150$$

Table 9. Measurements of the sheet of Saremco Print Crowntec -resin.

	1	**2**	**3**	**4**	**5**	**6**
Measurement [mm]	0.823	0.816	0.843	0.817	0.800	0.800

Exposure time for bottom layers of the Saremco Print Crowntec:

$$t_{E,B} = \left[\left(\frac{100}{\bar{X}}\right) \cdot t_{E1}\right] \cdot 10$$

$$t_{E,B} = \left[\left(\frac{100}{816.50}\right) \cdot 30\right] \cdot 10$$

$$t_{E,B} = [3.7] \cdot 10$$

$$t_{E,B} \approx 37$$